HERON is jointly edited by:
STEVIN-LABORATORY of the faculty of Civil Engineering, Delft University of Technology, Delft, The Netherlands
and
TNO BUILDING AND CONSTRUCTION RESEARCH. Rijswijk (ZH), The Netherlands
HERON contains contributions based mainly on research work performed in these laboratories on strength of materials, structures and materials science.

ISSN 0046-7316

This publication has been issued in close co-operation with the Netherlands Technology Foundation (STW)

HERON vol. 39 1994 no. 3

Contents

THE FATIGUE BEHAVIOUR OF MULTIPLANAR TUBULAR JOINTS

A. Romeijn
Faculty of Civil Engineering
Delft University of Technology
The Netherlands

Publication in HERON since 1970

Abstract

Circular hollow sections are frequently used in structures subjected to fatigue loading such as bridges, offshore structures and cranes. These sections are generally connected by direct welding of the sections to each other. For the design of these welded connections, information is required on the fatigue behaviour. Especially for multiplanar connections, insufficient data is available regarding stress concentration factors (SCFs) which affect the fatigue life.

Also, there is no standard for determining the fatigue strength of welded tubular joints. This has led to a divergence in the methods being used both experimentally as well as numerically. This publication presents the results of experimental and numerical research on the fatique strength of welded tubular joints.

The research projects aim to provide guidelines and design recommendations on the fatigue strength of welded tubular joints, to be proposed for inclusion in international codes of practice such as Eurocode 3.

Keywords

Welded tubular joint, Lattice girder, Numerical modelling, Fatigue, Hot spot stress, Uniplanar, Multiplanar, Stress (strain) concentration factor.

1. INTRODUCTION

1.1 *The use of circular hollow sections*

In nature it is shown that circular hollow sections are excellent structural elements.
Their use offer many advantages over open structural sections such as I-beams because of:

- *Equal bending strength and stiffness in all directions.*
- *High strength-to-weight ratio.*
- *Low drag coefficient and shape factor.*
- *Possible use of internal void (buoyancy, transport, filling with concrete, etc.).*

Furthermore, compared to the open structural sections, the circular hollow sections offer an excellent profile for:

- *Resistance against buckling in all directions.*
- *Environmental corrosion protection.*
- *Fire resistance (water or concrete filling).*
- *Composite steel-concrete members.*
- *An economical construction (direct welded connection of members avoiding expensive stiffeners or gusset plates).*

In addition, the closed curved shape of circular hollow sections offers architecturally pleasing features making them increasingly popular, and for the near future, it is expected that the use of circular hollow sections will increase also because of robot welding, which makes the fabrication of the joints less labour intensive.
Circular hollow sections are frequently used in *bridges*, *offshore structures*, *cranes*, *amusement parks*, *agriculture* and *mechanical engineering*. These types of structures however, are generally subjected to fatigue loading, which requires knowledge on the fatigue strength of the joints between the tubular members in the structure. The welded tubular joints constitute the structural elements in a lattice girder, formed by the hollow sections identified as brace and chord members. The non-uniform stiffness around the perimeter of the brace to chord intersection results in a geometrical non-uniform stress distribution, which may be unfavorable in case of fatigue loading. The non-uniform stress distribution depends on the type of loading (axial, bending in plane, bending out of plane and torsion) and the connection (types and geometry). Thus many cases exist.
Therefore, the fatigue behaviour of welded tubular joints is treated in a different way than for example for welded connections between plates.

1.2 *Research objectives*

The fatigue behaviour of welded tubular joints can be determined either by σ_r - N methods or with a fracture mechanics (FM) approach.

- The various σ_r - N methods are based on experiments, resulting in $S_{r_{h.s.}}$ - N_f curves with a defined hot spot stress range also called geometric stress range on the vertical axis and the number of cycles N_f to a specified failure criterion on the horizontal axis. The advantage of a σ_r - N method, so-called hot spot stress method, is that all types of welded tubular joints are related to the same $S_{r_{h.s.}}$ - N_f curve by the stress concentra-

tion factors (SCFs), which depend on the global connection geometry and loading.

- The FM approach is based on a fatigue crack growth model. The material crack growth parameters of the model can be determined from standardized small specimens and the influence of the connection geometry is incorporated in the stress intensity factor ΔK.

This publication deals with the σ_r - N methods

The design of welded uniplanar tubular joints by means of $S_{r\ h.s.}$ - N_f curves and parametric formulae for determining SCFs is implemented in the different design codes like API [*F1*], AWS [*F2*], IIW [*F22*], DEn [*F9*] and EC3 [*F12*]. However, the work carried out so far on uniplanar joints has some major drawbacks. This is because of:

- *Fairly "open" guidelines on how the hot spot stresses should be determined.*
- *Assumptions are made for converting experimentally measured hot spot strains into hot spot stresses for use in fatigue design $S_{r\ h.s.}$ - N_f curves, by the use of a constant average conversion factor of snf = 1.2 .*
- *Large variations in the predicted SCFs can occur depending on the parametric formulae adopted [F26], and many design codes do not specify which formulae to use.*

Furthermore, SCF parametric formulae for uniplanar joints obtained from numerical work, mainly cover:

- *The use of FE models where the shape of the weld is not included. This has been found to give large differences, particularly for the brace member locations. (This problem also exists for SCF parametric formulae obtained from experimentally tested small acrylic models where the weld shape is not included).*
- *The use of principal stresses instead of stresses in a direction perpendicular to the weld toe (chord member locations) and parallel to the axis of the brace member (brace member locations), which is found to be more realistic.*
- *SCFs for limited locations around the perimeter of the brace to chord intersection.*
- *SCFs caused by brace member loads, so that no information on SCFs caused by chord member loads exist. Also, no information exists on SCFs caused by torsional moments.*
- *SCFs, which are dependent upon the combination of boundary and loading conditions used. Therefore, the hot spot stresses caused, for instance by brace member loads in a T joint incorporate the effect of bending in the chord member (the so-called α influence).*

For multiplanar tubular joints, which are more frequently encountered in comparison to uniplanar joints, only limited numerical information [*F13*] and limited experimental information [*F3*, *F30*, *F47*, *F63*] is available.
No recommendations on fatigue design $S_{r\ h.s.}$ - N_f curves and SCFs specifically for these types of joints in codes exist. The above mentioned lack of information on fatigue strength of welded tubular joints has been the reason for setting up two projects, namely:

- A STW sponsored numerical research project entitled:
  "***Numerical and experimental investigation for the stress concentration factors of tubular joints***", carried out at Delft University of Technology, The Netherlands.
- An ECSC sponsored experimental research project entitled:
  "***Fatigue behaviour of multiplanar welded hollow section joints and reinfor cement measures for repair***", carried out by the following partners:
  The Netherlands: - Delft University of Technology.
  - TNO Building and Construction Research.
  Germany: - Mannesmannröhren-Werke A.G.

- Universität Karlsruhe.

Additional work is sponsored by Cidect in the programme entitled:
"*7A: Fatigue strength of multiplanar welded unstiffened CHS and RHS joints*".

The projects aim at providing guidelines and design recommendations on fatigue strength of (unstiffened) welded tubular joints, and information on joint flexibility behaviour. Information on joint flexibility behaviour is found to be necessary to determine the correct load distribution, so that the hot spot stress range can be accurately determined.

This publication, which mainly concerns the numerical work, contains the following three topics:

1 ***Numerical modelling of welded tubular joints.***
- *Numerical modelling of tubular joint stress concentration factors.*

2 ***Fatigue behaviour of multiplanar welded tubular joints in lattice girders.***
- *Experimental investigation.*
- *Calibration of numerical results with experimental results.*

3 ***Parameter study on SCFs and SNCFs.***
- *Method of SCF and SNCF determination.*
- *Numerical determination of stress and strain concentration factors of unstiffened uniplanar and multiplanar welded tubular joints with a gap and having no eccentricity.*
- *Calibration of numerical results with experimental results.*
- *Comparison between numerical results from the parameter study and existing parametric formulae on SCFs.*
- *The influence of the presence of a carry-over brace member on SCFs due to reference loading.*
- *The importance of carry-over effects.*
- *The relationship between SCF and SNCF.*

1.3 *Definitions*

1.3.1 Definitions related to fatigue

Finite Element (FE) modelled joint
The translation of a joint and its loading into a mathematical model which can be solved numerically by the use of finite elements (shell, solid, etc.), and which have geometrical and material properties and load and boundary conditions which correspond to the real behaviour of the joint in an acceptable manner.

Fatigue
For a structure subjected to fluctuating loads, because of:
- *geometric peak stresses caused by the non-uniform stiffness of the welded tubular joint;*
- *the geometry of the weld;*
- *the condition at the weld toe;*

micro structural changes resulting in the development of cracks are likely to occur at the weld toe locations of the joint. The development of such cracks is identified as a fatigue

phenomenon.

Fatigue life

The fatigue life of a structural component (joint) is defined as the number of load cycles N of stress or strain up to which a failure of a specified nature occurs [*F58*]. Various modes like *first visible crack, certain crack length, crack through the wall* and *end of test* (because of complete loss of strength) can be considered. Nowadays, a crack through the wall so-called first through-thickness cracking is adopted as the failure criterion for welded tubular joints.

Nominal stress

The nominal stress σ_{nom} is defined as the maximum stress (linear-elastic behaviour) in a cross section of a loaded chord or brace member according to the equations:

$$\sigma_{axial;nom} = \frac{F_{axial}}{A_x} \quad , \quad \sigma_{ipb;nom} = \frac{M_{ipb}}{W_y} \quad \text{and} \quad \sigma_{opb;nom} = \frac{M_{opb}}{W_z} .$$

For the fatigue loaded multiplanar KK joints in the triangular lattice structures tested (described in chapter 4), extrapolated nominal stresses for the braces under axial tension loading are used as illustrated in figure 1, for which:

$$\sigma_{extrap;nom} = \sigma_{axial;nom} + \sqrt{\sigma^2_{extrap;ipb} + \sigma^2_{extrap;opb}}$$

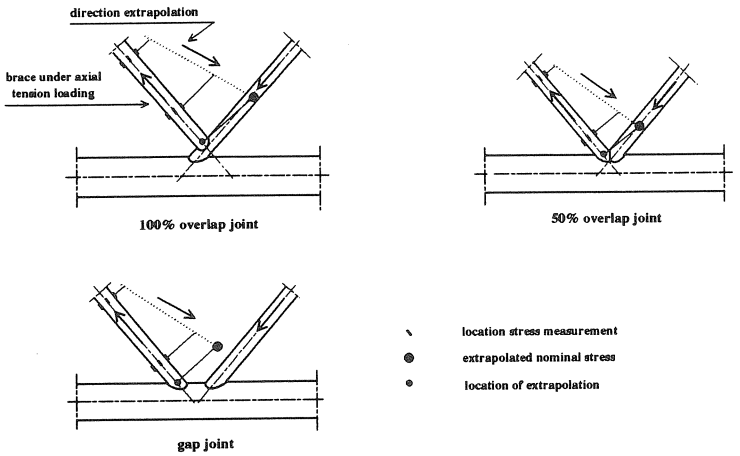

Fig. 1. Definitions of extrapolated nominal stresses $\sigma_{extrap.;nom}$ for the tested multiplanar KK joints placed inside a structure.

Stress range

The stress range σ_r, is the main parameter to be determined for fatigue analysis.
In case of constant amplitude loading (see figure 2), the stress range is defined as $\sigma_r = \sigma_{max} - \sigma_{min}$. The nominal stress range σ_r is based on nominal stresses, while the hot spot stress range $S_{r\ h.s.}$ is based on hot spot stresses.

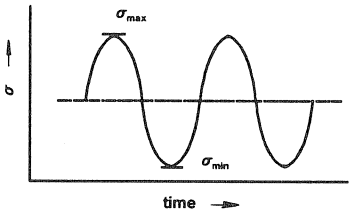

Fig. 2. Stress range for constant amplitude loading.

Stress ratio

The stress ratio R, is defined as the ratio between the minimum and maximum stress for constant amplitude loading (see also figure 2).

$R = \sigma_{min} / \sigma_{max}$: tension is taken positive and compression as negative.

Hot spot stress or also called geometric stress

A hot spot is a critical point at a discontinuity, usually a weld toe location, where fatigue crack initiation is expected and joint failure starts. The hot spot stress $\sigma_{h.s.}$ is the extrapolated stress to the weld toe, which takes the global joint geometrical effects into account only. The definition of the hot spot stress is closely related to the choice of the fatigue design $S_{r\ h.s.}$ - N_f curve. A standard procedure for the determination of the hot spot stress is an extrapolation of stresses from a defined distance to the weld toe (see figure 3). On the basis of this procedure, *S-N* data for tubular joints within a large range of geometries, fall within a common $S_{r\ h.s.}$ - N_f scatterband.

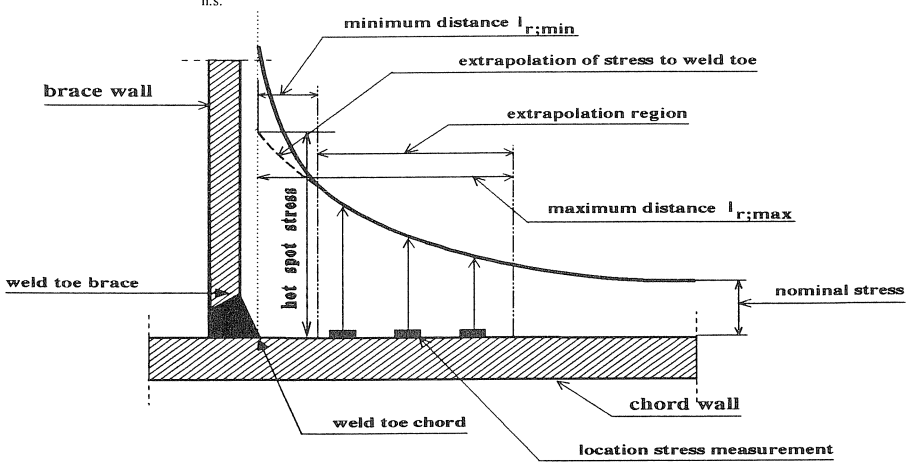

Fig. 3. Definition on hot spot stress.

Extrapolation region

The extrapolation region is defined by a specified minimum and maximum distance from the weld toe of the joint (see figure 3). The region is defined in such a way that the effects of the global geometry of the weld (flat, concave, convex) and the condition at the weld toe (angle, undercut) are not included in the hot spot stress. Therefore, the first point of

extrapolation should be outside the influence area of the weld. The extrapolation region according to the recommendations given by ECSC WG III are summarized in table 1.

Chord member		Brace member
crown location (cc)	saddle location (cs)	crown location (bc) and saddle location (bs)
$l_{r;min} = 0.4 \cdot t_o$ $l_{r;min} \geq 4$ mm*		$l_{r;min} = 0.4 \cdot t_1$ $l_{r;min} \geq 4$ mm*
$l_{r;max} = 0.4 \cdot (r_1 \cdot t_1 \cdot r_0 \cdot t_0)^{1/4}$	$l_{r;max} = 5°$	$l_{r;max} = 0.65 \cdot (r_1 \cdot t_1)^{1/2}$

* Minimum distance given by IIW.

Table 1. Extrapolation region (with linear extrapolation of the stresses to the weld toe) recommended by ECSC WG III [*F3*]. Distance l_r measured from the weld toe location in a direction perpendicular to the weld toe (chord member locations) and parallel to the axis of the brace member (brace member locations).

Stress concentration factor
(parameter study on isolated joints)
The hot spot stresses are determined around the connection of the reference brace member '*a*' to the chord member (see figures 4 and 5). The stress concentration factor (SCF) for an isolated joint loaded individually by separate chord member loads $F_{ch;ax}$, $M_{ch;ip}$ and $M_{ch;op}$ and brace member loads $F_{br;ax}$, $M_{br;ip}$ and $M_{br;op}$ is defined as:
for the chord member loads:

$$SCF_{m.n.o} = \frac{\sigma_{h.s.;m.n.o}}{\sigma_{ch;nom;o}}$$ and

for the brace member loads:

$$SCF_{m.n.o} = \frac{\sigma_{h.s.;m.n.o}}{\sigma_{br;nom;o}}$$ with:

m = *Chord member at the connection of brace 'a', or brace 'a' member.*
n = *Location around the perimeter of the brace 'a' to chord intersection, e.g. crown, saddle or inbetween.*
o = *Type of loading (axial, in plane bending or out of plane bending).*

Stress concentration factor
(numerical calibration of tested joints placed inside a structure)
For the multiplanar KK joints in the triangular lattice girders tested (described in chapter 4), the stress concentration factor (SCF) includes the influence of all chord and brace member loads as follows:

$$SCF_{m.n.o} = \frac{\sigma_{h.s.;m.n.o}}{\sigma_{extrap;nom}}$$ with:

m = *Chord member or a brace member.*
n = *Location around the perimeter of a brace to chord intersection, e.g. crown, saddle or inbetween.*
o = *Combination of all chord and brace member loads.*
$\sigma_{extrap.;nom}$ = *Extrapolated nominal stress of the in-plane axial tensile loaded brace member.*

Total hot spot stress based on stress concentration factors

The total hot spot stress $\sigma_{h.s.;m.n}{}_{total}$ for an isolated joint under combined loads at a particular location around the brace to chord connection, is defined as the superposition of the individual hot spot stress components $\sigma_{h.s.}$ according to the following equations:

$$\sigma_{h.s.;m.n}{}_{total} = \sigma_{h.s.;m.n}{}_{chord\ loads} + \sigma_{h.s.;m.n}{}_{brace\ loads}$$

with for the chord member loads (reference loads exist only):

$$\sigma_{h.s.;m.n}{}_{chord\ loads} = SCF_{m.n;F}{}_{ch;ax} \cdot \sigma_{nom;F}{}_{ch;ax} + SCF_{m.n;M}{}_{ch;ip} \cdot \sigma_{nom;M}{}_{ch;ip} + SCF_{m.n;M}{}_{ch;op} \cdot \sigma_{nom;M}{}_{ch;op}$$

and for the brace member loads (reference loads and carry-over loads exist):

$$\sigma_{h.s.;m.n}{}_{brace\ loads} = \sum_{i=1}^{p} SCF_{m.n;F}{}_{br;ax;i} \cdot \sigma_{nom;F}{}_{br;ax;i} + SCF_{m.n;M}{}_{br;ip;i} \cdot \sigma_{nom;M}{}_{br;ip;i} + SCF_{m.n;M}{}_{br;op;i} \cdot \sigma_{nom;M}{}_{br;op;i}$$

with: i = *The brace number (defined as 'a', b, c, d etc. shown in figures 4 and 5).*
p = *The total number of connecting braces.*

Joint type

Different types of welded tubular uniplanar and multiplanar gap joints are considered in the parameter study on SCFs and SNCFs (chapter 6). The joints are grouped into two parts, namely:

- *Joints with braces perpendicular to the chord axis (T, X, TT and XX joints). (See figure 4).*
- *Joints with braces inclined to the chord axis (Y, K and KK joints). (See figure 5).*

Uniplanar joint

A uniplanar joint is a type of joint with braces lying in the same plane along the chord axis. The considered uniplanar joints are: T, Y, X also called TT (180°), K and KK (180°) joints.

Multiplanar joint

A multiplanar joint is a type of joint with braces lying in different planes along the chord axis. The considered multiplanar joints are: TT (45°, 70°, 90°, 135°), KK (60°, 90°) and XX (90°-180°-270°) joints.

Reference effect

The reference effect on SCFs is caused by:

- *Loads on the reference brace, identified as brace member 'a', i.e. SCFs due to* $F_{br;ax;a}$, $M_{br;ip;a}$ *and* $M_{br;op;a}$
- *Loads on the chord member, i.e. SCFs due to* $F_{ch;ax}$, $M_{ch;ip}$ *and* $M_{ch;op}$

The reference brace shown in figures 4 and 5, is the brace for which SCFs around the connection to the chord member for all load cases considered are determined.

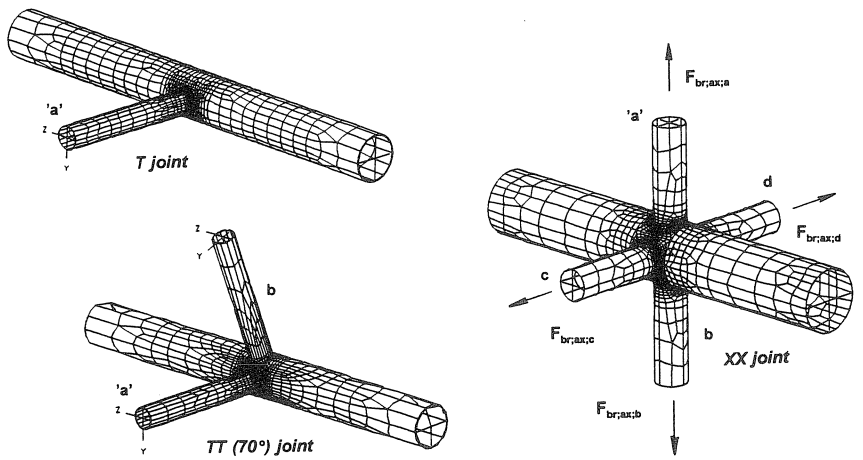

Fig. 4. Joints with braces perpendicular to the chord axis.

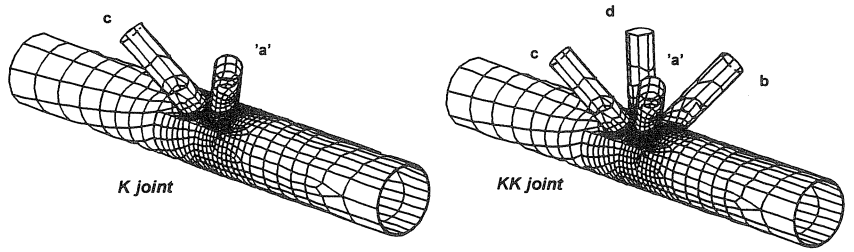

Fig. 5. Joints with braces inclined to the chord axis.

Carry-over effect

The carry-over effect on SCFs around the connection of brace member '*a*' to the chord member is caused by loads on the other (carry-over) brace members, identified as brace member *b*, *c*, *d* etc., i.e. SCFs caused by:

- *Axial forces:* $F_{br;ax;b}$, $F_{br;ax;c}$, $F_{br;ax;d}$ *etc.;*
- *In-plane bending moments:* $M_{br;ip;b}$, $M_{br;ip;c}$, $M_{br;ip;d}$ *etc.;*
- *Out-of-plane bending moments:* $M_{br;op;b}$, $M_{br;op;c}$, $M_{br;op;d}$ *etc.*

Locations of interest on SCFs

The locations of interest for the SCF determination (around the connection of brace member *'a'* to the chord member) are shown in figure 29. For the parameter study, a total of 16 locations for the SCF determination are considered; namely 8 locations on the chord member and 8 locations on the reference brace *'a'* member.

$S_{r_{h.s.}}$ - N_f curve

The $S_{r_{h.s.}}$ - N_f curve gives for a specified probability of failure, the hot spot stress range to the number of cycles to fatigue failure. The hot spot stress range is given on the vertical axis and the number of cycles to fatigue failure on the horizontal axis, both on a logarithmic scale as illustrated in figure 6.

Thickness effect

The fatigue strength is dependent upon the wall thickness of the member considered, and tends to decrease with increasing wall thickness. This is called the thickness effect. The thickness effect is attributed to three sources, namely *geometrical effects*, *statistical effects* and *technological effects* [*F58*]. Based on results of ECSC and CIDECT sponsored research programmes, the following thickness corrections for hollow section joints have been proposed for uniplanar joints [*F12*]:

- For wall thicknesses of 4 to 16 mm:

$$S_{r_{h.s.;t = 4\text{-}16}} = S_{r_{h.s.;t = 16}} \cdot (16/t)^{0.11 \cdot \log N_f}$$

- For wall thicknesses of 16 mm and more:

$$S_{r_{h.s.;t \geq 16}} = S_{r_{h.s.;t = 16}} \cdot (16/t)^{0.30}$$

For thicknesses below 4 mm, no guidance is given, since the fatigue behaviour may be adversely affected by the welding imperfections at the root of the weld.

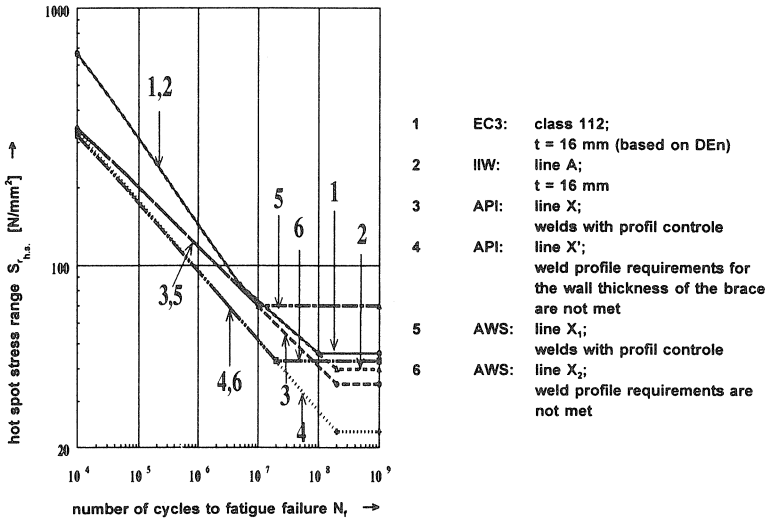

Fig. 6. Major $S_{r_{h.s.}}$ - N_f curves for hollow section joints. (Butt weld).

2. LITERATURE REVIEW

Literature studies have been carried out on the following main aspects:

1 *Fatigue behaviour of welded uniplanar and multiplanar tubular joints.*
2 *Design codes and recommendations on the fatigue behaviour of welded tubular joints.*

2.1 *Fatigue behaviour of welded uniplanar and multiplanar tubular joints*

d. Back [*F3*, *F4*, *F5*, *F6*]
Data on SCFs (or hot spot stresses) and fatigue life for uniplanar as well as multiplanar joints are published. The data is mainly obtained from tested steel models. Furthermore, based on a large number of tested steel specimens, results on the influence of weld improvement techniques, plate thickness and environmental conditions on the fatigue behaviour of joints are published.

Efthymiou [*F13*]
SCF formulae and generalized influence functions based on FE analysis for use in fatigue analysis of tubular joints are given.

Irvine [*F20*]
Different approaches on the determination of SCFs are compared. This includes work carried out on steel models, acrylic models (using gauges and photoelastic technique) and numerical FE models using shell elements without the weld shape included.

Lalani [*F26*]
Data on the fatigue behaviour is reviewed and assessed. An extensive reliability assessment of various SCF equations using test results from large scale steel model tests is carried out. The SCF equations given by Kuang et al [*F24*], Gibstein [*F15*], Wordsworth and Smedley [*F62*], UEG [*F56*], Efthymiou [*F13*] and Marshall [*F30*] have been screened, which shows that the SCF formulae giving the best correlation to test data are those given by Wordsworth and Smedley and Efthymiou. Attention on the correlation between numerical and experimental work is mainly given to the chord saddle locations only.

Kurobane [*F25*]
A large number of reports on various topics are published, such as fatigue design of welded joints in trussed legs of offshore jack-up platforms, research on fatigue strength of thin walled tubular joints, ultimate limit state criteria for design of tubular K joints, investigation into estimation of fatigue crack initiation life in tubular joints, fatigue tests of tubular T and K joints and developments in the fatigue design rules in Japan.

Marshall [*F30*, *F31*, *F32*]
Work on the fatigue design of welded tubular connections, which is implemented in the American API and AWS codes is presented. Topics covered are failure modes for offshore structures, problems in long-life fatigue assessment for fixed offshore structures, fatigue analysis of dynamically loaded offshore structures and recent developments in the fatigue design rules in the USA .

Niemi [*F34*]
Published recommendations concerning stress determination for fatigue analysis of welded components .

Packer [*F35*]
A "*Design guide for hollow structural section connections*" is published together with Henderson, which is a compendium of current design information directed to practicing structural engineers, on the topic of Hollow Structural Section (HSS) connections.

Puthli [*F36*]
Some publications, which have formed a basis for the present work are: "*Numerical and experimental determination of strain (stress) concentration factors of welded joints between square hollow sections*" and "*Geometrical non-linearity in collapse analysis of thick walled shells with application to tubular steel joints*" .

Wardenier [*F58, F59*]
Papers, reports and design guides on a large number of topics are used for the present work. These include "*Fatigue design of tubular joints*", and the "*Design guide for circular hollow section (CHS) joints under predominantly static loading*", which is published together with Kurobane, Packer, Dutta and Yeomans.

v. Wingerde [*F60, F61*]
Based on knowledge gained from experimental and numerical work on square hollow sections, design recommendations and comments regarding the fatigue behaviour of hollow section joints are given.

Wordsworth and Smedley [*F64*]
SCF formulae for the chord crown and saddle locations are developed on the basis of tested small scale acrylic models and FE analyses. The formulae cover uniplanar gap joints. The SCFs for the brace side are related to the SCFs for the chord side by means of a function: $SCF_{brace} = 1 + 0.63 \cdot SCF_{chord}$.
The SCFs obtained from the SCF formulae, are the values at the toe and heel of the intersecting tubular members. For T and TT (180°) joints, they recommended that the SCF for the chord member locations is corrected for the leg length of the weld as follows:

$$SCF_{corrected} = \frac{SCF_{formulae}}{(1 + \frac{x}{T})^{0.33}}$$ with:

x = The leg length of the weld on the chord side;
T = The wall thickness of the chord member.

2.2 *Design codes and recommendations on fatigue behaviour of welded tubular joints*

The developments of fatigue research on welded tubular joints are reflected in design codes, such as IIW [*F22*], DEn [*F9*], EC3 [*F12*], AWS [*F2*] and API [*F1*]. For the mentio-

ned design codes, recommendations on how hot spot stresses should be determined, which parametric SCF formulae to use, weld profile effect on the fatigue strength, and the influence of secondary bending moments on fatigue strength are summarized in table 2.

Recommendations	IIW	DEn	EC3	AWS	API
Determining hot spot stresses. *Type of stress*: - principal stresses; - stresses perpendicular to the weld toe.	x	x	x	x	x
Determining hot spot stresses. *Extrapolation method*: - no extrapolation procedure; - linear extrapolation; - non-linear extrapolation.	*(1)	*(2) *(2)	*(1)	*(3)	*(3)
Parametric SCF formulae: - uniplanar joints; - multiplanar joints.	*(4)			*(5)	*(5)
Weld type and profile effect on the fatigue behaviour.		30%(6)	classes(7)	*(8)	*(8)
Secondary bending moments.			coefficients (9)		

(1) No clear guidance is given on the location of the extrapolation region and the type of extrapolation method.

(2) A linear extrapolation is used for T and X joints, and a non-linear extrapolation is recommended for Y and K joints.

(3) The hot spot stress is taken as the stress adjacent and perpendicular to the weld toe. Therefore, no extrapolation is carried out.

(4) SCF graphs are given for uniplanar T, Y, X, K and N joints. These formulae are fairly provisional.

(5) The AWS and API codes recommend using the formulae given by Marshall [*F30*], which are based on an analogy of the behaviour of a circular cylinder subjected to uniform circumferential loads established by Kellogg.

(6) A 30% higher fatigue strength is allowed for a grounded weld toe.

(7) The influence of weld type and profile on the fatigue behaviour is included using classes. (Comments on this are among others given by [*F60*, *F61*]).

(8) In the AWS and API codes the hot spot stress at $N_f=2\cdot10^6$ range from 79 N/mm^2 to 100 N/mm^2 for an improved weld profile.

(9) EC3 gives factors to account for the secondary bending effects if these are not calculated. The stress ranges obtained for axial loading should be multiplied by these factors if the secondary bending moments are not included in the analysis.

Table 2. Design codes: recommendations on fatigue of welded tubular joints.

As shown in table 2, no systematic recommendations exist, which results in different values particularly for SCFs. Inconsistency in determining hot spot stresses exists. For instance according to AWS and API, the SCFs should be based on hot spot stresses adjacent and perpendicular to the weld toe locations, without the use of an extrapolation method. The IIW and EC3 specify that hot spot stresses should be based on the use of an extrapolation method perpendicular to the weld toe. However, no clear guidance is given on the location of the extrapolation region and the type of extrapolation method. It is also not always clear to which location the extrapolation needs to be carried out. Some

identified locations to which extrapolation of stresses take place are:

- *The intersection of the outer surface of the connecting member walls. (For tested small scale acrylic models without the weld shape included);*
- *The fictitious intersection of the midplanes of the connecting member walls. (Numerical investigation without the weld shape included in the FE model);*
- *The weld toe location.*

3. NUMERICAL MODELLING OF WELDED TUBULAR JOINTS

3.1 *General*

The fatigue design of structures containing welded tubular joints requires knowledge of the joint stiffness (flexibility) behaviour and the stress concentration factors. These can be obtained experimentally by the use of test specimens, or by numerical work using finite element (FE) analyses. However, because of high costs using solely experimental methods, investigations based on numerical work together with experimental calibration are more widely accepted nowadays. The numerical modelling of welded tubular joints puts certain obligations on the use of finite element programs, because results can be obtained without having an insight of the actual behaviour. Also, for the problem to be solved, in case of inexperienced use, the analysis results can have either a low accuracy or e.g. high computer costs. As no systematic guidance concerning the numerical modelling of welded tubular joint flexibility behaviour and welded tubular joint stress concentration factors exists, a study is carried out on several main aspects which affect the numerical results (and computer costs).

General purpose FE programs being used

For the numerical modelling of tubular joints, a (pre-processing) FE package is essential. Several of such packages are available around the world, like *Diana*, *Marc*, *I-Deas*, *Patran*, *Ansys*, *Sesam* and *Abaqus*. Each of them have their own specific (dis)advantages, like conditions of use, hardware required, user-friendliness, available types of finite elements and element generation of joints. After comparison of the (dis)advantages of the above mentioned packages, the decision was made to use the module *Pretube* of the Norwegian *Sesam* package and the module *Supertab* of the American *I-Deas* package for the numerical modelling of welded tubular joints.
The analysis was carried out on a Sun Sparc station and using the general purpose finite element computer program *Diana* and the solver module of the *I-Deas* package. There is an interface linking *Diana* to *I-Deas*. However, as no link exist between *Pretube* (*Sesam*) and *I-Deas*, an interface program was developed between the *Sesam* and *I-Deas* package.

3.2 *Aspects of importance for modelling*

For numerical modelling, correct choices have to be made on the use of *element type*, *mesh refinement*, *integration scheme*, *weld shape* modelling and *boundary conditions*. No standard answer exists, because it entirely depends on the combination of geometry (thin

walled, thick walled), type of forces (membrane, plate bending), analysis (linear, non-linear) and the desired accuracy (global load distribution, local stress pattern).
A study has been carried out on the effect of numerical modelling on tubular joint stress concentration factors [*F46*]. From this study, several conclusions have been made (chapter 3.3.2), which should be considered when linear-elastic flexibility and stress concentration factors of tubular joints are analysed numerically.

Computational aspects of finite element (FE) modelling

The aim here is not to discuss theoretical aspects that can be obtained from textbooks [*N1-N4*]. However, brief details are given as background information.

Element types
Depending on the FE package used, various types of elements, such as membrane elements, plate bending elements and solid elements, are available. For each type of element, differences in topology (triangular, quadrilateral) and order (linear, parabolic, cubic) exist. Using the same number of elements, a joint modelled with elements having midside node(s) gives generally much more accurate analytical results compared to a joint modelled with elements having corner nodes only.
Mesh refinement
Generally, increasing the number of elements (mesh density), in which the elements meet all compatibility and equilibrium conditions, gives more accurate analytical results. However, computer costs also increase.
Integration scheme
In the practical use of the numerical integration procedures, for finite element analyses, basically two questions arise. Namely, what kind of integration scheme is to be used and what order of integration is to be selected. The correct choice for the problem to be solved is important, because firstly, the cost of analysis might increase when a high order integration is employed, and, secondly, using a different integration order, the results can be greatly affected. These considerations are particularly important for the complex three dimensional behaviour of welded tubular joints.

3.3 *Numerical modelling of tubular joint SCFs*

From literature studies, it has been found that recommendations for the numerical SCF determination of uniplanar as well as multiplanar tubular joints are limited [*F34*]. There is no standard guidance, which has led to a divergence in the numerical methods in SCF determination being used. Differences on the effect of numerical modelling on tubular joint SCFs exist, because of:

- *The use of different types of elements, mesh refinements and boundary conditions.*
- *FE modelling with and without the weld shape included.*
- *Disregarding the effect of a chosen integration scheme for the numerical integration procedures on SCFs.*

The effect of various aspects like the type of element, mesh refinement, integration scheme and weld shape on numerical modelling for tubular joint SCFs are considered in this chapter.

3.3.1 Effect of modelling on tubular joint SCFs

For the determination of SCFs, various methods of numerical modelling are applied. For a proper understanding of the effects of the various methods of numerical modelling on SCFs, knowledge regarding the definition of hot spot stress from which SCFs are obtained, is necessary. Chapter 1.3.2 explains the definition on hot spot stress. A comparison of the various methods of numerical modelling on SCFs has been carried out for a multiplanar KK and XX joint with joint parameters as summarized in table 3.

Joint	Joint parameters						Chord dimension [mm]
	γ	β	τ	α	φ_{ip}	φ_{op}	
KK	24	0.40	1.00	8.5	60°	180°	ø 400.0 · 8.33
XX	20	0.30	1.00	10.0	90°	90°-180°-270°	ø 406.4 · 10.00

Table 3. Joints considered for a comparison of the various methods of numerical modelling on SCFs.

Since the results of the comparisons were found to be the same for the KK and XX joints investigated, the results are presented for one type of joint, either KK or XX.

Influence of element type on SCFs

The following four types of FE models have been compared:

FE model a: *4-n thin shell elements; weld shape not included and SCFs defined at the intersection of the midplanes of the connecting walls.*

FE model b_1: *8-n thin shell elements; weld shape not included and SCFs defined at the intersection of the midplanes of the connecting walls.*

FE model b_2: *8-n thin shell elements; weld shape not included and SCFs defined at the fictitious weld toe location.*

FE model c: *8-n solid elements; weld shape included and SCFs defined at weld toe position.*

FE model d: *20-n solid elements; weld shape included and SCFs defined at weld toe position.*

The SCFs are determined using the extrapolation method and region as described in chapter 6.2. Because FE model *d* can be regarded as the most accurate FE model (as the weld shape is included and the element type has a high degree of accuracy [*N2*, *N4*]), the results of FE models *a*, b_1, b_2 and *c* have been compared to those of FE model *d* using the same mesh refinement. For the investigated KK joint with the reference brace '*a*' (see figure 5) loaded by a nominal stress of 1 N/mm^2 and bending moments in the chord compensated, the stress pattern at the crown (heel) position of the chord member is given in figure 7. For the influence of the investigated types of elements on the stress distribution (SCFs) it is found that small differences on SCFs for the brace member locations and large differences on SCFs for the chord member locations exist. Especially for the chord crown location large differences in the stress gradient to the weld toe position occurs. The reason for the different influence of the element types on the SCF results for the chord and brace member locations is caused by the numerical formulation of the element types, especially in case of shear deformation and bending stresses, which are more prevalent in the chord member. From figure 7, it is obvious that ignoring the weld and defining SCFs at the intersection of the midplanes of the member walls leads to entirely different results

(especially for the brace member differences up to 300% are expected). This is because although the distance between this intersection point and the weld toe position is small, the stress gradients are high. If this distance is taken into account, in other words, if the SCFs are calculated at the fictitious weld toe locations, a considerable improvement, especially for the brace member, arises. Considering the degree of element accuracy (using the same number of elements, 20-n solid elements gives much more accurate results compared to 8-n solid elements), the results on SCFs for the investigated element types and the information given by [*NI-3*], the use of 20-n solid elements with the weld shape included and determining the SCFs at the weld toe location is recommended.

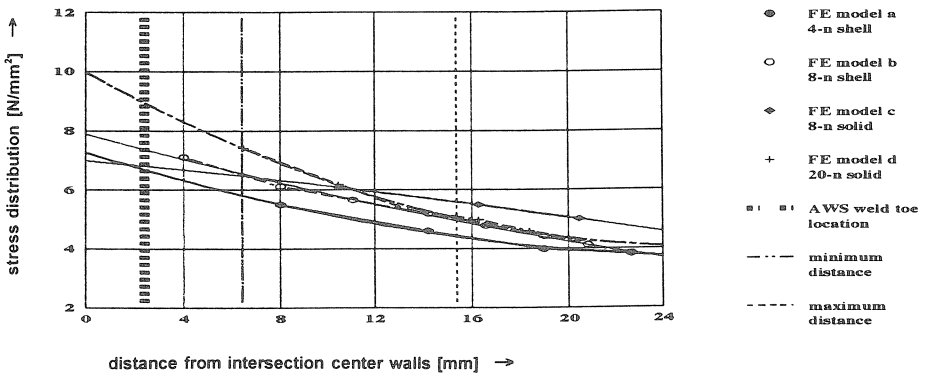

Fig. 7. Stress distribution for the cc;1 location of a KK joint.

Influence of mesh refinement on SCFs

For the influence of changes in mesh refinement on SCFs, the variation is mainly concentrated at the locations where SCFs are defined. As an illustration of this, figure 8 shows the mesh refinements considered for the KK joint investigated, using FE model *d*.
The corresponding number of nodes and elements are given in table 4.

Mesh refinement : KK joint	Nodes	Elements
mf_1	15171	2227
mf_2	10323	1557
mf_3	8238	1330

Table 4. Investigated mesh refinements regarding SCFs (see also figure 8).

For the mesh refinements mf_1-mf_3 as shown in figure 8, the analysed SCFs for the chord member of the KK-joint using FE model *d* are shown in figure 9. The SCFs are given for fifteen load cases (with compensating moments as described in chapter 6.2.7), namely:
Three chord member loads : $F_{ch;ax}$; $M_{ch;ip}$ and $M_{ch;op}$.
Twelve brace member loads : $F_{br;ax;a\text{-}d}$; $M_{br;ip;a\text{-}d}$ and $M_{br;op;a\text{-}d}$.

Generally, an increase of mesh refinement, when the element type meets all consistency

criteria (this is the case for 20-n solid elements), results in a convergence of deformation, stresses and strains to an optimum value [*NI*]. Therefore, refinement of the mesh should be such that any further refinement does not result in a substantial change of the stress distribution (outside the notch effect area). Comparison of the SCF results for the three analysed mesh refinements justifies the use of mesh refinement mf_2. Using mf_2, the length of the 20-n solid element measured along the intersection area is approximately 1/16 of the total length of the intersection area.

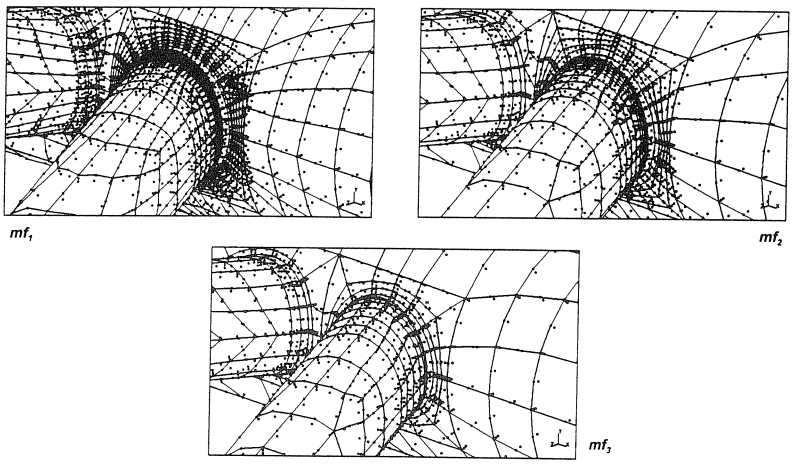

Fig. 8. Investigated mesh refinements mf_1-mf_3 for the determination of SCFs of a KK joint.

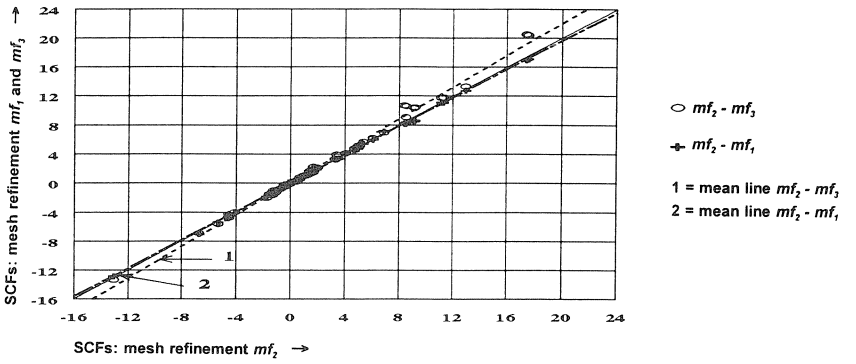

Fig. 9. Influence of mesh refinement on SCFs for the chord member locations 1-8 of a KK joint.

Influence of the integration scheme on SCFs

Regarding the effect of the integration scheme on the SCFs, two types of FE models have been studied, namely:

FE model d: *Joint modelled with 20-n solid elements, and the weld shape included. Variations in integration scheme are: int_1 (2x2x2) and int_4 (3x3x3).*

FE model e: *Joint modelled with 8-n shell elements and the weld shape included by 20-n solid elements. Between the shell and solid elements, 13-n transition elements have been used. The variations in integration scheme for the shell elements are int_1 (2x2x2); int_2 (2x2x3); int_3 (2x2x5) and int_4 (3x3x3).*

The SCFs for balanced axial loads on the vertical brace members *'a'* and *b* (load case $F_{br;ax;a,b}$ as shown in figure 4), and balanced loads on the horizontal brace members *c* and *d* (load case $F_{br;ax;c,d}$) of the XX joint, using the various integration schemes int_{1-4} are together with test results [*F47*] summarized in table 5. The test results used are described in chapter 6.5.5.

XX joint γ = 20 β = 0.50 τ = 1.00	SCFs						
	20-n solid + 8-n shell + 13-n transition				20-n solid		test results [*F47*]
FE model	Load case: vertical braces *'a'* and *b* balanced axial loaded ($F_{br;ax;a,b}$)						
Integration scheme	int_1 2x2x2	int_2 2x2x3	int_3 2x2x5	int_4 3x3x3	int_1 2x2x2	int_4 3x3x3	
cs;3,7	20.7	35.7	35.7	33.0	33.7	33.3	30.7
cc;1,5	1.7	1.6	1.6	2.0	1.9	2.0	2.2
bs;3,7	9.8	14.1	14.1	14.1	14.7	16.0	14.2
bc;1,5	-0.4	0.0	0.0	0.0	0.0	- 0.1	0.4
	Load case: horizontal braces *c* and *d* balanced axial loaded ($F_{br;ax;c,d}$)						
cs;3,7	-15.3	-25.7	-25.7	-23.2	-24.0	-23.7	-25.6
cc;1,5	0.3	1.5	1.5	0.9	0.8	0.8	0.8
bs;3,7	-7.1	-10.6	-10.6	-10.3	-11.2	-12.2	-13.6
bc;1,5	1.0	0.7	0.7	0.7	0.6	0.7	0.1

Table 5. The effect of integration schemes int_{1-4} on SCFs.

Using the recommended 20-n solid elements, table 5 shows small differences in SCFs for the alternative integration schemes and a reasonable agreement with the test results. Therefore, the use of integration scheme 2x2x2 is recommended.
For shell elements the reduced integration scheme 2x2x2 gives much lower SCFs compared to other integration schemes, and seems to be inaccurate.

Influence of weld shape on SCFs
The influence of weld shape on SCFs has been studied using three types of weld shapes, as shown in figure 10. The first weld shape with a weld footprint L_{w1} ($\approx 1.3 \cdot t_1$) is modelled according to the AWS specifications for a weld accessible from one side. For the second and the third weld shape, only increases in length of the chord weld footprint have been made, so that $L_{w2} = 1.5 \cdot L_{w1}$ and $L_{w3} = 2.0 \cdot L_{w1}$. In an identical way as described for the influence of element type on SCFs caused by a brace member load $F_{br;ax;a}$ (with compensating moments), the stress pattern using FE model *d* for the three alternative types

of weld shapes considered is given in figure 11. Figure 11 shows, that an increase of the chord weld footprint for the geometry and joint parameters considered leads to a substantial increase of the SCFs for the brace member (and decrease for the chord member). As illustrated by the SCFs for the brace member locations (constant weld toe location for the three types of weld shapes considered), the SCF differences are mainly caused by differences in the shape of the weld toe (angle between the weld and the member).

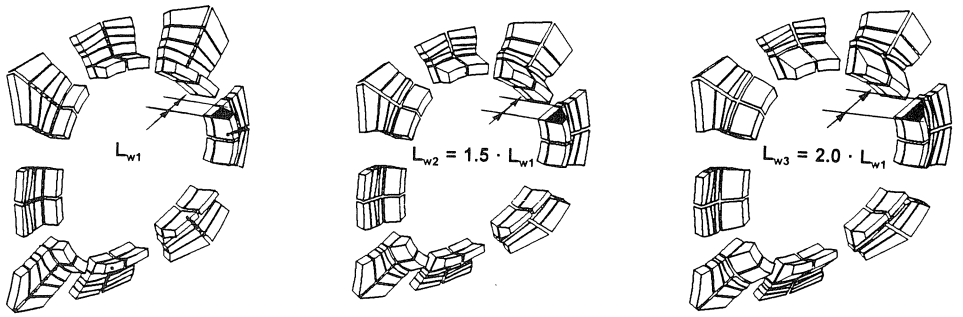

Fig. 10. Different types of weld shapes considered.

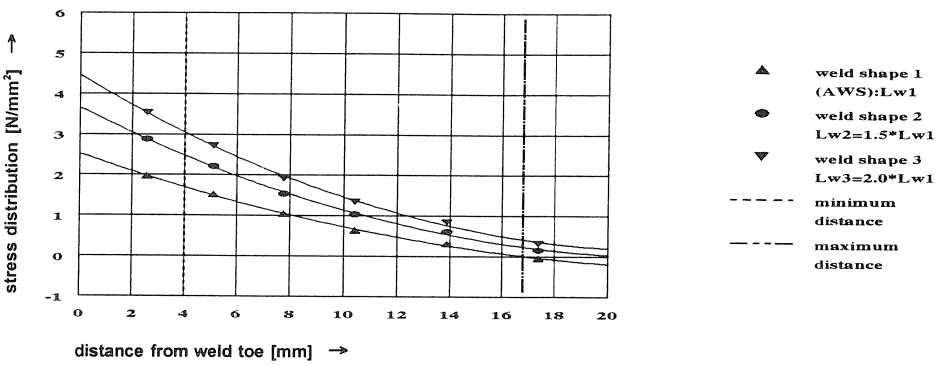

Fig. 11. Influence of weld shape on the stress distribution for the bc;5 location of a KK joint.

Influence of boundary condition on SCFs

For the sake of equilibrium the (chord) member(s) should be adequately supported. This is particularly true for unbalanced load cases. At the supports, boundary conditions arise, which cause reaction forces and moments in the members.

The effect of boundary conditions (*bdc*) on SCFs has been studied using three alternatives, namely:

bdc_1. SCFs determined with chord member ends pin-ended.

bdc_2. SCFs determined with chord member ends fully-clamped.

bdc_3. SCFs determined with chord member ends pin-ended and a correction applied to the SCFs to account for the forces and moments introduced. A method on this is given in chapter 6.2.7.

Using FE model *d*, for the three alternative boundary conditions bdc_{1-3} considered, results on SCFs for the chord member locations of a KK joint loaded by the load cases $F_{br;ax;a}$, $F_{br;ax;b}$, $F_{br;ax;c}$ and $F_{br;ax;d}$ are given in figure 12. Large differences in SCFs are found for the three alternative boundary conditions bdc_{1-3} considered. The magnitude of the differences depends on the load case and joint considered and on the relevant location between crown and saddle. The influence of the boundary conditions on the SCFs from the carry-over effects (SCFs caused by brace member loads $F_{br;ax;b,c,d}$) is much larger than for the reference effects (SCFs caused by brace member load $F_{br;ax;a}$), because the former effect is smaller than the latter, while the effect due to moments from boundary conditions can be the same.

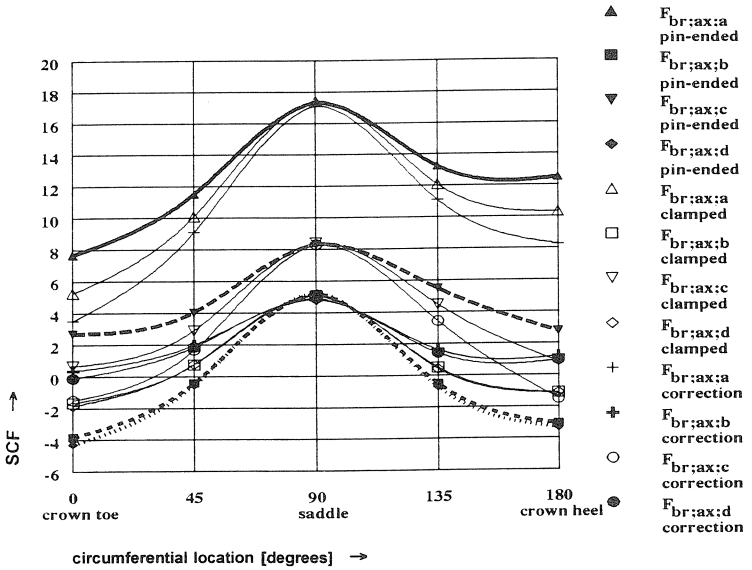

Fig. 12. Influence of boundary conditions on SCFs for the chord member of a KK joint.

3.3.2 Conclusions on modelling for tubular joint SCFs

It is found that the results of numerical models of tubular joint SCFs are greatly influenced by the method used, which causes problems in the interpretation of numerical FE results (as well as experimental results). From the observations obtained, the following conclusions are made:

Position SCF determination:

- *SCFs should always be determined at the weld toe position and not at the intersection of the member wall midplanes or at the intersection of the member wall outer surfaces.*

Element type:

- *Modelling the weld shape improves the accuracy of SCFs largely.*
- *Using solid elements to model the weld area is recommended, as it is a more realistic representation compared to model the weld area using shell elements.*
- *Because of high accuracy requirements, the use of 20-n solid elements is recommended above 8-n solid elements.*
- *The use of transition elements is disadvised. Because these types of elements increase rather than decrease computer costs. Thus a combination of solid and shell elements should not be used.*

Mesh refinement:

- *The length of the 20-n solid element, measured along the intersection area, should be less than 1/16 of the total length of the intersection area.*

Integration scheme:

- *When using 20-n solid elements, the integration scheme 2x2x2 is preferred to 3x3x3. This because an investigation on numerical modelling for tubular joint flexibility shows that the 3x3x3 integration scheme underestimates the joint flexibility behaviour largely.*

Boundary condition:

- *It is preferable to compensate for the influence of boundary conditions when determining SCFs. This is particularly true in case of multiplanar joints (having carry-over effects). However, such an approach is not always possible to simulate experimental work, so that SCFs particularly at crown locations include the influence of boundary conditions.*

4. EXPERIMENTAL INVESTIGATION ON THE FATIGUE BEHAVIOUR OF MULTIPLANAR TUBULAR JOINTS IN LATTICE GIRDERS

Nearly all published experimental work on the fatigue behaviour of welded tubular joints carried out so far has been on uniplanar joints. On the fatigue behaviour of multiplanar KK joints, which are one of the most common types of joints e.g. in offshore structures, limited experimental work on SCFs using acrylic test specimen without including the weld have been carried out by Lloyd's Register of Shipping. The lack of sufficient information on SCFs is because of the complexity of such joints and the high costs of adequately strain gauging experimental steel models.

4.1 *Experimental investigation*

To investigate the fatigue behaviour of tubular multiplanar joints in lattice girders, experiments have been carried out on four different multiplanar triangular lattice girders. The configuration and joint parameters of the tested girders are given in figures 13 and 14 and table 6. For the joints of the lower chord of girders 5 to 8, measurements to determine the hot spot strains $\varepsilon_{h.s.}$ have been carried out. The girders have been subjected to fatigue loading until each joint of the lower chord has failed in succession.
Based on this investigation, a $S_{r_{h.s.}}$ - N_f design curve is determined for multiplanar KK joints.

Type of multiplanar joint	Joint parameters		
	chord ø193.7; τ = 0.50		
	γ	β	
gap + 100% overlap	12	0.40	tested girder 5
gap + 100% overlap	6	0.40	tested girder 6
gap + 50% overlap	12	0.60	tested girder 7
gap + 50% overlap	6	0.60	tested girder 8

Table 6. Tested girders 5, 6, 7 and 8.

Details of Test Specimens

The circular hollow sections used for the girders are hot finished, with a steel grade S235 in accordance with EN 10210-1. The dimensions of the members as well as the welds at the crown and saddle positions for the main joints have been measured. The material properties f_y (minimum yield strength), f_u (tensile strength) and ε_u (elongation) of the hollow sections have been determined with tensile tests (dp5). The overlap joints in girders 5 and 6 have a 100% overlap and in the girders 7 and 8 a 50% overlap. The angle in transverse direction to the chord axis between the braces φ_{op} is 60°. The eccentricity (*e*) between the chord axis and the intersection of the brace axis is zero for the gap joints in girders 5 and 6. For the joints in girders 7 and 8, the eccentricity is 48 mm, which avoids an out-of-plane overlap. Figures 13 and 14 show the relevant details. The girders are welded with rutile electrodes in accordance with the standards ASME SFA-5.1 and ISO 2560. Figure 15 shows the weld preparation, the welding details and the welding sequences. The test rig is shown in figure 16. A load F on the girder is applied by means of a jack. The jack load is measured with a dynamometer fitted on the jack. All the girders are tested first under a static loading, followed by a sinusoidal constant amplitude fatigue loading with a load ratio $R = F_{min} / F_{max} = 0.1$ and a frequency of 1 Hz. Failure of the joint is assumed to have occurred when a through wall crack is observed.

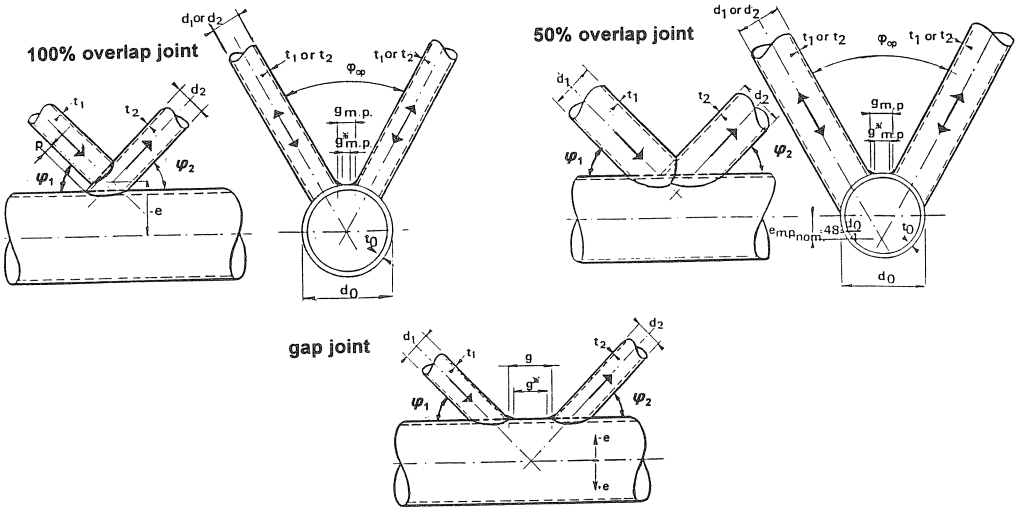

Fig. 13. Configuration of basic types of tested joints.

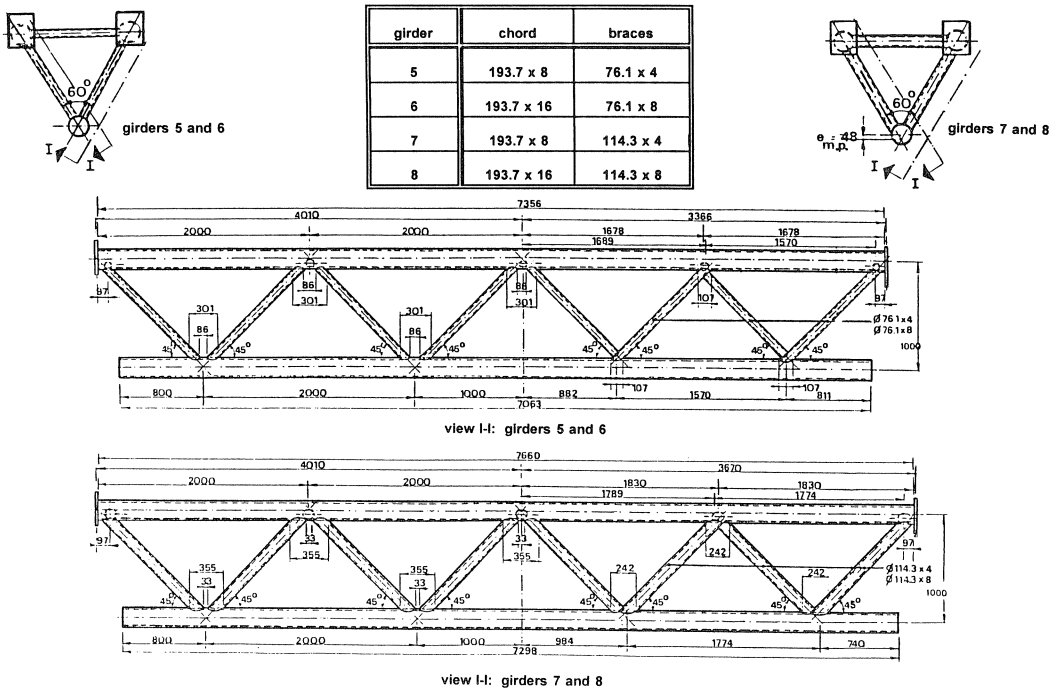

girder	chord	braces
5	193.7 x 8	76.1 x 4
6	193.7 x 16	76.1 x 8
7	193.7 x 8	114.3 x 4
8	193.7 x 16	114.3 x 8

Fig. 14. Configuration of tested girders 5, 6, 7 and 8.

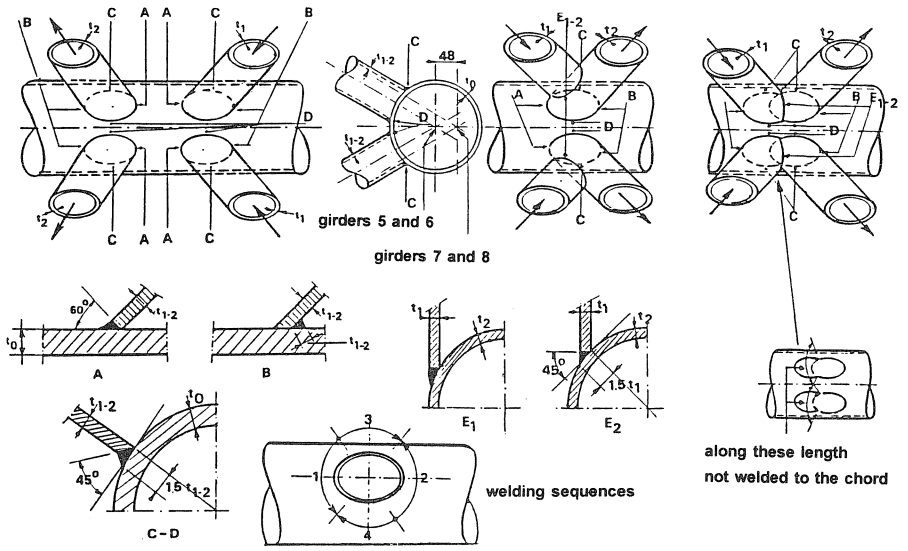

Fig. 15. Welding details and welding sequences for the tested girders 5, 6, 7 and 8.

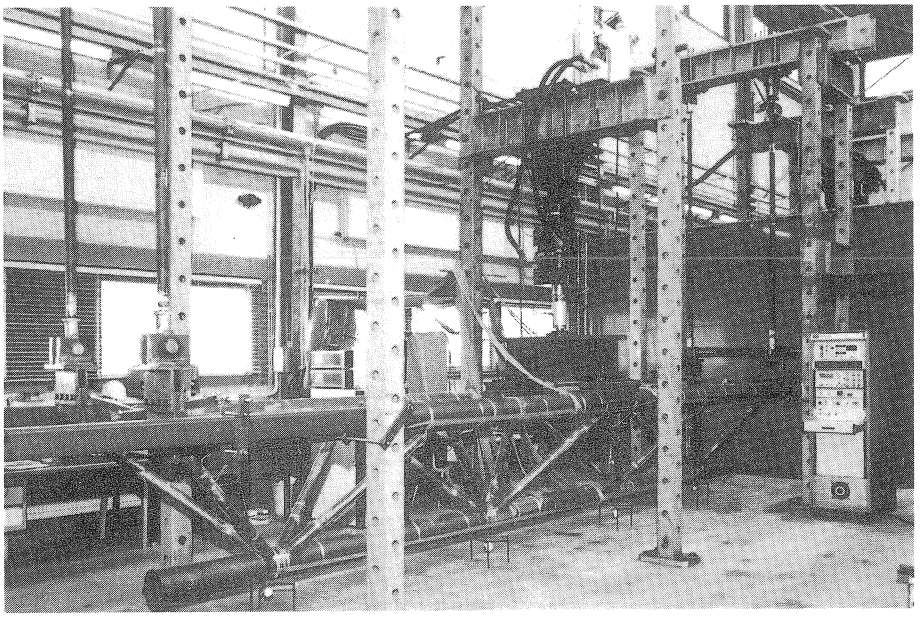

Fig. 16. Fully instrumented girder in test rig.

4.2 *Experimental measurements*

Hot spot strains (and SNCFs).
For the determination of the hot spot strain $\varepsilon_{h.s.}$ at the weld toes, all four joints of the lower chord of the girders have been provided with strip gauges in a number of crown, saddle and inbetween locations.

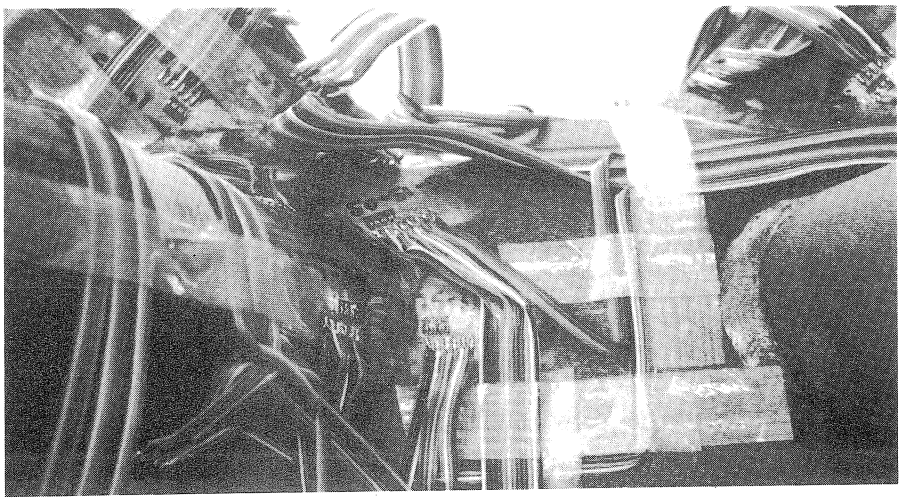

Fig. 17. Strip gauges around a multiplanar joint.

As an example, figure 17 shows some strip gauges around a multiplanar gap joint in girder 5.
The hot spot strain $\varepsilon_{h.s.}$ at the weld toes in chord and braces is determined from a linear extrapolation method according to table 1 and figure 3. From the strain measurements, SNCFs have been determined as described in chapter 1.3.
Table 7 gives a summary of the hot spot strains $\varepsilon_{h.s.}$ and SNCFs at the weld toes of chord and braces for the main joints in girder 7. For complete details of $\varepsilon_{h.s.}$ and SNCF results for all the tested girders 5 to 8, reference is made to [*F23*].
For the value of $\varepsilon_{h.s.}$ around the brace to chord intersection, the following conclusions can be drawn:

- *For the gap and 100% overlap joints.*
  The highest (positive) $\varepsilon_{h.s.}$ around the intersection of the tensile loaded brace to the chord occurs in the gap region at the toe and the inbetween locations of both the chord and brace member. The $\varepsilon_{h.s.}$ around the entire intersection of the compression loaded brace to the chord (gap joints) are negative.
- *For the 50% overlap joints.*
  The highest (positive) $\varepsilon_{h.s.}$ around the intersection of the tensile and compression loaded brace to the chord occurs at the brace heel location of the tensile loaded brace and at the chord heel location of the compression loaded brace.
- Generally, for all three main types of multiplanar KK joints investigated, the $\varepsilon_{h.s.}$ for both the chord saddle and brace saddle locations are when compared to the $\varepsilon_{h.s.}$ for the chord and brace crown and inbetween locations small. This is caused by the combination of chord and brace member loads, namely:
  - *Chord member loads $F_{ch;ax}$, $M_{ch;ip}$ and $M_{ch;op}$ result in largest $\epsilon_{h.s.}$ at the crown locations of the chord member.*
  - *Combined brace member loads $F_{br;ax;a-d}$, $M_{br;ip;a-d}$ and $M_{br;op;a-d}$, result in largest $\epsilon_{h.s.}$ at some of the saddle, crown and inbetween locations of the chord and brace members.*

- The highest SNCF in the gap joints due to the combined loading varies from 1.3 to 2.3 and for the overlap joints from 0.9 to 2.5.

Fatigue life.
The fatigue tests have been carried out for determination of the number of cycles to initiation of cracks and failure of the joints. During the fatigue tests, the strain distribution in the members and around the main joints have been measured at regular intervals, so that changes in hot spot strains and nominal strains due to initiation of cracks and crack growth could be determined. For all joints, with the exception of the overlap joints in girder 7, the cracks start at the location where the highest hot spot strains (and SNCFs) occurs and extends along the weld toe of chord or brace over a certain length until a through crack occurs. All of the 16 main joints, with the exception of gap joint 2 of girder 6, and gap joint 2 as well as overlap joint 2 of girder 7, failed in the chord. In the gap joint 2 of girders 6 and 7 failure occurred in the brace, whereas in overlap joint 2 of girder 7 a combined failure occurred in the chord and brace.
Table 8 summarizes the test results from the static load tests and the fatigue tests. As an example, figure 18 shows a joint failure.

Gap joint 1					Gap joint 2					Overlap joint 1					Overlap joint 2				
line	$\varepsilon_{h.s.}$	$\varepsilon_{h.s.}$ aver.	ε_{nom}	SNCF aver.	line	$\varepsilon_{h.s.}$	$\varepsilon_{h.s.}$ aver.	ε_{nom}	SNCF aver.	line	$\varepsilon_{h.s.}$	$\varepsilon_{h.s.}$ aver.	ε_{nom}	SNCF aver.	line	$\varepsilon_{h.s.}$	$\varepsilon_{h.s.}$ aver.	ε_{nom}	SNCF aver.
E.1-B	142	132	168	0.78	A.1-B	88	103	169	0.61	K.1-B		138	137	1.00	O.1-B	130	134	159	0.80
F.1-B	121		170		B.1-B	117		169		L.1-B	188		138		P.1-B	138		175	
G.1-B	-42		168	-0.25	C.1-B	-30		169	-0.18		87								
E.1-C	41	41	168	0.24	A.1-C	85	85	169	0.50	K.1-C	-98	-98	137	-0.78	O.1-C	-50	-50	159	-0.31
E.2-B	253	264	168	1.56	A.2-B	308	284	169	1.68	K.2-B	95	95	137	0.69	O.2-B	205	205	159	**1.29****
F.2-B	275		170		B.2-B	260		169											
G.2-B	-187		168	-1.11	C.2-B	-		169	-1.68	K.2-C	60	60	137	0.44	O.2-C	-7	-6	159	-0.04
						283				L.2-C	60		138		P.2-C	-4		175	
E.2-C	300	296	168	1.75	A.2-C	180	175	169	1.04	K.3-B	53	81	137	0.59	O.3-B	120	125	159	0.75
F.2-C	291		170		B.2-C	170		169		L.3-B	108		138		P.3-B	130		175	
E.3-B	122	122	168	0.73	A.3-B	113	113	169	0.67	K.3-C	13	13	137	0.10	O.3-C	-15	-15	159	-0.09
E.3-C	96	96	168	0.57	A.3-C	108	108	169	0.64	I.4-C	230	230	137	**1.68****	M.4-C	180	180	159	1.13
E.4-C	100	100	168	0.60	A.4-C	-26	-26	169	-0.15	K.5-B	56	56	137	0.41	O.5-B	39	39	159	0.25
E.5-C	380	380	168	**2.26****	A.5-C	283	283	169	**1.68****	K.6-C	-62	-62	137	-0.45	O.6-C	-2	-2	159	-0.01

** Maximum SNCF.

*** $\epsilon_{nom} = \epsilon_{ax} + \sqrt{\epsilon^2_{ipb} + \epsilon^2_{opb}}$.

Table 7. Measured hot spot strains $\varepsilon_{h.s.}$ and SNCFs in girder 7 at F = 100kN.

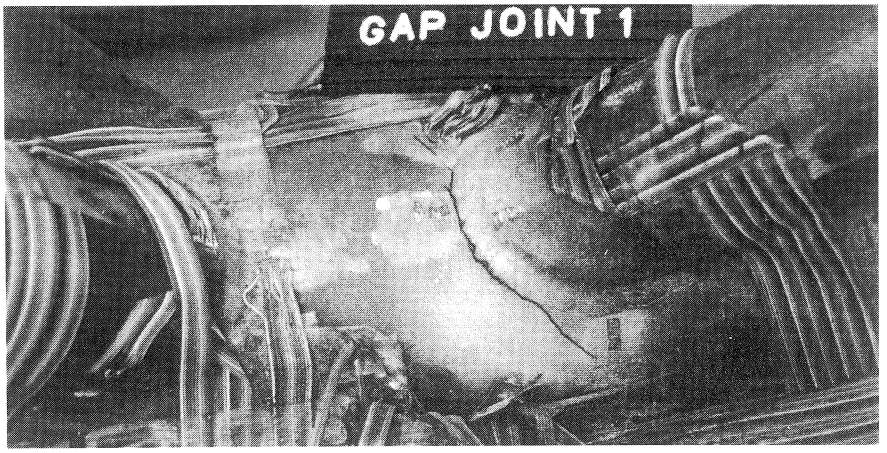

Fig. 18. Failure in a gap joint.

From the fatigue test results, $S_{r_{h.s.}}$ - N_f curves have been derived.
Since these curves are based on stresses and the measurements on strains, a conversion is carried out from the measured strains into stresses by using an average factor as given below, which is on the basis of existing information [*F3*] and the results of the numerical calibration given in chapter 5.

$SCF = 1.2 \cdot SNCF.$

Figure 19 shows the mean $S_{r_{h.s.}}$ - N_f line for all the multiplanar KK joints tested together with the DEn S_r - N curve (see also figure 6), which is also used for uniplanar joints with

t = 16 mm. From figure 19 it is found that the scatter of the fatigue data is small, and the slope of the mean line is m = -3.7. Also, it can be seen that the mean line and slope through the data points is in good agreement with those of the DEn mean line. As shown in figure 20, a thickness correction for the fatigue data results in an increase of scatter.
From the results given in figures 19 and 20, it is proposed that the DEn design curve for uniplanar joints in CHS should also be applied for the multiplanar KK joints for thicknesses of 4 to 16 mm. No thickness correction is therefore needed. The equation of this design curve is :

$$\log(N_f) = 12.4756 - 3 \log(S_{r_{h.s.}})$$

with: $(10^3 < N_f < 5 \cdot 10^6)$.

t [mm]	joints in CHS
4	o
8	o
16	o

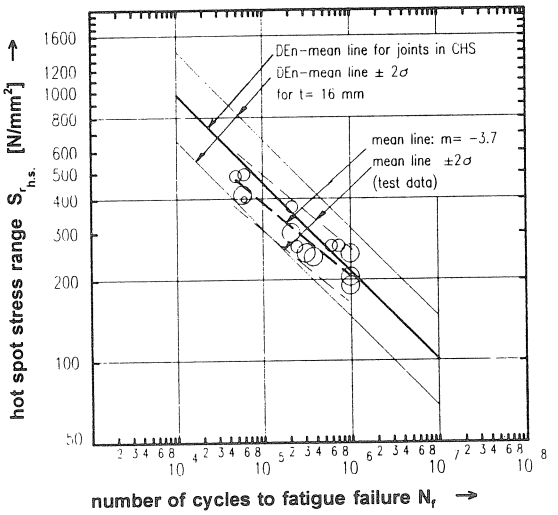

Fig. 19. Main fatigue data derived from multiplanar KK joints without thickness correction.

t [mm]	joints in CHS
4	o
8	o
16	o

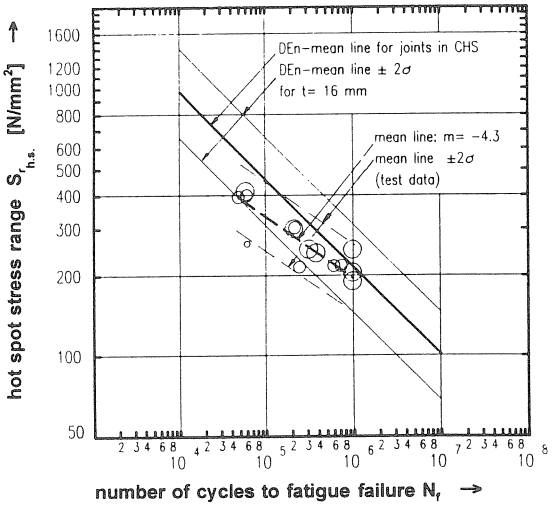

Fig. 20. Main fatigue data derived from multiplanar KK joints with thickness correction.

Joint	Dimensions		R	Load range F_r [Kn]	ε_{nom} ($*10^{-6}$)	S_{nom} [N/mm^2]	$\varepsilon_{h.s.}$ ($*10^{-6}$)		$S_{h.s.}$ [N/mm^2]		SNCF		SCF		Location		N_i ($*10^6$)	N_f ($*10^6$)	Mode of failure	N_f / N_i	$S_{h.s.}$ corrected to thickness [N/mm^2] (DEn)
	chord	brace					Chord	Brace	Chord	Brace	Chord	Brace	Chord	Brace	Chord	Brace					
GIRDER 5																					
Gap 1	ϕ193.7x8	ϕ 76.1x4	0.1	321	703	148	1059	-	267	-	1.51	-	1.81	-	E.2-C	-	0.200	0.723	chord	3.62	217
Gap 2					812	171	1059	-	267	-	1.30	-	1.56	-	B.2-C	-	0.130	0.598	chord	4.60	217
Overlap 1					600	126	1477	-	372	-	2.46	-	2.95	-	K.4-C	-	0.030	0.214	chord	7.13	302
Overlap 2					1053	221	1920	-	484	-	1.82	-	2.18	-	O.4-C P.4-C	-	0.010	0.048	chord	4.80	393
GIRDER 6																					
Gap 1	ϕ 193.7x16	ϕ 76.1x8	0.1	585	632	133	965	-	243	-	1.53	-	1.83	-	F.2-C	-	0.100	0.375	chord	3.75	243
Gap 2					725	152	-	1053	-	265	-	1.45	-	1.74	-	B.2-B	0.010	0.244	brace	24.40	215
Overlap 1					632	133	1188	-	299	-	1.88	-	2.25	-	K.4-C	-	0.020	0.210	chord	10.50	299
Overlap 2					1000	210	1638	-	413	-	1.64	-	1.97	-	O.4-C	-	0.006	0.058	chord	9.67	413
GIRDER 7																					
Gap 1	ϕ 193.7x8	ϕ 114.3x4	0.1	513	862	181	1949	-	491	-	2.26	-	2.71	-	E.5-C	-	0.030	0.060	chord	2.0	399
Gap 2					867	182	-	1580	-	398	-	1.82	-	2.19	-	A.2-B A.5-B	0.010	0.060	brace not	6.0	263
Overlap 1					708	149	-	-	-	-	-	-	-	-	-	-	-	>0.220+	failed	-	-
Overlap 2					856	180	-	-	-	-	-	-	-	-	O.3-C	-	0.025	0.093	chord brace	3.72	-
GIRDER 8																					
Gap 1	ϕ 193.7x16	ϕ 114.3x8	0.1	603	512	108	995	-	251	-	1.94	-	2.32	-	F.5-C	-	0.065	0.310	chord	4.77	251
Gap 2					494	104	814	-	205	-	1.65	-	1.97	-	A.5-C	-	0.310	0.978	chord	3.15	205
Overlap 1					458	96	994	-	250	-	2.17	-	2.60	-	K.4-C	-	0.310	>0.978+	not	>3.15	250
Overlap 2					500	105	754	-	190	-	1.51	-	1.81	-	O.4-C	-	0.320	>0.978+	failed	>3.06	190

Table 8. Test results from the static load tests and fatigue tests.

5. CALIBRATION OF NUMERICAL WORK WITH EXPERIMENTAL RESULTS

5.1 *Introduction*

For the calibration of the numerical work on stress and strain concentration factors described in chapter 6, sixteen experimentally investigated joints of girders 5 to 8, as described in chapter 4, have been used.
Based on the results given in previous chapters, it is decided for the numerical hot spot strain (and SNCF) calibration, to model the weld of the joint by 20-n solid elements and the joint member parts by 20-n solid or 8-n shell elements and placing this joint in a beam modelled girder. This means that all other joints are modelled with rigid ended beam elements only, without taking the effect of joint flexibility into account. An example is given in figure 21.

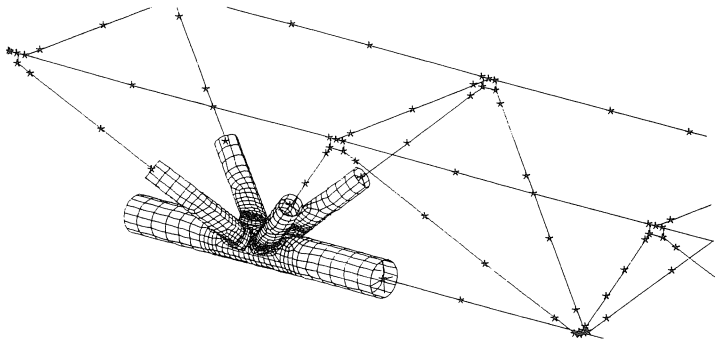

Fig. 21. Numerical model for the hot spot strain calibration of KK gap joint 2 in girder 5.

Since the measured dimensions of the hollow sections were nearly the same as the nominal dimensions, the last mentioned are used for both the joint and girder members. Numerical calibration of experimental results are carried out for:

- *Extrapolated nominal strains ϵ_{nom} for the brace members under tension of the joints tested.*
- *Strain concentration factors (SNCFs).*
- *Ratio SCF/SNCF.*
- *Hot spot strains $\epsilon_{h.s.}$ using the individual measured chord and brace member strains and multiplication of these strains by SNCFs obtained from a parameter study of welded multiplanar KK joints as described in chapter 6.*

5.2 *Numerical calibration*

5.2.1 Calibration of extrapolated nominal strains

Because the experimentally defined SNCFs are determined by $SNCF_{m.n.o} = \frac{\epsilon_{h.s;m.n.o}}{\epsilon_{extrap;nom}}$, a calibration of $\varepsilon_{extrap.;nom}$ has been carried out firstly. The results of this calibration (using a FE model as shown in figure 21) are summarized in table 9.

Girder	Joint no.	Extrapolated nominal strains ($\cdot 10^{-6}$)						Ratio	Ratio	Ratio
		Numerical			Experimental			$\frac{\varepsilon_{nom;num}}{\varepsilon_{nom;exp}}$	$\frac{\varepsilon_{nom;num}}{\varepsilon_{ax;num}}$	$\frac{\varepsilon_{nom;exp}}{\varepsilon_{ax;exp}}$
		ε_{ax}	ε_{ip}	ε_{op}	ε_{ax}	ε_{ip}	ε_{op}			
5	gap 1	170	38	18	151	62	28	0.97	1.24	1.43
	gap 2	199	30	19	193	44	39	0.93	1.17	1.29
	overlap 1	154	52	16	136	40	31	1.12	1.35	1.35
	overlap 2	225	62	44	220	54	93	0.92	1.34	1.47
6	gap 1	91	16	10	89	14	5	1.06	1.39	1.29
	gap 2	105	11	10	104	9	15	0.99	1.14	1.17
	overlap 1	82	25	8	80	26	12	1.01	1.32	1.33
	overlap 2	120	36	23	119	38	36	0.95	1.36	1.42
7	gap 1	122	38	15	111	49	29	0.97	1.33	1.35
	gap 2	133	33	20	128	38	15	1.01	1.29	1.32
	overlap 1	120	4	18	111	5	25	1.01	1.15	1.24
	overlap 2	142	2	28	132	10	25	1.06	1.20	1.25
8	gap 1	64	20	6	62	21	5	1.01	1.33	1.47
	gap 2	69	13	6	67	14	5	1.02	1.21	1.23
	overlap 1	63	9	2	62	10	10	0.94	1.15	1.15
	overlap 2	74	5	16	70	6	11	1.09	1.23	1.23

Table 9. Comparison between numerically and experimentally determined extrapolated nominal strains (10^{-6}) in the tension braces for the joints tested by fatigue of girders 5, 6, 7 and 8.

From the results given in table 9, it is concluded that:

- A good agreement between numerical and experimental extrapolated nominal strains ε_{nom} exist. The maximum differences in ε_{nom} varies from

  $0.92 < \frac{\varepsilon_{nom;num}}{\varepsilon_{nom;exp}} < 1.12.$

- The ratios $\frac{\varepsilon_{nom;num}}{\varepsilon_{ax;num}}$ and $\frac{\varepsilon_{nom;exp}}{\varepsilon_{ax;exp}}$ show a large influence of axial strains compared to bending strains on the total strains.

5.2.2 Calibration of SNCFs

Results of the numerically determined strain concentration factors SNCFs (and SCFs) for the sixteen tested multiplanar joints are given in table 10, in which the comparison with experimental results is also given.
Figure 22 illustrates the results on calibration of SNCFs, showing a reasonable agreement, considering the small SNCF values.

girder 5

gap joint 1						gap joint 2						overlap joint 1						overlap joint 2					
line	numerical results			exp. results	num. exp.	line	numerical results			exp. results	num. exp.	line	numerical results			exp. results	num. exp.	line	numerical results			exp. results	num. exp.
	SNCF	SCF	SCF SNCF	SNCF	ratio SNCF		SNCF	SCF	SCF SNCF	SNCF	ratio SNCF		SNCF	SCF	SCF SNCF	SNCF	ratio SNCF		SNCF	SCF	SCF SNCF	SNCF	ratio SNCF
E.1-B	1.04	1.13	1.08	1.18	0.88	A.1-B	1.06	1.16	1.10	1.23	0.86	K.1-B	0.71	0.84	1.18	0.62	1.15	O.1-B	1.22	1.36	1.12	1.13	1.08
G.1-B	-1.00	-1.10	1.10	-1.28	0.78	A.2-B	0.71	0.76	1.08	1.19	0.60	K.1-C	-1.28	-1.34	1.04	-1.44	0.88	O.1-C	-0.33	-0.28	0.85	0.07	**
E.1-C	0.54	0.76	1.41	0.53	1.02	A.2-C	1.44	1.72	1.20	1.37	1.06	K.2-B	0.43	0.42	0.97	0.32	**	O.3-B	0.80	0.78	0.98	0.55	1.46
E.2-B	0.71	0.81	1.14	0.67	1.06	A.3-C	0.69	0.78	1.13	0.48	**	K.2-C	0.49	0.51	1.04	0.34	**	O.4-C	-2.17	2.44	1.13	1.86	1.17
G.2-B	-0.54	-0.59	1.10	-0.73	0.74	A.5-B	0.96	1.06	1.10	1.02	0.94	K.3-B	0.80	0.72	0.91	0.54	1.48						
E.2-C	1.74	2.08	1.20	1.51	1.15	A.5-C	1.11	1.37	1.23	1.07	1.04	K.3-C	-0.13	-0.13	1.00	-0.48	**						
E.3-B	0.81	0.85	1.05	0.86	0.94							K.4-C	2.15	2.73	1.27	2.46	0.88						
E.3-C	0.58	0.85	1.46	1.26	0.46							K.5-B	0.02	0.11		0.19	**						
E.4-B	0.81	0.86	1.06	0.27	**							I.5-B	-0.12	-0.04		-0.31	**						
G.4-B	-1.51	-1.68	1.11	-1.28	1.18																		
E.4-C	0.31	0.41	1.33	0.32	**																		
E.5-B	0.97	1.06	1.09	1.21	0.80																		
E.5-C	1.23	1.47	1.20	1.32	0.93																		

girder 6

gap joint 1						gap joint 2						overlap joint 1						overlap joint 2					
line	numerical results			exp. results	num. exp.	line	numerical results			exp. results	num. exp.	line	numerical results			exp. results	num. exp.	line	numerical results			exp. results	num. exp.
	SNCF	SCF	SCF SNCF	SNCF	ratio SNCF		SNCF	SCF	SCF SNCF	SNCF	ratio SNCF		SNCF	SCF	SCF SNCF	SNCF	ratio SNCF		SNCF	SCF	SCF SNCF	SNCF	ratio SNCF
E.1-B	0.99	1.11	1.12	1.15	0.86	A.1-B	0.86	0.95	1.11	1.16	0.75	K.1-B	0.53	0.02	0.04	0.75	0.71	O.1-B	0.83	0.60	0.73	0.96	0.87
G.1-B	-0.96	-1.03	1.08	-1.52	0.63	C.1-B	-0.91	-1.04	1.14	-0.95	0.96	K.1-C	-0.96	-0.95	0.99	0.76	1.26	O.1-C	-0.33	-0.28	0.85	-0.09	**
E.1-C	0.43	0.63	1.46	0.44	**	A.1-C	0.57	0.68	1.19	0.61	0.93	K.3-B	0.48	0.10	0.21	0.50	0.97	O.3-B	-0.71	0.49	0.69	0.58	1.22
E.2-B	1.34	1.57	1.17	1.51	0.89	A.2-B	1.37	1.49	1.09	1.49	0.93	K.3-C	-0.73	-0.83	1.14	-0.32	**	O.3-C	-0.48	0.42	0.88	-0.35	**
G.2-B	-0.93	-0.85	0.92	-0.91	1.02	C.2-B	-1.16	1.39	1.20	-1.09	1.06	K.4-C	2.38	2.72	1.14	1.88	1.27	O.4-C	2.11	2.38	1.13	1.64	1.29
E.2-C	1.45	1.69	1.17	1.38	1.05	A.2-C	1.30	1.52	1.18	1.16	1.12	K.4-B	0.36	0.23	0.64	0.26	**	O.5-B	0.49	0.41	0.83	0.49	1.00
E.3-B	1.01	1.10	1.09	0.97	1.04	C.2-C	-0.23	-0.40	1.74	-0.48	**												
E.3-C	0.75	1.02	1.36	0.89	0.85	A.3-B	1.04	1.11	1.07	0.84	1.23												
E.4-C	0.24	0.31	1.29	0.19	**	A.3-C	0.94	1.17	1.24	0.74	1.27												
						A.4-C	-0.11	-0.05	0.45	0.19	**												

Table 10. SNCF and SCF values at various locations of the joints in girders 5 and 6.
note: ** = very small SNCF values.

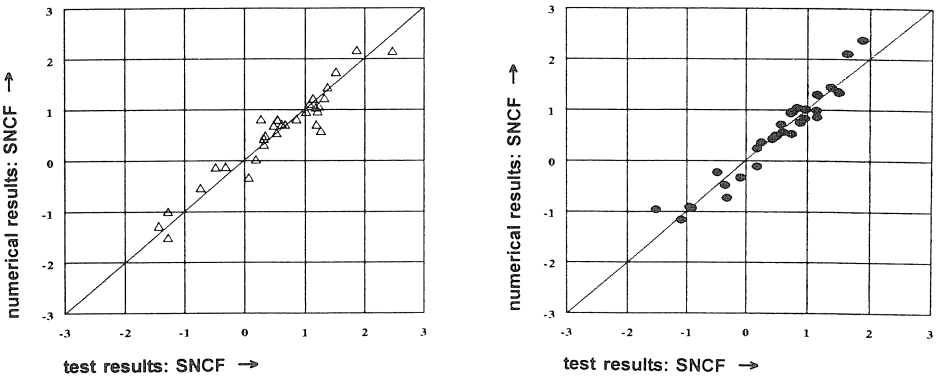

Fig. 22. Comparison between experimentally and numerically determined SNCF values. (Girder 5 left figure and girder 6 right figure).

5.2.3 Calibration of the ratio SCF/SNCF

As mentioned in chapter 4, a ratio for SCF/SNCF has to be established for converting measured hot spot strains $\varepsilon_{h.s.}$ into hot spot stresses $\sigma_{h.s.}$ for use in the fatigue design curves. Results of the numerically determined ratio for SCF/SNCF for the sixteen tested multiplanar joints, considering all locations around the perimeter, are given in table 11 and figure 23. An average ratio of SCF/SNCF = 1.2 is obtained, which supports previous work on uniplanar joints. It is mentioned, however, that for SCFs and SNCFs with absolute values smaller than 0.5, a large scatter on this ratio exist, namely: $0.80 < SCF/SNCF < 1.40$. For the locations along the weld toe where fatigue failure occurs, the average ratio SCF/SNCF is 1.14 and the ratio SCF/SNCF varies from $1.02 < SCF/SNCF < 1.27$ (see table 11). The existence of the scatter in SCF/SNCF is specifically for tubular joints by means of constitutive equations and parameter study results explained and discussed in chapter 6.

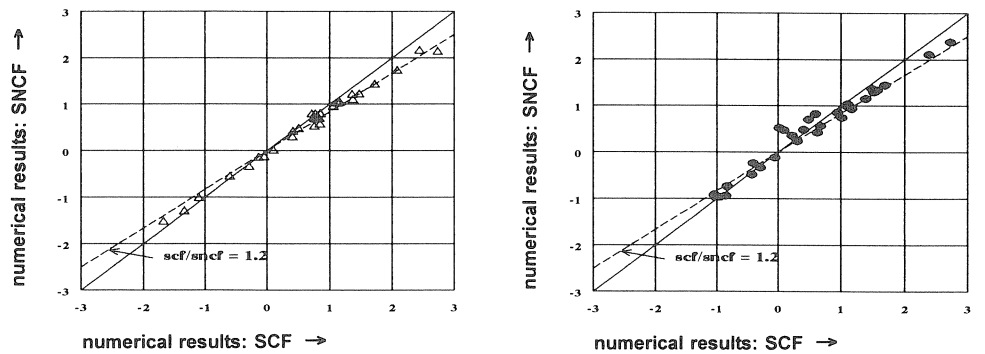

Fig. 23. Comparison between numerically determined SNCF and SCF values. (Girder 5 left figure and girder 6 right figure).

Girder	Joint							
	Gap 1		Gap 2		Overlap 1		Overlap 2	
	Location	SCF / SNCF	Location	SCF / SNCF	Location	SCF / SNCF	Location	SCF / SNCF
5	E.2-C	1.20	A.2-C	1.20	K.4-C	1.27	O.4-C	1.17
6	E.2-C	1.17	A.2-B	1.09	K.4-C	1.14	O.4-C	1.13
7	E.5-C	1.13	A.2-B	1.08	-	-	-	-
8	E.5-C	1.12	A.5-C	1.10	K.4-C	1.06	O.4-C	1.02

Table 11. Numerically determined ratio SCF/SNCF for the locations of fatigue failure.

5.2.4 Calibration of hot spot strains based on individual loads

Due to the non-uniform stiffness along the intersection of a brace to chord member connection, the magnitude of hot spot strain $\varepsilon_{h.s.}$ entirely depends on the location (crown, saddle and inbetween) considered.
As an example, for the reference effects of brace member loads, as explained in chapter 6, axial forces and out-of plane bending moments generally give the highest $\varepsilon_{h.s.}$ at the chord saddle and brace saddle locations, whereas in-plane bending moments give the highest $\varepsilon_{h.s.}$ at the chord and brace crown and inbetween locations. For the axial chord member loads, the highest $\varepsilon_{h.s.}$ always occurs at the chord crown locations. Besides reference effects, depending on the type of joint, joint parameters β, γ, τ, φ_{ip} and φ_{op} and type of loading, large carry-over effects at crown, saddle and inbetween locations occur. Therefore, no fixed locations of $\varepsilon_{h.s.}$ can be given, as in the case of reference effects. A calibration on $\varepsilon_{h.s.}$ using the individual measured brace and chord member strains (extrapolated) from the tested girders 5 to 8 and SNCFs obtained from a parameter study as described in chapter 6 has been carried out for the gap joints. The $\varepsilon_{h.s.}$ is determined according to the definition on total hot spot stress based on stress concentration factors given in chapter 1.3. Results of the $\varepsilon_{h.s.}$ determined in this way are given in figure 24 and table 12, together with experimental results of $\varepsilon_{h.s.}$.

From the results of the calibration of hot spot strains $\varepsilon_{h.s.}$ based on individual loads (measured chord and brace member strains) and numerically determined SNCFs (reference and carry-over effects), the following conclusions are given:

- *The numerical and experimental results on $\epsilon_{h.s.}$ as illustrated in figure 24 for gap joints 1 show an acceptable agreement.*
- *Generally, the largest determined $\epsilon_{h.s.}$ ($= \epsilon_{h.s.;br} + \epsilon_{h.s.;ch}$) for the gap joints 1 and 2 investigated occurs at the chord crown location in the gap region for the brace member under tension, which is the same location where fatigue cracking starts. At some chord and brace saddle and inbetween locations of the gap region for the brace member under tension, values of $\epsilon_{h.s.}$ are found which are only slightly smaller than the largest one.*
- *As shown in table 12, for the relevant total $\epsilon_{h.s.}$ of gap joints 1, the contribution of chord member loads (axial and in-plane bending) cannot be neglected. Therefore, chord member loads should always be considered when analysing $S_{r_{h.s.}}$.*
- *Comparison of $\epsilon_{h.s.}$ for the brace and chord member locations shows that the contribution of*

bending strains $\epsilon_{h.s.;ip}$ and $\epsilon_{h.s.;op}$ on the total strains $\epsilon_{h.s.}$ varies around the brace to chord intersection line. But for the brace member loads with large values of $\epsilon_{h.s.}$, the ratio α_{br} (see column 6 of table 12) varies approximately within the range of $1.0 < \alpha_{br} < 1.6$.
For the chord member loads with large values of $\epsilon_{h.s.}$ however, the ratio α_{ch} (see column 9 of table 12) varies largely.

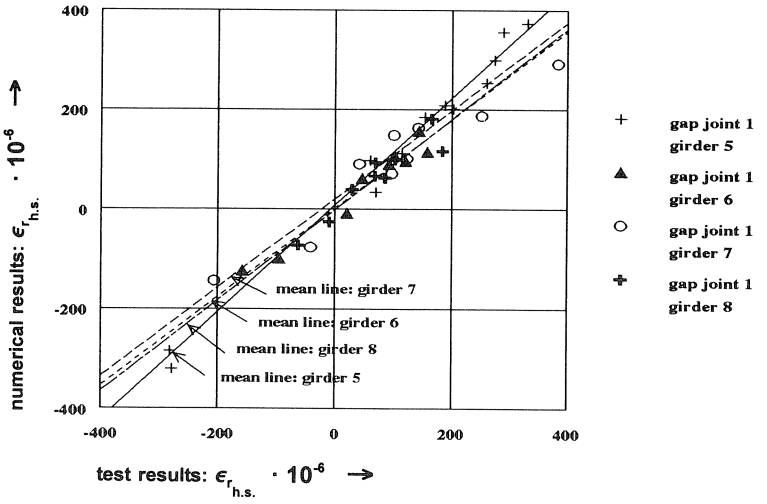

Fig. 24. Comparison between numerically and experimentally determined hot spot strains $\varepsilon_{h.s.}$ for gap joint 1 of girders 5 to 8. Numerical determined hot spot strains based on measured chord and brace member strains (axial + bending) and multiplied by the corresponding SNCFs obtained from the parameter study results (see chapter 6).

Line	Girder	Brace loads: $\varepsilon_{h.s.;br}$ ***				Chord loads: $\varepsilon_{h.s.;ch}$ ***			Brace + chord loads: $\varepsilon_{h.s.} = \varepsilon_{h.s.;br} + \varepsilon_{h.s.;ch}$	Ratio $\varepsilon_{h.s.}$ **** numerical / experimental
		$\varepsilon_{h.s.;ax}$ [3]	$\varepsilon_{h.s.;ip}$ [4]	$\varepsilon_{h.s.;op}$ [5]	α_{br} ** [6]	$\varepsilon_{h.s.;ax}$ [7]	$\varepsilon_{h.s.;ip}$ [8]	α_{ch} ** [9]		
E.1-B	5	170	13	54	1.39	38	-22	0.42	253	0.97
	6	92	1	-4	0.96	12	-5	0.58	96	0.80
	7	78	9	32	1.52	44	0	1.00	163	1.15
	8	40	0	6	1.15	21	-1	0.95	66	1.14
G.1-B	5	-181	5	-125	1.66	38	-22	0.42	-285	1.01
	6	-90	-1	-40	1.46	12	-5	0.58	-124	0.79
	7	-75	1	-47	1.61	44	0	1.00	-77	1.83
	8	-38	0	-6	1.16	21	-3	0.86	-26	
E.1-C	5	206	8	-94	0.58	-31	23	0.25	112	0.98
	6	66	2	-3	0.99	-17	13	0.24	61	1.32
	7	82	10	35	1.55	-37	0	1.00	90	2.19
	8	25	3	3	1.24	20	0	1.00	39	
E.2-B	5	141	38	0	1.27	3	-9	-2.00	185	1.25
	6	105	7	0	1.07	9	-7	0.22	114	0.72
	7	136	37	9	1.33	0	5	--	187	0.74
	8	82	14	1	1.17	6	-4	0.33	99	0.97
G.2-B	5	-145	20	0	0.86	3	-9	-2.00	-131	0.82
	6	-110	14	0	0.88	9	-12	-0.33	-99	1.04
	7	-133	26	-26	1.00	0	-11	--	-144	0.77
	8	-79	11	0	0.87	6	-11	-0.83	-73	1.16
E.2-C	5	270	68	13	1.30	143	-120	0.16	374*	1.13
	6	134	10	0	1.07	79	-67	0.15	156*	1.09
	7	238	67	-5	1.26	125	-3	0.98	422	1.41
	8	94	28	0	1.30	77	-18	0.77	181	1.10
E.3-B	5	155	-3	50	1.30	40	-34	0.15	208	1.11
	6	107	0	-4	0.96	13	-10	0.23	106	1.05
	7	110	0	-59	0.46	50	0	1.00	101	0.83
	8	58	0	-10	0.83	19	-5	0.73	62	0.73
E.3-C	5	201	17	118	1.67	-3	-33	12.0	300	1.09
	6	102	3	17	1.20	-20	-12	1.60	90	0.98
	7	113	15	-32	0.85	-25	0	1.00	71	0.74
E.4-B	5	236	-126	0	0.47	-9	-4	1.44	97	1.62
G.4-B	5	-241	-67	0	1.28	-9	-4	1.44	-321	1.15
E.4-C	5	42	-33	0	0.21	150	-125	0.17	34	
	6	-18	-2	0	1.11	87	-75	0.14	-8	
	7	17	-19	-3	-0.29	153	0	1.00	148	1.48
E.5-B	5	186	34	-15	1.10	17	-21	-0.23	201	0.99
	8	76	11	-4	1.09	18	-8	0.56	93	1.34
E.5-C	5	304	72	-22	1.16	73	-71	0.02	356	1.23
	7	206	62	-33	1.14	57	0	1.00	292*	0.76
	8	81	19	-6	1.16	30	-8	0.73	116*	0.63

* Indicates positions of joint failure

** Using the column numbering: $\alpha_{br} = [6] = ([3] + [4] + [5]) / [3]$; $\alpha_{ch} = [9] = ([7] + [8]) / [7]$

*** Using the column numbering: $\varepsilon_{h.s.;br} = [3] + [4] + [5]$; $\varepsilon_{h.s.;ch} = [7] + [8]$

**** Ratio given for $|\varepsilon_{h.s.;br} + \varepsilon_{h.s.;ch}| > 50 \cdot 10^{-6}$

Table 12. Contribution of individual measured axial and bending strains ($\cdot 10^{-6}$) of the chord and brace members on the total hot spot strains for gap joint 1 of girders 5 to 8.

6. PARAMETER STUDY ON SCFs AND SNCFs OF WELDED UNIPLANAR AND MULTIPLANAR TUBULAR JOINTS

6.1 *Introduction*

For uniplanar joints considerable research on stress concentration factors has been carried out, but there is still a lack of information. It is found that large differences in SCFs exist between those published in various publications. This is due to the difference in numerical modelling of tubular joints (see chapter 3.3) and the method of determining SCFs (see chapter 6.2). Furthermore, only a few load cases (brace member loads) have been considered in the past. From the calibration results given in chapter 5.2.4 however, it is shown that chord member loads can in a large number of instances be as important as brace member loads. Also, the SCFs have been determined in the past, for a limited number of locations around the perimeter of the brace to chord intersection (mainly the saddle locations). The results of the numerical calibration on the ratio *SCF/SNCF* given in chapter 5.2.3 have shown the existence of a large scatter. No thorough investigation, particularly numerical, is carried out on this ratio for tubular joints. For multiplanar joints, which are frequently used, only limited information on SCFs is available.
For the reasons given above, a parameter study on the determination of SCFs as well as SNCFs for several types of uniplanar and multiplanar joints has been carried out. The SCFs are required for practical use so that the hot spot stress range $S_{r_{h.s.}}$ can be determined. The SNCFs are required to determine the SCF/SNCF ratios for each type of joint as well as for direct comparison of SNCF values with experiments to establish accuracy of the numerical work.

6.2 *Method of SCF and SNCF determination*

Before commencing a parameter study on SCFs (and SNCFs), the following points have to be established:

1 *The finite element (FE) model and weld shape to be used.*
2 *Method of extrapolation and extrapolation region.*
3 *Limits of the extrapolation region with reference to size effect.*
4 *Type of stress to be considered.*
5 *The locations around the reference brace for SCF and SNCF determination.*
6 *Load cases to be analysed.*
7 *Boundary conditions to be used in the FE model.*

Other points, such as the influence of element type, mesh refinement, integration scheme, weld shape and boundary conditions on SCFs have already been discussed in chapter 3.3.

6.2.1 FE model and weld shape to be used

From the conclusions given in chapter 3.3, the joints are modelled with 20-n parabolic solid elements, with the weld shape included. For practical reasons, a butt weld shape that complies with the AWS-code [*F2*], is used in the FE model.

6.2.2 Extrapolation method

For exclusion of effects caused by the global geometry of the weld (flat, concave, convex) and the condition at the weld toe (angle, undercut), an extrapolation of stresses (and strains) to the weld toe location from a defined extrapolation region is carried out for the hot spot stress approach. The extrapolation region, as shown in figure 3, is defined by a specified minimum distance $l_{r;min}$ and a maximum distance $l_{r;max}$ measured from the weld toe location.

Because of the existence of various extrapolation methods (see table 2), a study has been carried out on the influence of extrapolation methods on SCFs.

The three main methods of extrapolation (*a*, *b* and *c)* considered are:

a. Linear curve fitting (by means of the least squares method) through all the data points in and around the region considered, and extrapolating the obtained curve to the weld toe location.

b. Parabolic (quadratic) curve fitting through all the data points in and around the region considered, and extrapolating the obtained curve to the weld toe location.

c. Parabolic (quadratic) curve fitting through all the data points in and around the region considered, and determining stresses at the two specified positions of the extrapolation region using the obtained curve. A linear extrapolation to the weld toe location is carried out from the stresses of these specified locations.

Figure 25 illustrates the use of the three extrapolation methods *a*, *b* and *c*.

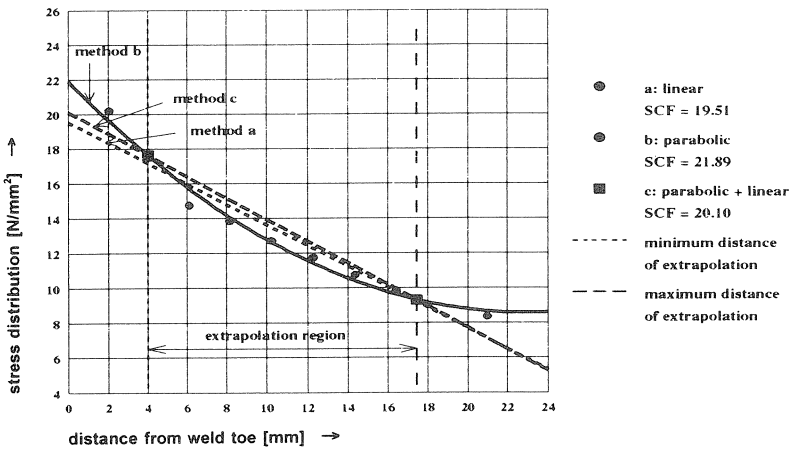

Fig. 25. Influence of extrapolation method on the determination of SCFs.

In this figure the stress distribution is shown for the chord saddle location of an axially loaded reference brace member ($F_{br;ax;a}$) of a KK joint with joint parameters $\beta = 0.40$, $\gamma = 12$, $\tau = 1.00$, $\varphi_{ip} = 60°$ and $\varphi_{op} = 180°$. The study on the extrapolation region is directly related to the study on the extrapolation method, namely the possibility on accuracy of linear or parabolic curve fitting through the data points in and around the

extrapolation region nearby the weld toe. From the study on the influence of extrapolation methods (and region of extrapolation) on SCFs for crown - saddle - inbetween locations, carried out using different types of joints and load cases, it is found that:

- *When no extrapolation method is used at all, i.e. where the SCFs are numerically determined on the basis of nodal stresses at the weld toe only, smaller SCFs (especially for the chord member locations) are to be expected, as compared to SCFs obtained by using an extrapolation method. The reason for the different results is that at the weld toe node, an average stress of the elements of different thicknesses common to this node is determined.*
- *Inside the extrapolation region proposed by the Working Group III, Tubular joints, of the ECSC (see table 1 and figure 3) the stress gradient can be properly described only as a parabolic function. This because, in general, a parabolic stress gradient exist, which continuous beyond the proposed region. However, a parabolic extrapolation of stresses to the weld toe location is very sensitive to small changes in the data points. For that reason, the extrapolation method c (parabolic curve fitting through the data points and linear extrapolation to the weld toe) will be used for the subsequent work.*

6.2.3 Limits of the extrapolation region with reference to scale effect

For one type of a TT joint (180°) so-called an X joint with joint parameters $\beta = 0.70$, $\gamma = 18.0$, $\tau = 1.00$ and various chord dimensions (d_0 = 100; 200; 400 and 800 mm), a study has been carried out on the differences in SCF. For all four chord dimensions, a weld shape that complies to the AWS-code has been modelled.
The influence of changes in chord diameter on the stress distribution near the weld toe, when using the extrapolation method *c* and extrapolation region as described in table 1, is shown in figure 26. SCFs for the chord saddle location are shown in figure 27.
The distances for the extrapolation region of the four chord dimensions used are summarized in table 13.
When using the extrapolation region according to table 1, limits with reference to joint size (chord diameter d_0 and joint parameter γ) are found.
As shown in table 13, decrease of d_0 might result in a large reduction of $\Delta l_r / t_0$.
As illustrated in figures 26 and 27, it is found that the combination of the defined extrapolation region Δl_r and the location of the start of the extrapolation region given by $l_{r;min}$ causes an increase of differences in SCFs when decreasing the chord diameter d_0. This is especially the case when using small values of γ ($\gamma < 10$). Beside this, an increase of d_0 results in a decrease of the gradient of the stress distribution to the weld toe (see also figure 26) and so a decrease of sensitivity on extrapolation.
For the parameter study, in order to avoid the possible large sensitivity of extrapolation region on SCFs when using the equations given in table 1, a chord diameter $d_0 > 400$ mm with $\gamma > 12$ is advised.

To the authors opinion, compared to the extrapolation region defined in table 1, a more simplified and less sensitive extrapolation region can be used for both the chord and brace member locations, namely:

chord member: $l_{r;min} = 0.4 \cdot t_o$ and $l_{r;max} = 1.4 \cdot t_o$
brace member: $l_{r;min} = 0.4 \cdot t_1$ and $l_{r;max} = 1.4 \cdot t_1$

This region is similar to the region used for rectangular hollow section joints [*F61*].

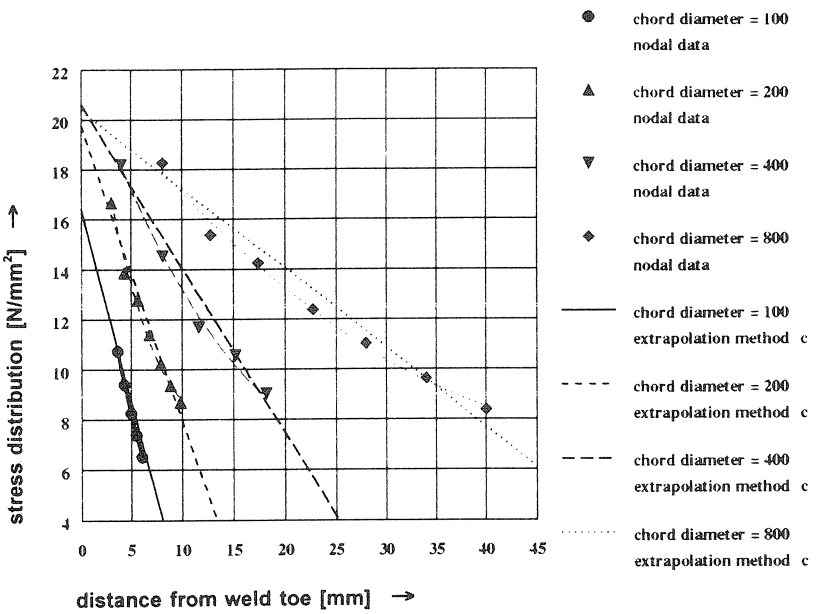

Fig. 26. The influence of changes in chord diameter on numerically determined gradient of the stress distribution nearby the weld toe location.

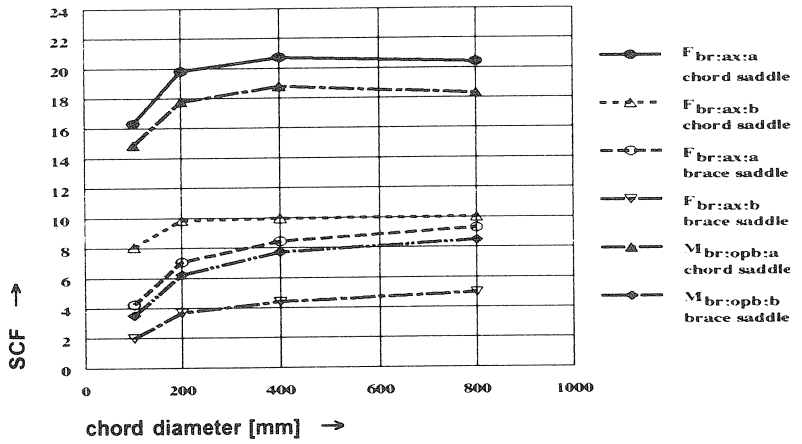

Fig. 27. The influence of changes in chord diameter on the determined SCFs for the chord saddle and brace saddle location of an X joint.

T joint (180°) with: $\beta = 0.70$; $\gamma = 18$; $\tau = 1.00$							
Chord [mm]		Minimum distance [mm]		Maximum distance [mm]		Extrapolation region [mm]	
d_o	t_o	$l_{r;min}$	$l_{r;min} / t_o$	$l_{r;max}$	$l_{r;max} / t_o$	$\Delta l_r = l_{r;max} - l_{r;min}$	$\Delta l_r / t_o$
100	2.78	4.00	1.44	4.36	1.57	0.36	0.13
200	5.56	4.00	0.72	8.73	1.57	4.73	0.85
400	11.11	4.44	0.40	17.45	1.57	13.01	1.17
800	22.22	8.89	0.40	34.91	1.57	26.02	1.17

Table 13. Distances of the extrapolation region for the chord saddle location according to the formulae given in table 1.

6.2.4 Type of stress to be considered

In most studies up till now, the SCFs determined numerically are based on the use of principal stresses only [*F13*, et al]. A limited investigation has been carried out for some types of multiplanar joints on the influence of type of stress used on SCFs. Two types of stresses are considered, namely:

- *Principal stresses.*
- *Primary stresses in a direction perpendicular to the chord weld toe for the chord member locations and in a direction parallel to the axis of the brace member for the brace member locations (this direction mostly differs from the direction perpendicular to the brace weld toe).*

Figure 28 shows an example of the difference obtained on SCF by using the principal and primary stresses.

From the investigation on the influence of type of stress used for SCFs, it is found that:

- *The direction of principal stresses inside the extrapolation region changes, which causes problems when extrapolating stresses to the weld toe location.*
- *For the extrapolation method and extrapolation region used, use of principal stresses (and strains) can result in lower SCFs compared to SCFs due to primary stresses [F46]. For instance, the orientation of the principal stress near the weld toe is perpendicular to the toe. Further away, inside the extrapolation region, the orientation may change, and therefore the extrapolated principal stress drops in comparison to the extrapolated primary stress. Figure 28 illustrates this phenomenon.*

Although, generally small differences (<10%) in SCFs are found in the limited investigation carried out for some types of joints, it has been decided to use primary stresses only. The use of primary stresses is also supported by the direction of crack growth, which is usually along the toe of the weld.

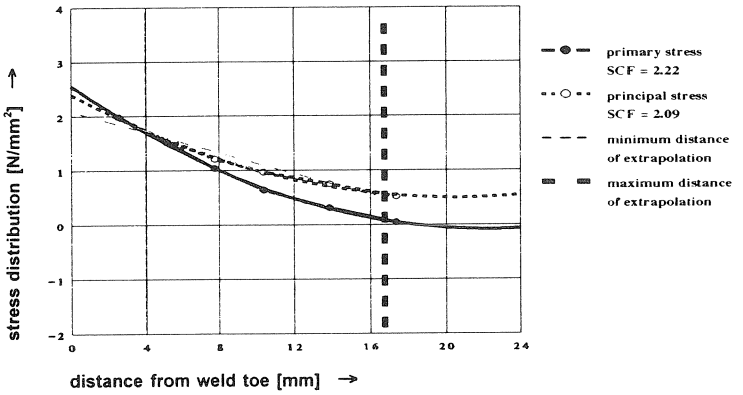

Fig. 28. Difference in SCF by using primary and principal stresses.

6.2.5 Locations around the reference brace for SCF (SNCF) determination

From the investigation on modelling for tubular joint SCFs and results on calibration of numerical work based on individual loads as described in chapter 5.2.4, the locations of interest for both chord and brace member are the crown, saddle and inbetween.
Figure 29 shows the 8 locations of the chord and 8 locations of the brace member, where SCF and SNCF values are determined.

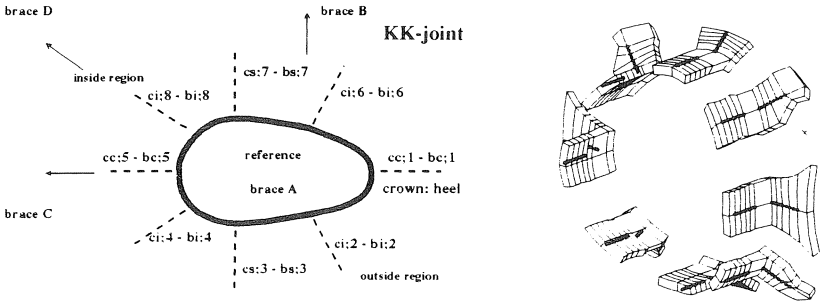

Fig. 29. Selected elements and nodes for the SCF and SNCF determination.

6.2.6 Load cases to be analysed

The following load cases are analysed:
Brace member(s): $F_{br;ax}$; $M_{br;ip}$; $M_{br;op}$.
Chord member: $F_{ch;ax}$; $M_{ch;ip}$; $M_{ch;op}$.
As an example, analysing a KK joint results in $2_{(a)} \cdot 8_{(b)} \cdot 15_{(c)} = 240$ SCF and 240 SNCF values, where:

(a) = *Chord + reference brace member (totally 2 member parts).*
(b) = *Number of locations of interest on a member, see figure 29 (totally 8 on each member part).*
(c) = *Number of load cases, three load cases for the chord member and three load cases for each brace member: KK joint ⇒ four brace members.*

Because of the large resistance of tubular members against torsion, torsional brace moments $M_{br;t}$ might occur which causes non-negligible hot spot stresses.
No information on this exist and therefore, a study on the influence of torsional brace moments $M_{br;t}$ on SCFs has been carried out [*F46*]. It appears that as an acceptable approximation, SCFs due to $M_{br;t}$ can be determined by resolving $M_{br;t}$ into an out-of-plane bending component $M_{br;op}$ as shown in figure 30, and considering the SCFs due to this component only (the SCFs caused by $M_{br;w}$ are found to be small compared to SCFs caused by $M_{br;op}$) [*F65*]. To avoid unnecessary SCF data, this load case is therefore not analysed separately.

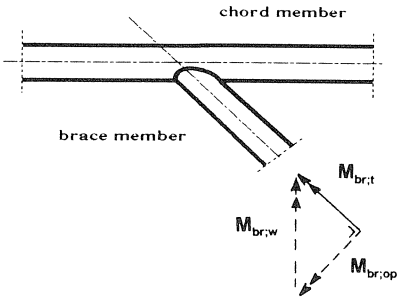

Fig. 30. Principle of resolving $M_{br;t}$ into $M_{br;op}$.

6.2.7 Boundary conditions to be used in the FE model

The decision is made to use a boundary system with a pin ended chord member and a free ended brace member. In addition to this, for equilibrium purpose, one side of the chord member is also fixed against rotation around the chord axis. For the boundary conditions used, in case of brace member loads, moments in the chord member are introduced which affect the SCFs (see chapter 3.3.2). To obtain data on SCFs and SNCFs which are independent of the boundary condition used, compensating moments are applied to obtain the effect of the brace member loading only. An example is given in figure 31, in which the compensating moments for an axially loaded brace member of a T joint are given for the locations of interest (crown, saddle and inbetween), namely:

locations 1, 5 (crown)	$M_{compensating} = 0.50 \cdot F_{br;ax} \cdot x1$
locations 2, 4, 6, 8 (inbetween)	$M_{compensating} = 0.50 \cdot F_{br;ax} \cdot x2$
locations 3, 7 (saddle)	$M_{compensating} = 0.25 \cdot F_{br;ax} \cdot L$

In all previous studies, the obtained SCFs incorporate the effect of the bending moment in the chord for e.g. by inclusion of an α parameter with $\alpha = 2L / d_o$. Therefore, the results on SCFs, especially those for carry-over effects (see chapter 3.3.2), are largely boundary depending. The method used is found to be more realistic, since the results are independent of the boundary condition used.

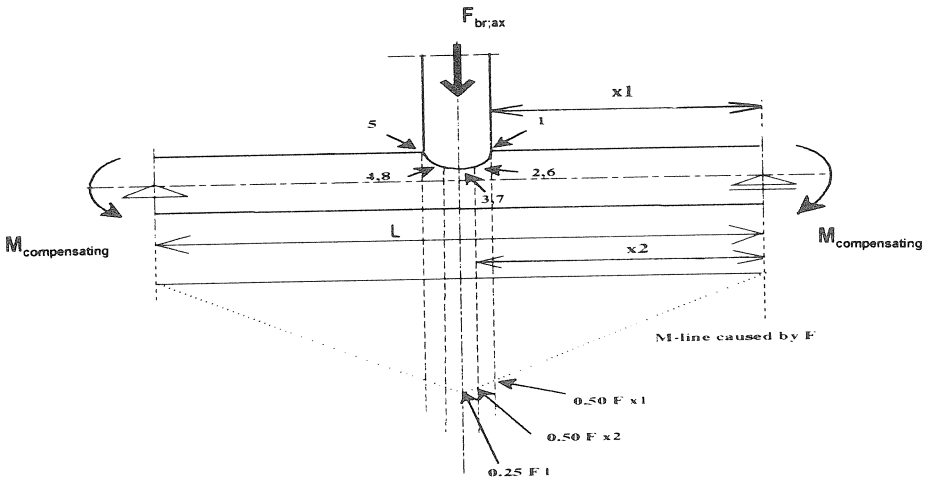

Fig. 31. An example on compensating moments applied to obtain SCFs independent of boundary conditions used.

6.3 *Relationship between SCF and SNCF*

Because of the almost isotropic behaviour of steel and assuming that $\sigma_z = 0$ (plane-stress condition), the relationship between σ_x and ε_x can be written as:

$$\frac{\sigma_x}{E \cdot \epsilon_x} = \left(\frac{1 + \nu \cdot \frac{\epsilon_y}{\epsilon_x}}{1 - \nu^2}\right)$$

in which:

x = The direction perpendicular to the weld toe (chord member locations), or parallel to the axis of the brace member (brace member locations).
y = The direction parallel to the weld toe (chord member locations), or along the brace member surface perpendicular to the axis of the brace member (brace member locations).
z = The direction perpendicular to the member surface.
ν = 0.30 (Poissons ratio for steel).

With $\nu = 0.30$, this equation when expressed in hot spot terms results in the simplified form of:

$$\frac{\sigma_{x;h.s.}}{E \cdot \epsilon_{x;h.s.}} = \left(1.10 + 0.33 \cdot \frac{\epsilon_y}{\epsilon_{x;h.s.}}\right) \quad \text{so that:} \quad \frac{SCF}{SNCF} = \left(1.10 + 0.33 \cdot \frac{\epsilon_y}{\epsilon_{x;h.s.}}\right).$$

It follows that the ratio SCF/SNCF entirely depends on the ratio $\frac{\epsilon_y}{\epsilon_{x;h.s.}}$.

The assumption that $|\frac{\epsilon_y}{\epsilon_{x;h.s.}}| < 1.0$, which is expected to be correct for large values for SCF, results into the relationship: $0.8 < \frac{SCF}{SNCF} < 1.4$.

6.4 *Joint types and geometries analysed*

The type of (gap) joints and geometries analysed and discussed are summarized in tables 14 and 15.

Type of joint. (FE models are shown in figure 4)	Number of joints analysed	Joint parameters			Number of SCFs and SNCFs analysed
		β	γ	τ	
T joint	48	$0.30 \le \beta \le 0.90$	$12 \le \gamma \le 30$	$0.25 \le \tau \le 1.00$	9216
TT joint					
$\varphi_{op} = 45°$	12	$\beta = 0.30$			3456
$\varphi_{op} = 70°$	12	$\beta = 0.30$			3456
$\varphi_{op} = 90°$	36	$0.30 \le \beta \le 0.65$	$12 \le \gamma \le 30$	$0.25 \le \tau \le 1.00$	10368
$\varphi_{op} = 135°$	36	$0.30 \le \beta \le 0.70$			10368
$\varphi_{op} = 180°$ (X joint)	48	$0.30 \le \beta \le 0.90$			13824
XX joint (φ_{op} = 90°-180°-270°)	60	$0.30 \le \beta \le 0.60$	$8 \le \gamma \le 32$	$0.25 \le \tau \le 1.00$	17280

Table 14. Geometries used for the parameter study (braces perpendicular to the chord axis).

Type of joint. (FE models are shown in figure 5)	Number of joints analysed	Joint parameters			Number of SCFs and SNCFs analysed
		β	γ	τ	
Y joint					
$\varphi_{ip} = 30°$	48	$0.25 \le \beta \le 0.75$			23040
$\varphi_{ip} = 45°$	48	$0.25 \le \beta \le 0.90$	$12 \le \gamma \le 30$	$0.25 \le \tau \le 1.00$	23040
$\varphi_{ip} = 60°$	48	$0.25 \le \beta \le 0.90$			23040
K joint					
$\varphi_{ip} = 30°$	48	$0.25 \le \beta \le 0.75$			23040
$\varphi_{ip} = 45°$	36	$0.25 \le \beta \le 0.60$	$12 \le \gamma \le 30$	$0.25 \le \tau \le 1.00$	17280
$\varphi_{ip} = 60°$	24	$0.25 \le \beta \le 0.40$			11520
KK joint					
$\varphi_{ip} = 30°$: $\varphi_{op} = 45°$	36	$0.25 \le \beta \le 0.40$			17280
: $\varphi_{op} = 90°$	36	$0.25 \le \beta \le 0.60$			17280
: $\varphi_{op} = 180°$	48	$0.25 \le \beta \le 0.75$			23040
$\varphi_{ip} = 45°$: $\varphi_{op} = 45°$	36	$0.25 \le \beta \le 0.50$			17280
: $\varphi_{op} = 90°$	36	$0.25 \le \beta \le 0.60$	$12 \le \gamma \le 30$	$0.25 \le \tau \le 1.00$	17280
: $\varphi_{op} = 180°$	36	$0.25 \le \beta \le 0.60$			17280
$\varphi_{ip} = 60°$: $\varphi_{op} = 45°$	24	$0.25 \le \beta \le 0.40$			11520
: $\varphi_{op} = 90°$	24	$0.25 \le \beta \le 0.40$			11520
: $\varphi_{op} = 180°$	24	$0.25 \le \beta \le 0.40$			11520

Table 15. Geometries used for the parameter study (braces inclined to the chord axis).

For the joints analysed, the chord length is taken $L_{ch} \geq 6d_o$, and the brace length $L_{br} \geq 3d_1$. The joint parameters (β, γ, τ and φ_{ip}) of the carry-over brace member(s) are taken equal to those of the reference brace member. Because of the enormous amount of data obtained when analysing a joint (see column 6 of tables 14 and 15), the results of SCFs and SNCFs are stored in data files. Besides the data files, graphs for SCFs are made for convenience in use and understanding of the behaviour. The results given as data files, graphs and evaluation of the SCF and SNCF results are presented in separate reports for each type of joint investigated. The reports also contain results (and evaluation) of the comparison with other available experimental and numerical work.
Experimentally obtained SCFs for $\beta > 0.95$ are excluded for comparison because of the large sensitivity of the weld shape on SCFs. Also, SCFs for $\alpha < 8.0$ are excluded because of the influence of boundary condition on SCFs.

6.5 *Results of the investigation for joints with braces perpendicular to the chord axis*

The results of the investigation on joints with braces perpendicular to the chord axis are reported in detail in [*F41-F45*, *F47*] and therefore, only the main results and conclusions will be summarized in this publication. This chapter summarizes results and conclusions on T joints, TT joints and XX joints independently. Results on SCFs due to chord member loads and results on the ratio SCF/SNCF, which are found to be common to all types of T, TT and XX joints investigated, are given separately in chapter 6.5.6.

6.5.1 Results and conclusions of the investigation on T joints

Comparison with experimental data.
From literature study it is found that most experimental work on T joints have been carried out using acrylic models without fillets [*F62*], and only limited experimentally determined SCF values based on steel models with $\beta \leq 0.95$ and $\alpha \geq 8$ are available. Table 16 summarizes the results of the comparison between numerical data from this parameter study and experimental data from tested steel models. In the comparison, all brace and chord loads are considered.

Test results Steel models	Load case	Chord			Joint parameters			SCFs experimental		Ratio parameter study / experimental		Ratio wordsworth / experimental	Ratio efthymiou / experimental
		support	d_o [mm]	α	β	γ	τ	cs	bs	cs	bs	bs	bs
[*F3*]	$F_{br,ax}$	pin	457	10	0.50	14.3	0.50	6.7		1.16			
	$F_{br,ax}$	ended	457	10	0.25	14.3	0.39	4.7		1.00			
	$F_{br,ax}$		914	10	0.50	14.3	0.50	7.7		1.02			
[*F56*]	$M_{br,op}$	fixed	457	14	0.25	14.3	0.39	2.6	2.0	1.00	1.00	1.20	1.50
	$M_{br,op}$	ended	457	14	0.25	14.3	0.28	1.8	1.7	0.95	1.00	1.18	1.53
[*F29*]	$F_{br,ax}$	pin	508	8	0.80	20.0	1.00		8.2		1.01	1.40	1.11
	$M_{br,op}$	ended	508	8	0.80	20.0	1.00		7.3		1.12	1.82	1.22
	$M_{br,op}$		508	8	0.80	31.8	1.00		10.6		1.02	1.94	1.15

Table 16. Comparison between numerical and experimental data on SCFs for T joints.

From table 16 it is concluded that the results of this parameter study are in good agreement with the experimental results.

Comparison with numerical work from Wordsworth and Smedley [F62].

For the brace member loads $F_{br;ax}$, $M_{br;ip}$ and $M_{br;op}$, a set of T joint formulae are given by Wordsworth and Smedley (Lloyd's Register of Shipping Research Laboratory, UK.). These formulae are based on an extensive study of experimentally tested small acrylic models where welds are not modelled.

Chord member locations:

It is found that the relevant SCFs for the chord crown and chord saddle locations show an acceptable agreement (differences within ±15%) between these parameter study results and the results given by formulae from Wordsworth and Smedley. Figure 32 shows the differences in SCF results for a T joint with $\tau = 0.50$.

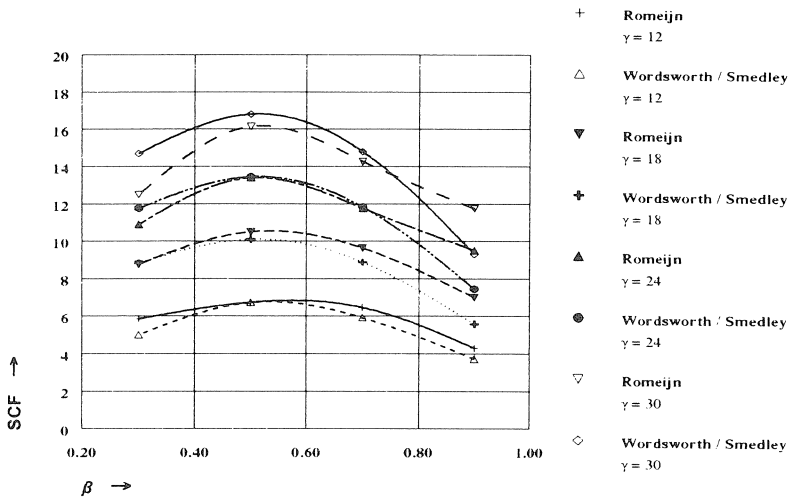

Fig. 32. T joint with $\tau = 0.50$: comparison of SCFs from the parameter study with SCFs from Wordsworth and Smedley.

Brace member locations:

The relevant SCFs for the brace crown and saddle locations show large differences (within ±100% ; see column 13 of table 16). The SCF formulae given by Wordsworth and Smedley give conservative values for the brace crown and brace saddle locations, because they are based upon measurements at the outer surface of the chord to brace connection, instead of the weld toe location, resulting in higher SCFs (see also results on modelling for tubular joint SCFs given in chapter 3.3).

Comparison with numerical work from Efthymiou [F13].

For the brace member loads $F_{br;ax}$, $M_{br;ip}$ and $M_{br;op}$, T joint formulae have been developed by Efthymiou at Shell International Petroleum Maatschappij B.V.), the Netherlands. These formulae are based on FE analyses only. The joints have been modelled with shell

elements and for the weld area solid elements. The SCFs given by Efthymiou are based on the maximum principal stress linearly extrapolated to the weld toe. For T joints, the primary stress perpendicular to the weld toe (crown and saddle locations) coincide with the maximum principal stress.

Chord member locations:

Comparison of the relevant SCFs from this parameter study and the SCF formulae given by Efthymiou, shows that for $\alpha > 12$ an acceptable agreement for the chord crown and chord saddle locations exist (differences within ±15%). For $\alpha < 12$, the formulae given by Efthymiou show for the saddle locations a large influence of α on the SCFs for the brace member loads $F_{br;ax}$ and $M_{br;op}$. This causes large differences between the SCFs from the Efthymiou formulae and those from the parameter study as well as from the experiments. As an example, figure 33 in which the SCF results are shown for a T joint with joint parameters $\beta = 0.50$, $\gamma = 30$ and $\tau = 1.00$ illustrates the differences.

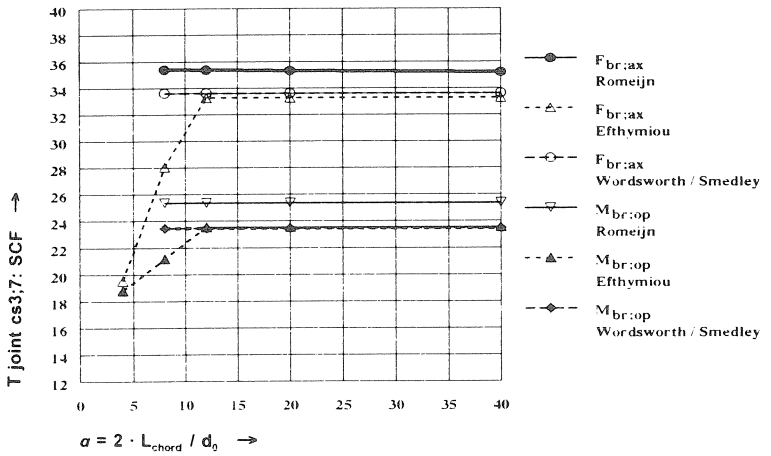

Fig. 33. Influence of short chord correction factors (for $\alpha < 12$) given by Efthymiou on the SCFs for the bs;3,7 location and comparison with parameter study results and results given by Wordsworth and Smedley.

Brace member locations:

Comparison of the relevant SCFs from the parameter study and the SCF formulae given by Efthymiou, with $\alpha > 12$ to avoid the sensitivity of the short chord correction factors on SCFs, shows large differences (within ±200%) for the brace crown and brace saddle locations.

The parameter study as well as the analyses carried out by Efthymiou include the weld shape, so that the method of modelling is not the reason for the differences. An explanation on the differences cannot directly be given. As shown in column 14 of table 16 large differences also exist between experimental data and SCFs from formulae given by Efthymiou. This is especially the case for $\alpha > 12$ (no short chord correction factor applied by Efthymiou).

6.5.2 Results and conclusions of the investigation on TT joints

Comparison with experimental data.

For the TT joint with φ_{op} = 90°, SCF results exist from steel models, and acrylic models where the SCFs are determined on the outer surface of the intersection between the brace and chord member [*F62*]. For the TT joints with φ_{op} = 45°, 70° and 135° no experimental data exist. From the comparison of T joint results between SCFs obtained on acrylic models without the weld shape included and SCFs obtained from steel models it is found that for the chord member locations an acceptable agreement in SCFs exist (differences within ±15%). Therefore, because of the very limited experimental results from steel models on SCFs for TT joints with φ_{op} = 90°, the SCF results on the chord member locations from acrylic models are also used for comparison purposes. The results of the comparison between the numerical data of this parameter study and experimental data are given in table 17 for the TT joints with φ_{op} = 90° and in table 18 for the TT joints with φ_{op} = 180°.

Test results	Load case	Chord			Joint parameters			SCFs experimental			Ratio parameter study / experimental			Ratio efthymiou / experimental		
		support	d_o [mm]	α	β	γ	τ	cs;3	cs;7	cc	cs;3	cs;7	cc	cs;3	cs;7	cc
[*F3*] (steel models)	$F_{br;ax;a}$ $F_{br;ax;b}$	pin ended	914.4	10	0.50	14.3	0.50	 -2.8	8.1 -5.5		 0.82	1.00 0.91		 1.36	0.91 0.69	
[*F62*] (acrylic models)	$F_{br;ax;a}$ $F_{br;ax;b}$ $M_{br;op;a}$ $M_{br;op;b}$ $M_{br;ip;a}$	pin ended	152.4	13.5	0.50	12.0	0.50	6.8 -2.3 -5.1 -1.4	6.6 -4.0 5.1 -0.7	3.7 2.3	1.05 0.87 1.06 0.80	1.03 1.05 1.06 1.00	1.00 0.87	0.94 1.39 0.92	0.94 0.80 0.92	0.81 0.91
[*F30*] (steel models)	$F_{br;ax;a}$ $F_{br;ax;b}$	pin ended	--	12	0.50	12.0	0.50	7.0 -2.3			1.02 0.87			0.91 1.39		

Table 17. Comparison between numerical and experimental data on SCFs for TT joints with φ_{op} = 90°.

Test results (steel models)	Load case	Chord			Joint parameters			SCFs experimental			Ratio par. study / experimental			Ratio efthymiou / experimental			Ratio smedley / experimental		
		support	d_o [mm]	α	β	γ	τ	cs	cc	bs	cs	cc	bs	cs	cc	bs	cs	cc	bs
[*F47*] (balanced loaded)	$F_{br;ax}$ $M_{br;ip}$ $M_{br;op}$	pin ended	406 406 406	12 12 12	0.60 0.60 0.60	20.0 20.0 20.0	1.00 1.00 1.00	41.2 18.5	2.6 4.2 	14.8 6.8	0.86 0.99	1.00 1.21 	0.93 1.03	0.79 0.90	1.19 0.73 	1.16 2.01	0.83 0.96	 1.23 	1.53 1.74
[*F3*] (balanced loaded)	$F_{br;ax}$	pin ended	914	10	0.50	14.4	0.50	10.9		7.3	1.00		0.98	1.02		2.18	1.07		1.15
[*F28*] (unbalanced loaded)	$F_{br;ax;a}$	fixed ended	473	8.46	0.72	10.4	0.94	13.1		8.8	0.92		0.92	0.65		0.69	no formulae		

Table 18. Comparison between numerical and experimental data on SCFs for TT joints with φ_{op}=180°.

From tables 17 and 18, it is concluded that the results of this parameter study are in reasonable agreement with the experimental results.

Comparison with numerical work from Wordsworth and Smedley [F65].
Wordsworth and Smedley give some SCF formulae for a TT joint (180°) with balanced axially loaded brace members $F_{br;ax;a}$ + $F_{br;ax;b}$ and for balanced out-of-plane bending moment loaded brace members $M_{br;op;a}$ + $M_{br;op;b}$. They also propose the use of the T joint formulae for (unbalanced) in-plane moment $M_{br;ip;a}$ loaded brace member '*a*' of the TT joint (180°). The comparison of SCF data from the parameter study with SCF formulae given by Wordsworth and Smedley results in similar conclusions as mentioned for the T joint, namely that acceptable agreement is obtained for the SCFs on the chord member, and large differences for the SCFs on the brace member. Those large differences also exist when comparing with experimental data (see column 20 of table 18). The reasons for the differences observed are the same as those given in chapter 6.5.1. which discusses the SCF comparisons for T joints.

Comparison with numerical work from Efthymiou [F13].
SCF formulae on TT joints (180°) are given by Efthymiou for a loaded reference brace member '*a*' ($F_{br;ax;a}$, $M_{br;ip;a}$ and $M_{br;op;a}$) and/or a loaded carry-over brace member *b* ($F_{br;ax;b}$, $M_{br;ip;b}$ and $M_{br;op;b}$). Efthymiou also published SCF influence functions on carry-over effects (due to $F_{br;ax;b}$ only) when varying the out-of-plane angle φ_{op} between the two braces '*a*' and *b*. A comparison of SCF data from this parameter study with the SCF formulae by means of influence functions given by Efthymiou shows large differences in SCF results for the saddle and crown locations of the chord and brace member. As an example, figure 34 illustrates the differences in SCFs due to $F_{br;ax;b}$ for the chord and brace saddle locations of a TT joint with various values of φ_{op}. From the parameter study results, and the test results given in table 17, it is shown that large differences in SCFs due to $F_{br;ax;b}$ exist for the two saddle locations cs;3 and cs;7. The influence functions on SCFs given by Efthymiou, however, assume the same SCF value for both saddle locations. For the chord crown and brace crown locations, the influence functions given by Efthymiou represent nominal chord bending stresses caused by axially loaded brace member *b*. These stresses do not include the hot spot stresses due to the non uniform stiffness of the joint, which makes a realistic comparison impossible.

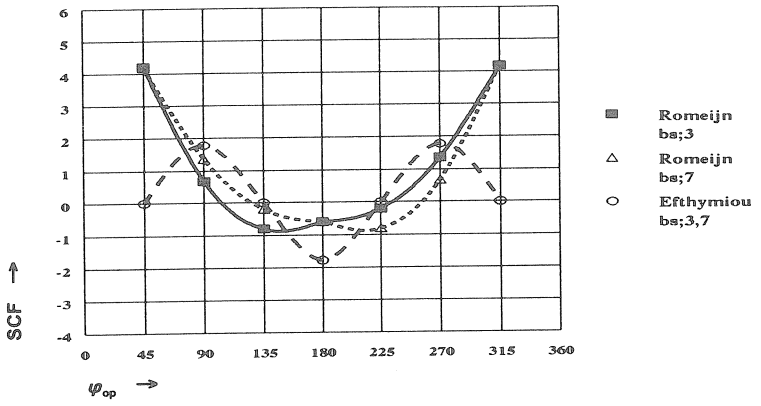

Fig. 34. SCFs due to $F_{br;ax;b}$ for the chord saddle locations of brace '*a*' of a TT joint with different φ_{op}. Results shown for $\beta = 0.30$, $\gamma = 30$ and $\tau = 1.00$.

6.5.3 Importance of out-of-plane carry-over effects on SCFs

From an investigation on SCFs caused by out-of-plane carry-over effects (SCFs due to load cases $F_{br;ax;b}$, $M_{br;ip;b}$ and $M_{br;op;b}$), with varying joint parameters β, γ, τ and φ_{op}, it is found that these SCFs in many cases cannot be neglected. This is dependent on a combination of the following aspects.

- *The type of carry-over loading considered.*
- *The location of interest.*
- *The joint parameters considered.*

Some results showing the importance of SCFs caused by out-of-plane carry-over effects are summarized in table 19. About the importance of SCFs caused by out-of-plane carry-over effects it is concluded that:

- *The influence of changes in γ and τ on out-of-plane carry-over effects, although considerable for γ, is generally small compared to the influence of changes in β and φ_{op}.*
- *For the chord saddle and brace saddle locations, the load cases $F_{br;ax;b}$ and $M_{br;op;b}$ cause large carry-over effects. This is especially the case with increasing β. Figure 35 shows for a TT joint with φ_{op} = 180° and τ = 1.00 the influence of β on SCFs caused by reference effects ($F_{br;ax;a}$) and carry-over effects ($F_{br;ax;b}$).*
- *As illustrated in figure 34 , depending on φ_{op}, the SCF results for the two saddle locations (chord and brace member) might differ entirely. Comparison of the test results given in columns 9 and 10 of table 17 results in the same conclusions on the existence of a large difference in SCFs between the two saddle locations.*
- *The carry-over effects caused by $M_{br;ip;b}$ are negligible for all locations considered.*
- *The carry-over effects caused by $M_{br;op;b}$ are negligible for the chord crown and brace crown locations.*
- *When varying φ_{op}, a harmonic function for SCFs due to carry-over effects exists, and the largest absolute SCFs caused by the carry-over effects are found in the region forming the shortest gap.*

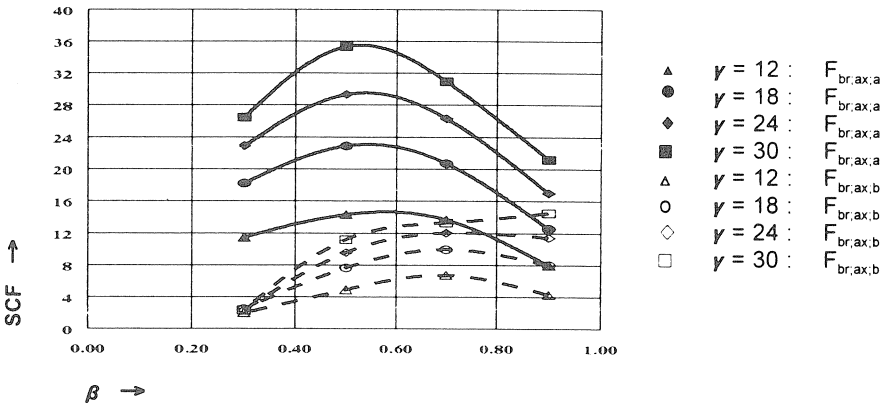

Fig. 35. Influence of β on SCFs caused by reference effects $F_{br;ax;a}$ and carry-over effects $F_{br;ax;b}$. TT joint with φ_{op} = 180° and τ = 1.00. SCFs given for the cs;3,7 locations of the reference brace.

φ_{op}	β	Load case			Location of interest					
		$F_{br;ax;b}$	$M_{br;ip;b}$	$M_{br;op;b}$	cc	bc	cs;3	cs;7	bs;3	bs;7
45°	0.30	*	*	*	- - -	- -- --	++ -- +	+ -- +	++ -- -	++ -- -
70°	0.50	*	*	*	++ - -	-- -- -	+++ -- +	++ -- +	+++ -- +	+ -- +
90°	0.30	*	*	*	- -- --	- -- --	+ -- +	+ -- +	+ -- -	+ -- -
	0.50	*	*	*	- -- --	- -- --	+ -- +	+++ -- +	+ -- +	+++ -- +
	0.65	*	*	*	++ - +	-- - -	++ -- ++	+++ -- +	++ -- ++	+++ -- ++
135°	0.30	*	*	*	-- -- --	-- -- --	+ -- -	-- -- -	+ -- --	- -- --
	0.50	*	*	*	- -- --	- -- --	+ -- +	- -- +	+ -- -	- -- +
	0.70	*	*	*	- - --	-- -- --	++ -- +	++ -- +	++ -- +	++ -- ++
180°	0.30	*	*	*	- -- --	- -- --	+ -- --		+ -- --	
	0.50	*	*	*	- -- --	- -- --	++ -- -		++ -- -	
	0.70	*	*	*	- - --	- -- --	+++ -- +		+++ -- +	
	0.90	*	*	*	+++ - --	- -- --	+++ -- ++		+++ -- ++	

SCF_{cc} are scfs caused by carry-over effects (brace member loads $F_{br;ax;b}$, $M_{br;ip;b}$ and $M_{br;op;b}$).
SCF_{re} are scfs caused by reference effects (brace member loads $F_{br;ax;a}$, $M_{br;ip;a}$ and $M_{br;op;a}$).

+++ = $SCFs_{cc} > 50\% \cdot SCFs_{re}$ and $SCFs_{cc} > 0.50$.
++ = $SCFs_{cc} > 30\% \cdot SCFs_{re}$ and $SCFs_{cc} > 0.50$.
+ = $SCFs_{cc} > 10\% \cdot SCFs_{re}$ and $SCFs_{cc} > 0.50$.
- = $SCFs_{cc} < 0.50$.
-- = $SCFs_{cc} < 0.10$.

Table 19. Importance of out-of-plane carry-over effects for TT joints. ($0.25 \leq \tau \leq 1.00$ and $12 \leq \gamma \leq 30$).

6.5.4 Influence of the presence of an out-of-plane member on SCFs due to reference loading

The influence of the presence of the carry-over brace member *b* on SCFs due to reference loading which was ignored up to now, is found to be dependent on a combination of the following aspects:

- *The reference loading considered.*
- *The location of interest.*

- *The joint parameters considered.*

From comparison of SCFs of T joints and TT joints it is found that the influence of the presence of the out-of-plane carry-over brace member *b* on SCFs due to reference loadings $M_{br;ip;a}$ and $M_{br;op;a}$ can be neglected. This because, for the T and TT joints analysed, the maximum differences in SCFs for all locations considered (crown, saddle and inbetween) are found to be smaller than ±10%. For the reference loading $F_{br;ax;a}$, however, the influence of the presence of the out-of-plane carry-over brace member *b* on SCFs due to reference loading cannot always be neglected.
As an example for $F_{br;ax;a}$, due to the existence of the out-of-plane carry-over brace member *b*, a large influence on SCFs (differences with relation to T joints within 40%) is found for the two saddle locations. Figure 36 illustrates the difference in SCFs between a T joint and a TT joint with $\varphi_{op} = 90°$. Figure 36 shows that for $\beta > 0.50$ and axial loading on the reference brace, the SCFs for the chord saddle location at the gap location between the two braces '*a*' and *b* are much smaller then those for the other chord saddle location.

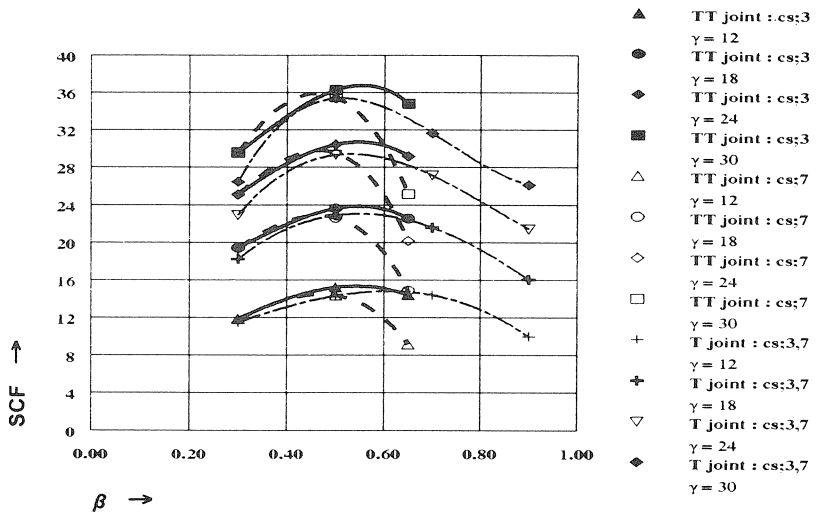

Fig. 36. Differences in SCFs caused by $F_{br;ax;a}$ for the saddle locations of a T joint and a TT joint with $\varphi_{op} = 90°$. $\tau = 1.00$.

Results showing the influence of the presence of the out-of-plane carry-over brace member *b* on SCFs caused by the reference loading $F_{br;ax;a}$ are summarized in table 20. This table shows the maximum range of the ratio *SCF T joint / SCF TT joint*, which exists for the combination $\gamma_{min};\tau_{min}$ (lower bound) and $\gamma_{max};\tau_{max}$ (upper bound). The results given in table 20 leads to the additional conclusion that the influence of the presence of the out-of-plane carry-over brace member *b* on SCFs due to reference loading $F_{br;ax;a}$ mainly depends on the size of the smallest gap region (combination of β and φ_{op}).
In general, for all locations considered, decrease of the size of the gap region results in a decrease of SCFs caused by the reference loading $F_{br;ax;a}$.

φ_{op}	β	Lower bound	Upper bound	Location of interest					
		γ=12;τ=0.25	γ=30;τ=1.00	cc	bc	cs;3	cs;7	bs;3	bs;7
45°	0.30	*	*	0.96 1.38	0.97 1.05	1.00 0.89	1.05 0.96	1.01 0.87	1.01 0.87
70°	0.50	*	*	1.05 1.31	1.00 1.03	1.10 1.21	1.13 1.21	1.01 1.03	1.05 1.07
90°	0.30	*	*	0.98 1.13	0.98 1.04	0.98 0.89	0.99 0.89	1.00 0.90	1.00 0.90
	0.50	*	*	1.06 1.21	1.01 1.03	0.96 0.98	0.99 1.00	1.00 1.00	1.00 1.00
135°	0.30	*	*	1.00 1.00	0.98 1.01	1.00 0.88	1.00 0.89	1.00 0.87	1.00 0.87
	0.50	*	*	1.00 0.98	1.01 1.01	0.99 1.10	0.98 1.10	1.04 1.12	1.03 1.11
	0.70	*	*	1.00 1.00	1.01 1.02	0.99 1.13	1.02 1.13	1.04 1.15	1.04 1.15
180°	0.30 and 0.50	*	*	all ≈ 1.00					
	0.70	*	*	1.00 1.01	1.00 1.01	1.02 1.03		1.02 1.03	
	0.90	*	*	1.00 1.02	1.00 1.03	1.16 1.23		1.13 1.21	

Table 20. Influence of the presence of carry-over brace member *b* on SCFs caused by the reference loading $F_{br;ax;a}$. Maximum range of the ratio *SCF T joint / SCF TT joint* shown.

6.5.5 Results and conclusions of the investigation on XX joints [*F47*]

Comparison with experimental data.

As part of a Joint Industry Programme for research on the ultimate static strength of multiplanar XX joints, measurements have also been carried out for the determination of SNCFs [*F47*]. Nine multiplanar XX joints have been investigated. As an illustration figure 37 shows the strip gauges for measuring the strains at the saddle and crown locations for one of the tested XX joints. All tested XX joints have the same joint parameters, namely, $\alpha = 12$, $\beta = 0.60$, $\gamma = 20$, $\tau = 1.00$ and a chord dimension of ∅ 406.4 x 10.

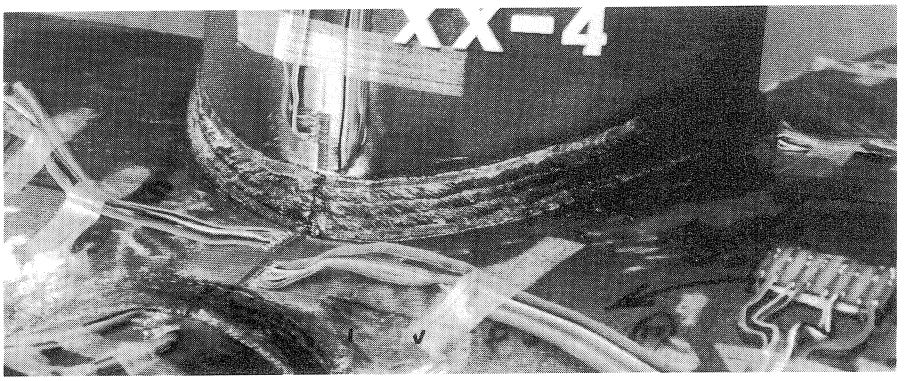

Fig. 37. Strip gauges for measuring the strains at the saddle and crown locations of an XX joint.

The results of the comparison between numerical and experimental data are given in table 21 and figure 38.

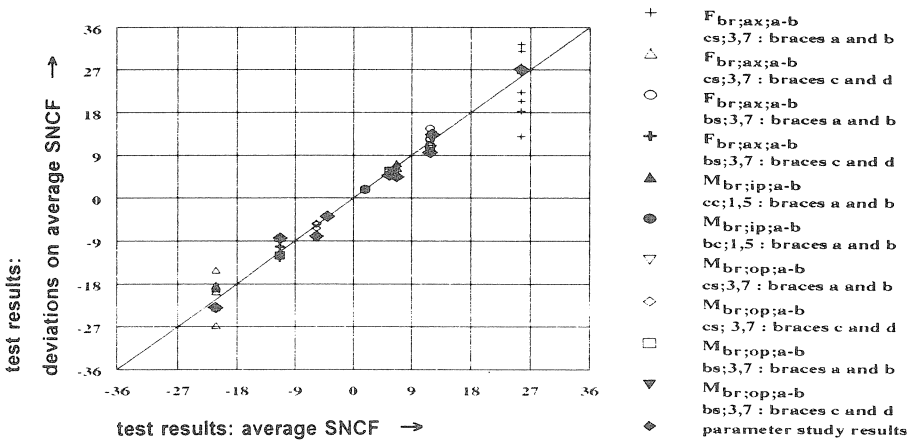

Fig. 38. XX joints: comparison of experimental data on SNCFs with results from the parameter study. (Relevant SNCFs > 2.0 shown only).

Tested joint	Load case (balanced)	Experimental data on SNCFs							
		loaded brace members				unloaded brace members			
		cs	cc	bs	bc	cs	cc	bs	bc
XX2	$F_{br;ax;a-b}$	26.4	1.5	12.3	0.3	-23.1	0.5	-11.4	0.2
XX3	$F_{br;ax;a-b}$	31.0	1.7			-26.7	0.4	-8.3	
XX3	$F_{br;ax;c-d}$		1.5	10.0			0.7	-9.0	
XX4	$F_{br;ax;a-b}$	26.3	2.0	14.7		-22.6	0.3	-12.2	
XX4	$F_{br;ax;c-d}$	27.8	2.6	12.5		-19.6	0.4	-12.5	
XX6	$M_{br;ip;a-b}$		7.3		2.1				
XX7	$F_{br;ax;c-d}$	22.2		11.2		-18.6	1.3	-13.1	-0.10
XX7	$M_{br;ip;a-b}$	0.0	6.4	-0.1	1.7	0.2		0.1	
XX8	$F_{br;ax;c-d}$	32.4		12.5		-22.6	1.1	-11.9	0.0
XX8	$M_{br;ip;a-b}$	0.1	6.3	-0.1	1.6	-0.1		-0.1	
XX10	$M_{br;op;a-b}$	13.4		5.9		-5.3		-3.9	
XX11	$F_{br;ax;c-d}$	20.4		10.5		-18.3		-12.7	
XX11	$M_{br;op;a-b}$	10.5		5.1		-6.3		-3.9	
XX12	$F_{br;ax;c-d}$	18.3		11.0		-19.0		-10.2	
XX12	$M_{br;op;a-b}$	12.4		5.4		-5.5		-4.3	
average test results	$F_{br;ax;a-b}$	25.6	1.8	11.8	0.3	-21.3	0.7	-11.3	0.1
	$M_{br;ip;a-b}$	0.0	6.7	-0.1	1.8	0.0		0.0	
	$M_{br;op;a-b}$	12.1		5.5		-5.7		-4.0	
ratio SNCF* parameter study / experimental	$F_{br;ax;a-b}$	1.06		0.81		1.08		0.74	
	$M_{br;ip;a-b}$		0.66						
	$M_{br;op;a-b}$	1.11		0.87		1.42		0.95	

* Ratio given for experimental SNCF > 2.0

Table 21. Comparison between numerical and experimental data on SNCFs for XX joints.

Taking into account the large scatter on SNCFs from the tested XX joints, which is mainly caused by deviations in size of weld shape, as shown in figure 38 a reasonable agreement with the results from this parameter study exists.

6.5.6 SCFs caused by chord member loads

From the parameter study it is found that the influence of the presence of an out-of-plane carry-over brace member *b* on SCFs caused by chord member loads can be neglected. Therefore, only the results of SCFs for the chord member loads on a T joint are discussed. A small variation in SCFs exists for the whole range of joint parameters considered.
The range of SCFs obtained are given in table 22, whereas the values for the chord crown locations for $F_{ch;ax}$ are shown in figure 39.

Location	Range of SCFs	
	load case	
	$F_{ch;ax}$	$M_{ch;ip}^{*}$
chord crown	1.00 < SCF < 1.60	1.10 < SCF < 1.70
brace crown	-0.15 < SCF < 0.10	-0.10 < SCF < 0.30
chord saddle	-0.20 < SCF < 0.10	-0.40 < SCF < 0.00
brace saddle	-0.30 < SCF < 0.70	-0.30 < SCF < 0.50

* Causing a nominal bending stress of 1 N/mm^2 at the chord outer surface along the plane of the crown.

Table 22. Range of SCFs caused by chord member loads (brace members: φ_{ip} = 90°).

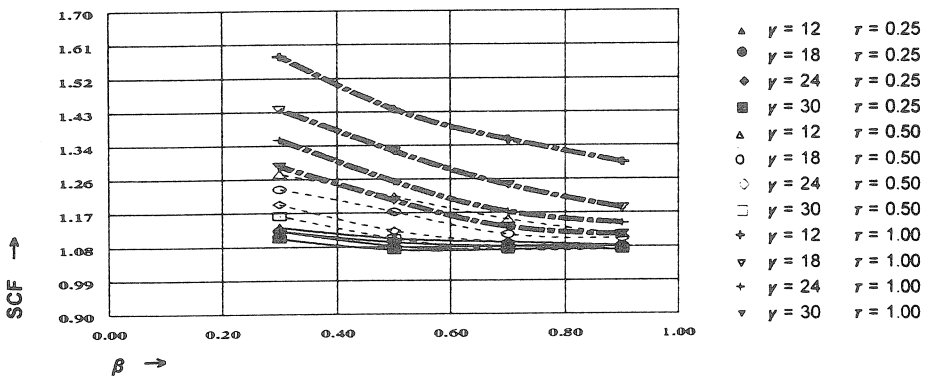

Fig. 39. SCFs for the chord crown location caused by $F_{ch;ax}$.

From the SCF results due to chord member loads (axial + bending), the following conclusions are made:

Chord crown location.

- As expected, the highest SCFs are found for this location.
- SCFs due to chord bending $M_{ch;ip}$ are found to be slightly larger (10%) compared to SCFs due to $F_{ch;ax}$.
- The value of SCF increases with decreasing β, γ and increasing τ.

Brace saddle location.

- SCFs due to chord bending $M_{ch;ip}$ are found to be smaller than SCFs due to $F_{ch;ax}$ (up to a maximum of 25%).
- The value of SCF increases with decreasing γ and τ, while for the β influence the maximum SCF occurs for about $\beta = 0.70$.

6.5.7 Results on the relationship between SCF and SNCF

The relationship between SCF and SNCF, identified as *snf* (=SCF/SNCF) is found to be dependent on the combination of load cases, locations of interest and joint parameters considered. The influence of the presence of an out-of-plane carry-over brace member *b* on *snf* caused by reference effects is found to be negligible (differences within 5%). The *snf* results of the investigation on joints with braces perpendicular to the chord axis are summarized in table 23, whereas the *sncf* results for the cc;1,5 location in case of $F_{ch;ax}$ and the *sncf* results for the bs;3,7 location in case of $F_{br;ax;a}$ are shown in figure 40.

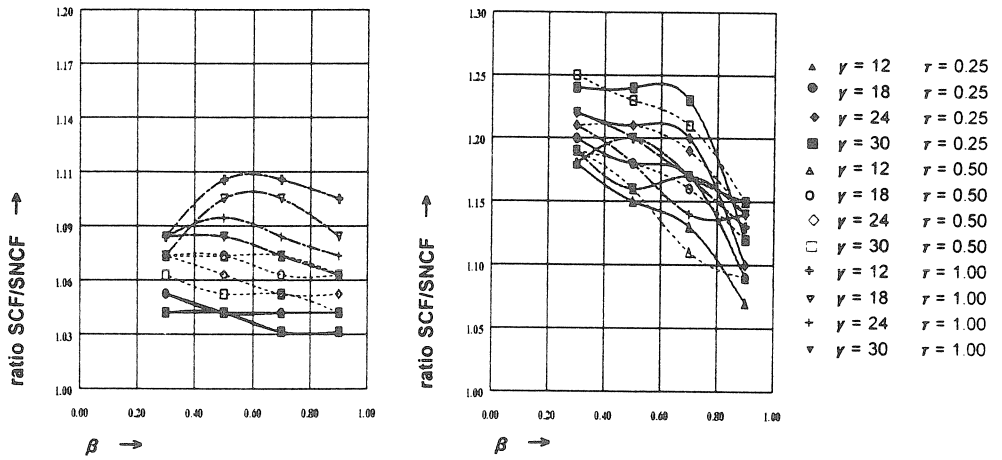

Fig. 40. Ratio SCF/SNCF for the cc;1,5 location of a T joint loaded by $F_{ch;ax}$ (left figure) and for the bs;3,7 location of a T joint loaded by $F_{br;ax;a}$ (right figure).

From the study on the relationship between SCF and SNCF, the following main conclusions are given:

- Chord member loads give smaller *snfs* and a smaller range of variation compared to brace member loads.
- For the reference effects as well as carry-over effects, the range of variation on *snfs* for the chord saddle locations is smaller than for the brace saddle locations.

Joint	Load case	Location	*snf* (=SCF/SNCF)		Influence of joint parameter		
			average	range	β	γ	τ
	Reference loading						
T	$F_{br;ax;a}$	cs	1.16	$1.12 < snf < 1.21$	-	o	-
		bs	1.18	$1.07 < snf < 1.25$	-	+	- : $\beta \leq 0.70$ + : $\beta > 0.70$
		cc	1.25	$1.16 < snf < 1.33$	o	-	- : $\beta \leq 0.70$ + : $\beta > 0.70$
		bc	*	*			
	$M_{br;ip;a}$	cc	1.28	$1.13 < snf < 1.35$	o	o	-
		bc	1.27	$1.18 < snf < 1.34$	o	+	+
	$M_{br;op;a}$	cs	1.18	$1.13 < snf < 1.21$	-	o	-
		bs	1.20	$1.11 < snf < 1.29$	-	-	- : $\beta \leq 0.70$ + : $\beta > 0.70$
	$F_{ch;ax}$	cc	1.05	$1.02 < snf < 1.12$	o	-	+
	$M_{ch;ip}$ **	cc	1.07	$1.02 < snf < 1.15$	o	o	+
	Carry-over loading						
TT φ_{op}=90°	$F_{br;ax;b}$	cs;3	1.17	$1.12 < snf < 1.19$	-	o	-
		cs;7	1.19	$1.11 < snf < 1.28$	-	o	-
		bs;3	1.18	$1.13 < snf < 1.23$	-	+	-
		bs;7	1.22	$1.09 < snf < 1.35$	-	+	-
TT φ_{op}=135°	$F_{br;ax;b}$	cs;3	1.23	$1.16 < snf < 1.26$	-	o	-
		cs;7	1.26	$1.22 < snf < 1.32$	-	o	-
		bs;3	1.27	$1.21 < snf < 1.33$	-	o	-
		bs;7	1.31	$1.22 < snf < 1.40$	-	o	-
TT φ_{op}=180°	$F_{br;ax;b}$	cs	1.15	$1.08 < snf < 1.21$	-	o	- : $\beta \leq 0.70$ + : $\beta > 0.70$
		bs	1.17	$1.05 < snf < 1.27$	-	o	- : $\beta \leq 0.70$ + : $\beta > 0.70$

- = Increase of β, γ or τ results in a decrease of *snf*.
- o = Influence of β, γ or τ on *snf* is negligible.
- \+ = Increase of β, γ or τ results in an increase of *snf*.
- * = SNCF < 1.00.
- ** = Causing a nominal bending stress of 1 N/mm² at the chord outer surface along the plane of the crown.

Table 23. Results of the investigation on the relationship between SCFs and SNCFs. (SNCF > 1.00).

6.6 *Results of the investigation for joints with braces inclined to the chord axis*

The main results and conclusions on the following subjects are summarized in this chapter.

- *Influence of φ_{ip} on SCFs caused by brace member loads.*
  (Loads considered are: $F_{br;ax;a}$, $M_{br;ip;a}$ and $M_{br;op;a}$).
- *Influence of φ_{ip} on SCFs caused by chord member loads.*

(Loads considered are: $F_{ch;ax}$ and $M_{ch;ip}$).

- *Importance of in-plane carry-over effects on SCFs.*
  (Loads considered are: $F_{br;ax;c}$, $M_{br;ip;c}$ and $M_{br;op;c}$).
- *Influence of the presence of an in-plane carry-over brace member 'c' on SCFs due to reference loadings.*
  (Loads considered are: $F_{br;ax;a}$, $M_{br;ip;a}$ and $M_{br;op;a}$).
- *Relationship between SCF and SNCF.*
  (Loads considered are: $F_{br;ax;a,c}$, $M_{br;ip;a,c}$, $M_{br;op;a,c}$, $F_{ch;ax}$ and $M_{ch;ip}$).

In an identical way as described for T joints, a comparison of Y, K and KK joint SCFs with available experimental work has been carried out. The comparison results in the same conclusion as those found for T joints, namely a good agreement (differences within ±10%) exists between numerical results from the parameter study and the experimental results.

6.6.1 Influence of φ_{ip} on SCFs caused by brace member loads

Generally, for all brace member loads $F_{br;ax;a}$, $M_{br;ip;a}$ and $M_{br;op;a}$, larger SCFs are found with increasing φ_{ip}. This is because increasing φ_{ip} results in a smaller brace to chord intersection area and hence a smaller region for stress distribution. Also in case of $F_{br;ax;a}$, increase of φ_{ip} results in a larger component perpendicular to the chord axis. A study on the SCFs for the chord crown and brace crown locations shows that the existing numerical work makes no distinction in toe and heel location. From the parameter study results however, it is found that the SCFs for those two locations entirely differ from each other. Depending on the load case $F_{br;ax;a}$ or $M_{br;ip;a}$ and joint parameters β, γ, τ and φ_{ip} considered, the largest SCF occurs at the toe or heel location. For Y joints with β = 0.40, γ = 30 and τ = 1.00, as an example the influence of φ_{ip} on SCFs due to brace member loads $F_{br;ax;a}$, $M_{br;ip;a}$ and $M_{br;op;a}$ is shown in figures 41, 42 and 43.

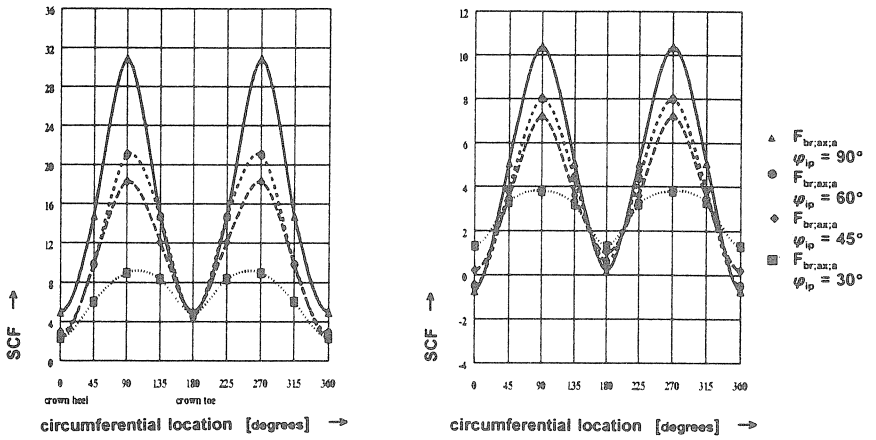

Fig. 41. Influence of φ_{ip} on SCFs due to $F_{br;ax}$. Results shown for the chord member locations (left figure) and brace member locations (right figure) of a Y joint with β = 0.40, γ = 30 and τ = 1.00.

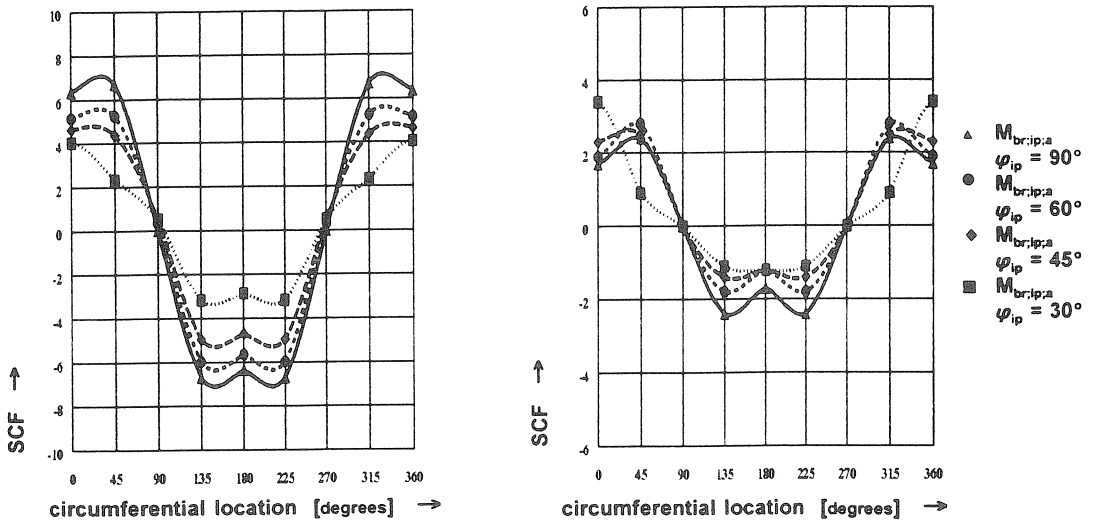

Fig. 42. Influence of φ_{ip} on SCFs due to $M_{br;ip}$. Results shown for the chord member locations (left figure) and brace member locations (right figure) of a Y joint with β = 0.40, γ = 30 and τ = 1.00.

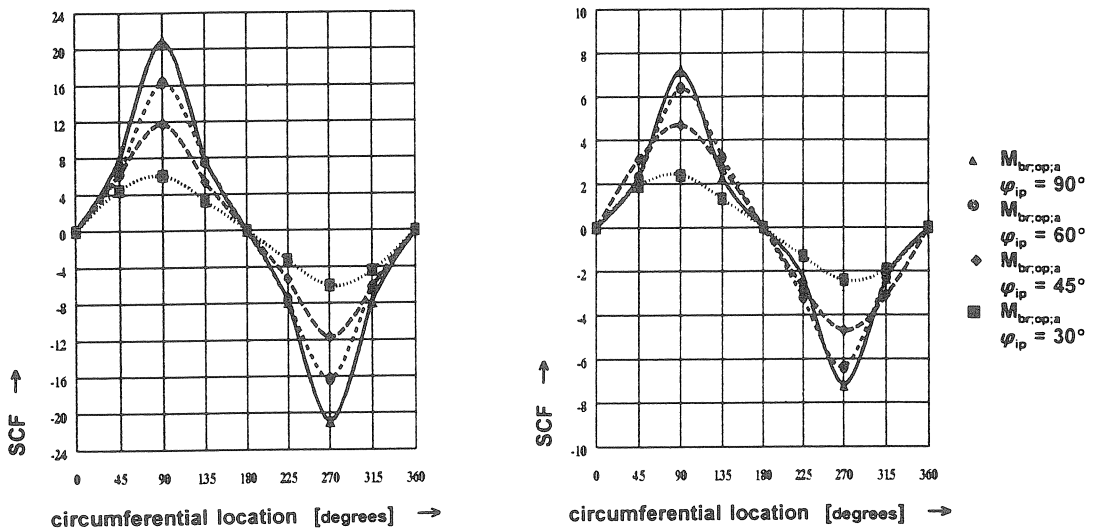

Fig. 43. Influence of φ_{ip} on SCFs due to $M_{br;op}$. Results shown for the chord member locations (left figure) and brace member locations (right figure) of a Y joint with β = 0.40, γ = 30 and τ = 1.00.

6.6.2 Influence of φ_{ip} on SCFs caused by chord member loads

The results of SCFs for the chord member loads on a Y joint are discussed only. This is

because the influence of the presence of in-plane and out-of-plane carry-over brace members on SCFs caused by chord member loads is found to be negligible. The range of SCFs obtained is given in table 24. As an example, SCFs for the chord crown heel location (cc;1) caused by $F_{ch;ax}$ are shown in figure 44. From the Y joint SCF results caused by chord member loads, the following conclusions are made.

- *For the whole range of φ_{ip} investigated, the significant SCFs occur on the chord crown (heel + toe) and brace saddle locations.*
- *Decrease of φ_{ip} results in an increase of SCFs. This is especially the case for the chord crown locations, and so, Y joints give larger SCFs for chord loads compared to T joints.*
- *The SCFs for the toe locations (chord and brace member) are smaller than the SCFs for the heel locations, and the differences increase with decreasing φ_{ip}.*
- *Regarding the influence of joint parameters β, γ and τ on the SCFs and the difference in SCFs caused by $F_{ch;ax}$ and $M_{ch;ip}$, identical conclusions are made as given for T joints (see chapter 6.5.6).*

Location	Range of SCFs	
	load case	
	$F_{ch;ax}$	$M_{ch;ip}$*
	$\varphi_{ip} = 60°$	
chord crown : heel	1.00 < SCF < 1.65	1.10 < SCF < 1.75
: toe	1.00 < SCF < 1.60	1.05 < SCF < 1.70
brace crown : heel	-0.25 < SCF < 0.15	-0.20 < SCF < 0.45
: toe	-0.15 < SCF < 0.10	0.00 < SCF < 0.20
chord saddle	-0.20 < SCF < 0.05	-0.35 < SCF < 0.10
brace saddle	-0.10 < SCF < 1.20	-0.20 < SCF < 0.80
	$\varphi_{ip} = 45°$	
chord crown : heel	1.05 < SCF < 2.00	1.20 < SCF < 2.20
: toe	1.00 < SCF < 1.95	1.00 < SCF < 2.10
brace crown : heel	-0.40 < SCF < 0.25	-0.30 < SCF < 0.60
: toe	-0.20 < SCF < 0.15	0.00 < SCF < 0.25
chord saddle	-0.25 < SCF < 0.05	-0.30 < SCF < -0.05
brace saddle	0.20 < SCF < 1.20	0.10 < SCF < 0.90
	$\varphi_{ip} = 30°$	
chord crown : heel	1.30 < SCF < 2.90	1.35 < SCF < 3.15
: toe	1.00 < SCF < 2.35	1.20 < SCF < 2.40
brace crown : heel	-0.50 < SCF < 0.45	-0.45 < SCF < 1.05
: toe	-0.20 < SCF < 0.40	0.10 < SCF < 0.50
chord saddle	-0.40 < SCF < 0.00	-0.50 < SCF < -0.10
brace saddle	0.40 < SCF < 1.20	0.30 < SCF < 0.95

* Causing a nominal bending stress of 1 N/mm^2 at the chord outer surface along crown plane.

Table 24. Range of SCFs caused by chord member loads on Y joints.

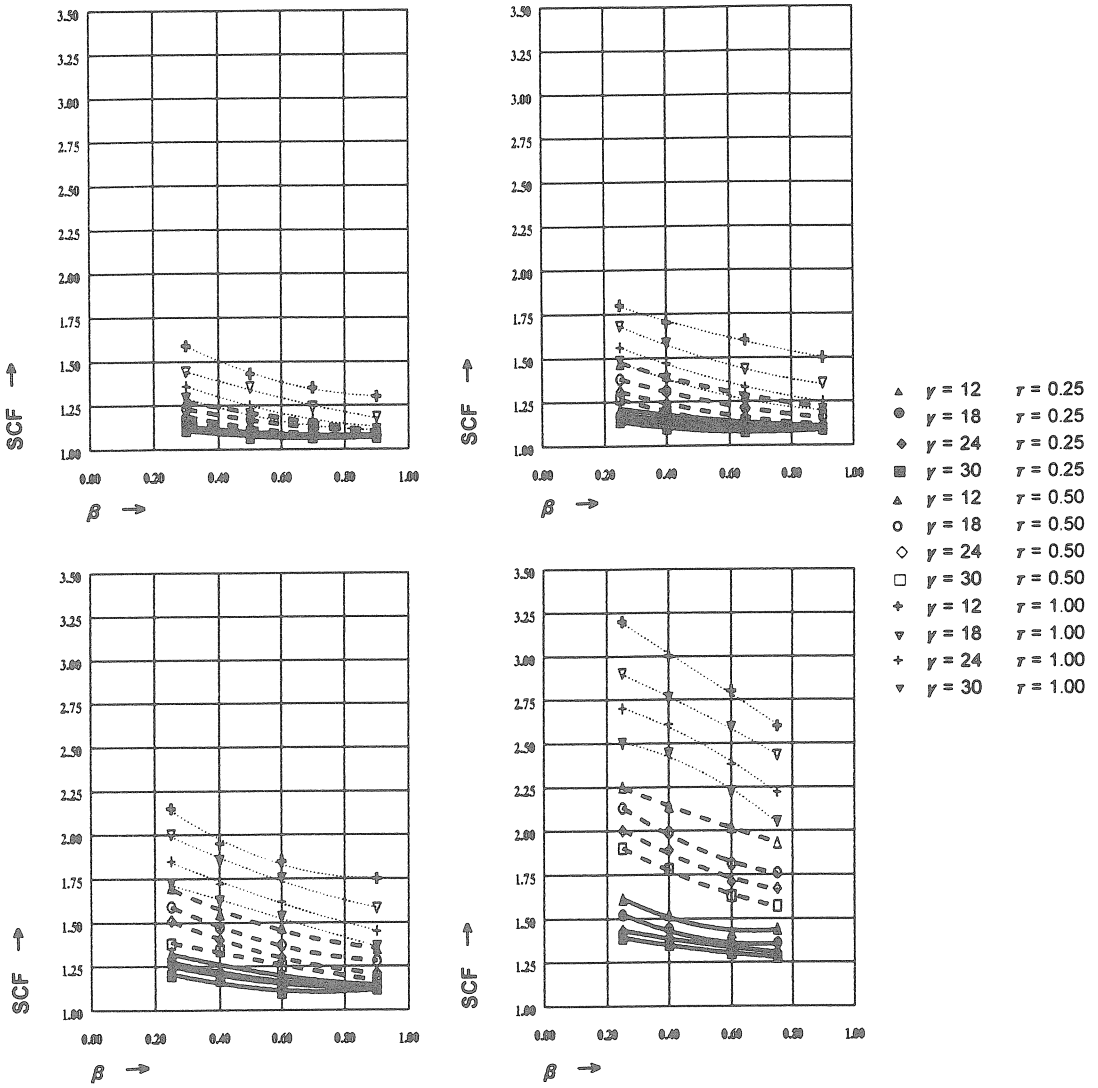

Fig. 44. Y joint: SCFs for the chord crown heel location (cc;1) caused by $F_{ch;ax}$. Top left figure φ_{ip} = 90° and top right figure φ_{ip} = 60°. Bottom left figure φ_{ip} = 45° and bottom right figure φ_{ip} = 30°.

6.6.3 Importance of in-plane carry-over effects on SCFs

In-plane carry-over effects on SCFs exist in case of brace member loads $F_{br;ax;c}$, $M_{br;ip;c}$ and $M_{br;op;c}$ of for example a K joint. The importance of SCFs due to in-plane carry-over effects of a K joint, is found to be as summarized in table 25. In this table, results of the importance of SCFs are given for $\gamma_{min};\tau_{min}$ (lower bound) and $\gamma_{max};\tau_{max}$ (upper bound). Figures 45 and 46 show some of the SCF results obtained.

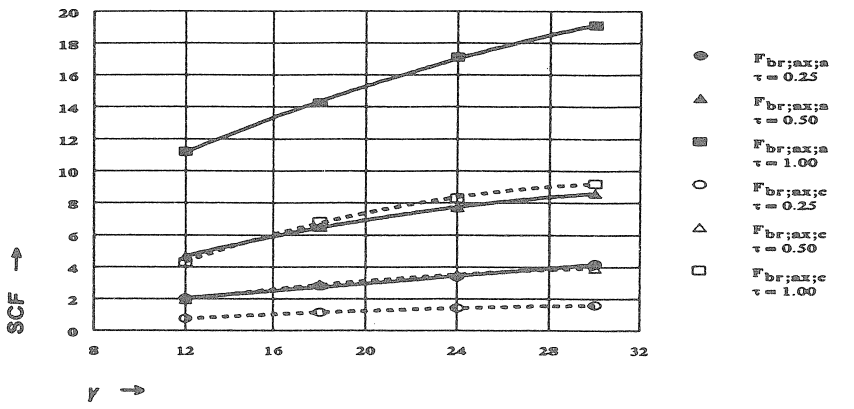

Fig. 45. Influence of γ and τ on SCFs caused by in-plane carry-over loading $F_{br;ax;c}$ and reference loading $F_{br;ax;a}$ for the chord saddle location of a K joint with β=0.40 and φ_{ip}=60°.

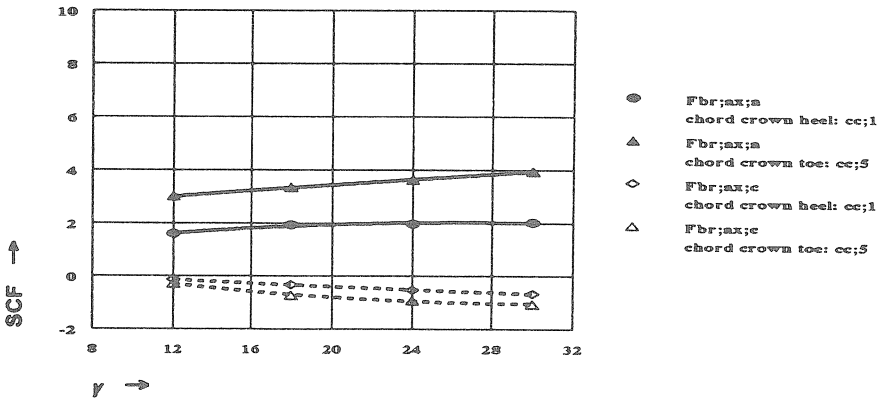

Fig. 46. In-plane carry-over SCF results ($F_{br;ax;c}$) and reference SCF results ($F_{br;ax;a}$) for the two chord crown locations (toe and heel) of a K joint with β=0.40, τ=0.50 and φ_{ip}=60°.

φ_{ip}	β	Load case	Location of interest											
			cc:1 (heel)		cc:5 (toe)		bc:1 (heel)		bc:5 (toe)		cs;3,7		bs;3,7	
			γ=12 τ=0.25	γ=30 τ=1.00	γ=12 τ=0.25	γ=30 τ=1.00	γ=12 τ=0.25	γ=30 τ=1.00	γ=12 τ=0.25	γ=30 τ=1.00	γ=12 τ=0.25	γ=30 τ=1.00	γ=12 τ=0.25	γ=30 τ=1.00
60°	0.25	$F_{br;ax;c}$	--	+	--	+	-	++	--	+	+	++	+	+
		$M_{br;ip;c}$	--	--	--	--	--	--	--	--	--	++	--	--
		$M_{br;op;c}$	--	--	--	--	--	--	--	--	-	+	--	-
	0.40	$F_{br;ax;c}$	--	+	--	+	-	+++	--	+	+	++	+	++
		$M_{br;ip;c}$	--	-	--	+	--	-	--	+	--	+++	-	++
		$M_{br;op;c}$	--	--	--	--	--	--	--	--	-	+	-	+
45°	0.25	$F_{br;ax;c}$	--	+	--	+	--	++	--	-	-	++	-	+
		$M_{br;ip;c}$	--	--	--	--	--	--	--	--	--	-	--	--
		$M_{br;op;c}$	--	--	--	--	--	--	--	--	--	+	--	-
	0.40	$F_{br;ax;c}$	--	++	--	+	--	++	--	-	-	+	-	+
		$M_{br;ip;c}$	--	--	--	-	--	--	--	--	--	+	--	-
		$M_{br;op;c}$	--	-	--	--	--	--	--	--	--	+	--	+
	0.60	$F_{br;ax;c}$	-	++	-	+	-	++	-	-	-	++	-	++
		$M_{br;ip;c}$	--	++	--	-	--	--	--	--	--	++	--	-
		$M_{br;op;c}$	--	-	--	--	--	--	--	--	-	+	--	+
30°	0.25	$F_{br;ax;c}$	--	+++	--	+	--	--	--	--	--	+	--	-
		$M_{br;ip;c}$	--	--	--	--	--	--	--	--	--	--	--	--
		$M_{br;op;c}$	--	--	--	--	--	--	--	--	--	--	--	--
	0.40	$F_{br;ax;c}$	--	+++	--	++	--	++	--	-	--	++	--	+
		$M_{br;ip;c}$	--	--	--	--	--	--	--	--	--	-	--	--
		$M_{br;op;c}$	--	--	--	--	--	--	--	--	--	-	--	--
	0.60	$F_{br;ax;c}$	--	+++	--	++	--	-	--	-	-	++	--	+
		$M_{br;ip;c}$	--	--	--	--	--	--	--	--	--	++	--	-
		$M_{br;op;c}$	--	--	--	--	--	--	--	--	--	++	--	-
	0.75	$F_{br;ax;c}$	-	++	-	++	--	-	--	+	--	++	--	+
		$M_{br;ip;c}$	--	--	--	-	--	--	--	--	--	--	--	--
		$M_{br;op;c}$	--	--	--	--	--	--	--	--	-	--	--	-

+++ = Very large SCFs due to carry-over effects (> 50 % of SCFs due to identical reference effects).
++ = Large SCFs due to carry-over effects (> 30 % of SCFs due to identical reference effects).
+ = Small SCFs due to carry-over effects (> 10 % of SCFs due to identical reference effects).
- = Negligible SCFs due to carry-over effects (SCF < 0.5).
-- = Approximately zero SCFs due to carry-over effects (SCF < 0.1).

Table 25. Importance of in-plane carry-over effects (SCFs caused by $F_{br;ax;c}$, $M_{br;ip;c}$ and $M_{br;op;c}$) related to SCFs due to reference effects (SCFs caused by $F_{br;ax;a}$, $M_{br;ip;a}$ and $M_{br;op;a}$) of a K joint.

About the importance of SCFs caused by in-plane carry-over effects it is concluded that:

- The influence of changes in γ and τ on in-plane carry-over effects cannot be neglected.
- For all locations, the load case $F_{br;ax;c}$ causes large in-plane carry-over effects. This is especially the case when increasing γ and τ. Figure 45 shows for the chord saddle location of a K joint with φ_{ip} = 60° and β = 0.40 the influence of γ and τ on SCFs caused by in-plane carry-over loading $F_{br;ax;c}$ and reference loading $F_{br;ax;a}$.
- As illustrated in figure 46, the in-plane carry-over SCF results for the two chord crown locations (toe and heel) might differ entirely. Existing formulae [*F13*, *F62*] makes no distinction on SCFs for the heel and toe locations.

6.6.4 Influence of the presence of an in-plane carry-over brace member on SCFs due to reference loading

The influence of the presence of the in-plane carry-over brace member *c* on SCFs due to reference loadings $F_{br;ax;a}$, $M_{br;ip;a}$ and $M_{br;op;a}$ has been investigated by comparison of SCF results from Y joints and K joints.
The results of comparison on SCFs between Y joints and K joints are summarized in table 26.
This table shows the maximum range of the ratio *SCF Y joint / SCF K joint*, which exists for the combination $\gamma_{min};\tau_{min}$ (lower bound) and $\gamma_{max};\tau_{max}$ (upper bound).
From the results given in table 26, the following conclusions are made:

- The influence of the presence of the carry-over brace member *c* on SCFs due to reference loadings $F_{br;ax;a}$, $M_{br;ip;a}$ and $M_{br;op;a}$, mainly depends on γ and τ, the size of the smallest gap region (combination of β and φ_{ip}) and the load case considered.
  In general, for all locations considered, increase of γ and τ and decrease of the size of the gap region results in an increase of the influence of the presence of the carry-over brace member *c* on SCFs caused by the reference loadings.
- The influence of the presence of the in-plane carry-over brace member *c* on SCFs due to reference loading, which was ignored up to now, is found to be only negligible for the following situations (differences smaller than ±10%):

  - The SCFs caused by reference loading $M_{br;op;a}$.
  - For low values of γ and τ, the SCFs caused by reference loadings $F_{br;ax;a}$ and $M_{br;ip;a}$.
  - The SCFs caused by reference loadings $F_{br;ax;a}$, $M_{br;ip;a}$ for the chord saddle, brace saddle and brace crown heel locations.

As an example, for $F_{br;ax;a}$, due to the existence of an in-plane carry-over brace member *c*, a large influence on SCFs (differences with relation to Y joints up to 50%) is found for the chord crown toe location. Figure 47 illustrates the differences in SCFs.

φ_{ip}	β	Load case	Location of interest											
			cc;1 (heel)		cc;5 (toe)		bc;1 (heel)		bc:5 (toe)		cs;3,7		bs;3,7	
			γ=12 τ=0.25	γ=30 τ=1.0	γ=12 τ=0.25	γ=30 τ=1.0	γ=12 τ=0.25	γ=30 τ=1.0	γ=12 τ=0.25	γ=30 τ=1.0	γ=12 τ=0.25	γ=30 τ=1.0	γ=12 τ=0.25	γ=30 τ=1.0
60°	0.25	$F_{br;ax;a}$	*	0.94	0.99	0.90	1.00	*	0.99	0.88	1.01	1.03	1.01	1.04
		$M_{br;ip;a}$	*	1.00	1.00	0.98	1.00	1.01	*	0.99	*	*	*	*
		$M_{br;op;a}$	*	*	*	*	*	*	*	*	1.00	1.01	1.00	1.01
	0.40	$F_{br;ax;a}$	*	0.77	0.93	0.51	0.96	*	0.95	*	1.03	1.10	1.02	1.09
		$M_{br;ip;a}$	*	1.03	0.98	0.82	1.01	1.04	0.98	0.77	*	*	*	*
		$M_{br;op;a}$	*	*	*	*	*	*	*	*	1.02	1.08	1.01	1.07
45°	0.25	$F_{br;ax;a}$	all 1.00											
		$M_{br;ip;a}$												
		$M_{br;op;a}$												
	0.40	$F_{br;ax;a}$	*	0.85	0.94	0.81	0.99	*	1.00	0.83	1.01	1.06	1.02	1.06
		$M_{br;ip;a}$	*	1.02	*	0.97	1.00	1.01	*	0.96	*	*	*	*
		$M_{br;op;a}$	*	*	*	*	*	*	*	*	1.00	1.02	1.00	1.02
	0.60	$F_{br;ax;a}$	*	0.74	0.92	0.50	0.97	*	0.98	*	1.03	1.09	1.00	1.01
		$M_{br;ip;a}$	*	1.04	0.98	0.80	1.01	1.06	0.99	*	*	*	*	*
		$M_{br;op;a}$	*	*	*	*	*	*	*	*	1.03	1.10	1.00	1.02
30°	0.25 and 0.40	$F_{br;ax;a}$	all 1.00											
		$M_{br;ip;a}$												
		$M_{br;op;a}$												
	0.60	$F_{br;ax;a}$	*	0.90	1.00	0.85	1.00	0.94	1.00	0.99	*	1.08	*	1.07
		$M_{br;ip;a}$	*	1.01	*	0.96	1.00	1.01	*	*	*	*	*	*
		$M_{br;op;a}$	*	*	*	*	*	*	*	*	*	1.02	*	1.02
	0.75	$F_{br;ax;a}$	*	0.98	0.97	0.58	0.99	*	1.01	*	*	1.09	*	1.09
		$M_{br;ip;a}$	*	1.02	*	0.88	1.00	1.02	*	*	*	*	*	*
		$M_{br;op;a}$	*	*	*	*	*	*	*	*	*	1.09	*	1.09

* = SCF < 1.00

Table 26. Influence of the presence of a carry-over brace member *c* on SCFs caused by reference loadings $F_{br;ax;a}$, $M_{br;ip;a}$ and $M_{br;op;a}$. Maximum range of the ratio *SCF Y joint / SCF K joint* shown.

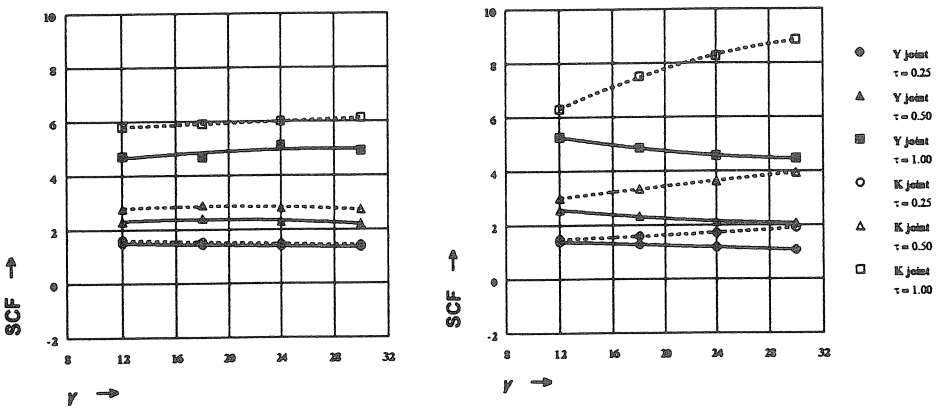

Fig. 47. SCFs caused by $F_{br;ax;a}$ for the chord crown toe location of a Y joint and a K joint. Left figure φ_{ip} = 45°, and right figure φ_{ip} = 60°: β=0.40.

6.6.5 Results on the relationship between SCF and SNCF

In an identical way as described for joints with braces perpendicular to the chord axis (see chapter 6.5.7), the relationship between SCF and SNCF has been investigated for joints with braces inclined to the chord axis.
The relationship between SCF and SNCF has been investigated for reference member loads $F_{br;ax;a}$, $M_{br;ip;a}$ and $M_{br;op;a}$ and carry-over member loads $F_{br;ax;c}$, $M_{br;ip;c}$ and $M_{br;op;c}$. The influence of the presence of an in-plane carry-over brace member *c* on *snf* related to reference member loads is found to be negligible (differences within 5%). The *snf* results of the investigation on joints with braces inclined to the chord axis are summarized in table 27. In addition to the conclusions given on the relationship between SCF and SNCF for joints with braces perpendicular to the chord axis, for joints with braces inclined to the chord axis, it is concluded:

- *For the chord member loads, increase of φ_{ip} results in a decrease of the average snf.*

Load case	Location	φ_{ip} = 30°		φ_{ip} = 45°		φ_{ip} = 60°		Influence of joint parameter		
		$snf_{average}$	range snf	$snf_{average}$	range snf	$snf_{average}$	range snf	β	γ	τ
Reference loading : Y joint										
$F_{ch,ax}$	cc;1	1.16	1.12 < snf < 1.18	1.10	1.06 < snf < 1.14	1.08	1.04 < snf < 1.12	o	o	+
	cc;5	1.10	1.06 < snf < 1.15	1.09	1.03 < snf < 1.14	1.07	1.02 < snf < 1.12	o	o	+
$M_{ch,ip}$***	cc;1	1.16	1.11 < snf < 1.20	1.13	1.08 < snf < 1.18	1.09	1.06 < snf < 1.15	o	o	+
	cc;5	1.13	1.08 < snf < 1.17	1.11	1.07 < snf < 1.15	1.08	1.05 < snf < 1.14	o	o	+
$F_{br,ax,a}$	cc;1	1.22	1.17 < snf < 1.25	1.21	1.13 < snf < 1.30	1.21	1.18 < snf < 1.29	o	-	+
	cc;5	1.28	1.24 < snf < 1.35	1.31	1.19 < snf < 1.43	1.30	1.21 < snf < 1.51	-	-	-
	bc;1	1.20	1.12 < snf < 1.25	1.25	1.17 < snf < 1.41	1.23	1.23 < snf < 1.33	o	+	-
	bc;5	1.32	1.22 < snf < 1.46	1.31	1.21 < snf < 1.43	1.34	1.23 < snf < 1.45	o	+	-
	cs;3,7	1.20	1.18 < snf < 1.22	1.19	1.15 < snf < 1.23	1.19	1.16 < snf < 1.23	o	o	-
	bs;3,7	1.39	1.10 < snf < 1.53	1.23	1.12 < snf < 1.40	1.18	1.13 < snf < 1.24	+ : $\varphi_{ip} \leq 45°$ - : $\varphi_{ip} > 45°$	o	+
$M_{br,ip,a}$	cc;1	1.27	1.23 < snf < 1.32	1.28	1.23 < snf < 1.33	1.27	1.24 < snf < 1.32	-	-	-
	cc;5	1.23	1.21 < snf < 1.26	1.26	1.22 < snf < 1.37	1.27	1.21 < snf < 1.34	o	o	-
	bc;1	1.20	1.14 < snf < 1.26	1.21	1.17 < snf < 1.27	1.23	1.18 < snf < 1.31	o	o	+
	bc;5	**	**	**	**	1.23	1.19 < snf < 1.31	o	+	+
$M_{br,op,a}$	cs;3,7	1.20	1.18 < snf < 1.23	1.20	1.16 < snf < 1.25	1.19	1.17 < snf < 1.22	o	o	-
	bs;3,7	1.48	1.35 < snf < 1.56	1.25	1.12 < snf < 1.39	1.18	1.12 < snf < 1.24	+ : $\varphi_{ip} \leq 45°$ - : $\varphi_{ip} > 45°$	+ : $\varphi_{ip} \leq 45°$ - : $\varphi_{ip} > 45°$	+ : $\varphi_{ip} \leq 45°$ - : $\varphi_{ip} > 45°$
Carry-over loading : K joint										
$F_{br,ax,c}$	cc;1	**	**	1.25	1.24 < snf < 1.27	1.33	1.31 < snf < 1.35	+	+	+
	cc;5	1.14	1.12 < snf < 1.16	1.22	1.19 < snf < 1.25	1.30	1.26 < snf < 1.35	+	+	+
	cs;3,7	1.13	1.10 < snf < 1.16	1.15	1.14 < snf < 1.16	1.18	1.16 < snf < 1.19	o	-	o
	bs;3,7	**	**	1.34	1.33 < snf < 1.36	1.25	1.23 < snf < 1.27	o	+	o
$M_{br,op,c}$	cs;3,7	1.16	1.15 < snf < 1.16	**	**	1.15	1.14 < snf < 1.17	o	-	o

- = Increase of β, γ or τ results in a decrease of *snf*.
o = Influence of β, γ or τ on *snf* is negligible.
\+ = Increase of β, γ or τ results in an increase of *snf*.
** = SNCF < 1.00.
*** = Causing a nominal bending stress of 1 N/mm² at the chord outer surface along the plane of the crown.

Table 27. Results of the investigation on the relationship between SCF and SNCF for joints with braces inclined to the chord axis.

7. SUMMARY AND CONCLUSIONS

7.1 *Design rules proposed*

Design rules are given on the following topics:
- *Numerical modelling of welded tubular joint stress concentration factors.*
- *Basics concerning fatigue analysis of welded tubular joints.*
- *Determination of stress concentration factors.*
- *Relationship between stress and strain concentration factor.*
- *Basic design fatigue resistance curve for welded multiplanar tubular joints.*
- *Fatigue design procedure of welded tubular joints.*

Numerical modelling of welded tubular joint stress concentration factors

As concluded in chapter 3, results on stress concentration factors based on numerical work using FE analyses largely depend on the type of element, mesh refinement, integration scheme and the weld shape considered.
The following recommendations are given:

Element type:
- The use of 20-n solid elements with a reduced integration scheme 2x2x2 is recommended.
- The use of transition elements is disadvised. Because these elements increase rather than decrease computer costs. Thus a combination of shell elements and solid elements should not be used.
- Regarding isolated joints, to avoid end effects, the length of the member parts outside the intersection area should be at least 3 times the diameter of the corresponding member.

Mesh refinement:
- The length of the 20-n solid element measured along the weld toe should be approximately less than 1/16 of the total length around the perimeter of the brace to chord intersection.
- Near the weld toe location, the length of the elements measured perpendicular to the intersection area for the chord member and measured parallel to the brace axis for the brace member should be based on a convergence criteria. For that, the influence of at least three alternative mesh refinements on joint flexibility and stress concentration factors should be investigated.

Weld shape:
- The real weld shape using 20-n solid elements should be included in the FE model, and the SCFs should be determined at the weld toe location.

Basics concerning fatigue analysis of welded tubular joints

From the research results described in chapter 6.2, based on the use of the hot spot approach, the following basics concerning fatigue analysis of welded tubular joints are recommended:

Stresses (strains) to be considered
- Stresses should be used in a direction perpendicular to the weld toe for the chord member locations and in a direction parallel to the axis of the brace member for the

brace member locations (this direction mostly differs from the direction perpendicular to the weld toe) should be used.

Extrapolation region

- For the chord and brace member locations, the following extrapolation region measured in a direction equal to the direction of stresses considered is preferred:
  - chord member (crown, inbetween and saddle):
    $l_{r;min} = 0.4 \cdot t_o$ and $l_{r;max} = 1.4 \cdot t_o$
  - brace member (crown, inbetween and saddle):
    $l_{r;min} = 0.4 \cdot t_1$ and $l_{r;max} = 1.4 \cdot t_1$

Method of extrapolation

- A parabolic quadratic curve fitting through all the data points in and around the extrapolation region and determining the stresses at $l_{r;min}$ and $l_{r;max}$ using the obtained curve should be carried out firstly.
  Secondly, for determining the hot spot stress, using the two determined coordinates $l_{r;min}$,$\sigma_{l_{r;min}}$ and $l_{r;max}$,$\sigma_{l_{r;max}}$, a linear extrapolation to the weld toe should take place.

Locations around the reference brace where the hot spot stress is determined

- The fixed weld toe locations of interest for both chord and brace member are crown, saddle and inbetween. This results, when analysing one load case, into eight hot spot stresses for the chord member and eight hot spot stresses for the brace member.
- Hot spot stresses at other weld toe locations can be determined from polynomial curve fitting through the hot spot stresses of the eight fixed weld toe locations around the intersection area along the member surface.

Boundary conditions

- The stress concentration factors analysed should be independent of boundary conditions used. Therefore, in case of brace member loads which causes bending in the chord member, to obtain the effect of brace member load only, compensating moment(s) on the chord member end(s) needs to be incorporated.

Determination of stress concentration factors

The stress concentration factors can be determined in three ways, namely:

- *Through experimental model studies.*
  Information on the test method used for the development of the fatigue resistance curve for welded multiplanar joints is given in [*F23*].
- *Through numerical model studies.*
  Recommendations on numerical modelling of welded tubular joint stress concentration factors are given on page 71, and basics concerning fatigue analysis of welded tubular joints are given on pages 71-72.
- *Data files and parametric formulae.*
  Stress concentration factors are determined for several common types of welded uniplanar and multiplanar tubular joints. Because of the enormous data obtained, the results are stored in data files, from which e.g. by the use of an input-file and a program-file the SCFs (SNCFs) and hot spot stresses (strains) can be obtained automatically. In addition to the data files, for multiplanar XX joints parametric formulae are developed.

By means of tables, conclusions are made on:

- *The importance of SCFs due to in-plane carry-over effects (see table 25).*
- *The importance of SCFs due to out-of-plane carry-over effects (see table 19).*

- *The influence of the presence of an in-plane carry-over brace member on SCFs due to reference loading (see table 26).*
- *The influence of the presence of an out-of-plane carry-over brace member on SCFs due to reference loading (see table 20).*

The information given in tables 19, 20, 25 and 26 are assumed to be helpful when analysing SCFs for any type of welded tubular joint. This because, in many cases the SCFs caused by carry-over loading are found to be negligible. Also, in many cases, the influence of the presence of a carry-over member on the SCFs due to reference loading is found to be negligible.

Relationship between stress and strain concentration factor

When assuming a plane-stress condition and a fully isotropic behaviour of steel with $E=2.068 \cdot 10^5 N/mm^2$ and $\nu=0.30$, the relationship between SCF and SNCF can be written as:

$$snf = \frac{SCF}{SNCF} = 1.10 + 0.33 \cdot \frac{\epsilon_y}{\epsilon_{x,h.s.}}$$

The parameter study results show the existence of a large variation on *snf*.
Related to the joint parameters β, γ, τ, φ_{ip} and φ_{op} and to the type of joint, for the relevant reference as well as carry-over effects, values of *snfs* are stored in data files. These *snfs* are recommended when converting hot spot strains into hot spot stresses. A summary of *snf* results is given in tables 23 and 27.

Basic design fatigue resistance curve for welded multiplanar tubular joints

There is sufficient evidence from de DEn design fatigue resistance curve for welded uniplanar tubular joints. This curve relies on an empirically derived relationship between the applied stress ranges and the fatigue life (*S-N* approach), based on a large amount of test data from simple tubular joints.
The characteristic DEn design curve for uniplanar tubular joints based upon the mean line minus two standard deviation (2σ) and a wall thickness of 16 mm is

for: $10^3 < N_f < 5 \cdot 10^6$: $\log N_f = 12.4756 - 3 \cdot \log (S_{r_{h.s.}})$

For wall thicknesses larger than 16 mm, a thickness correction of

$S_{r_{h.s.;t \geq 16}} = S_{r_{h.s.;t = 16}} \cdot (16/t)^{0.30}$ is applied for the whole curve.

The fatigue data based on first through-thickness cracking from the tested multiplanar KK joints with wall thicknesses of 4, 8 and 16 mm are in good agreement with the proposed DEn design curve for uniplanar tubular joints. Because of this agreement, for welded multiplanar KK joints with wall thicknesses between 4 and 16 mm, the use of the DEn design curve for welded uniplanar joints with a wall thickness of 16 mm is recommended. For multiplanar joints in a non-corrosive environment and those in a corrosive environment which are adequately protected, a fatigue cut-off limit is adopted at $N=5 \cdot 10^6$ cycles for constant amplitude loading in accordance with EC3 [*F12*]. For variable amplitude loading, a slope of m=-5 is used between $5 \cdot 10^6$ and the cut-off limit $1 \cdot 10^8$.

Fatigue Design Procedure

1. ***Replace the structure into an acceptable numerical model.***

2. ***Determine the load distribution by means of nominal stresses.***
   - This needs to be done for the brace and chord members of the joint(s) under consideration only.
   - Relevant member loads are:
     - Chord member: $F_{ch;ax}$, $M_{ch;ip}$ and $M_{ch;op}$;
     - Brace member: $F_{br;ax}$, $M_{br;ip}$ and $M_{br;op}$ (incl. $M_{br;t}$) .

3. ***Determine the extrapolated nominal stresses.***
   - The stresses should be extrapolated to the intersection of the brace center-line and the outerwall surface of the continuous member.

4. ***Determine the stress concentration factors using SCF formulae, graphs or data files.***
   For SCF results by means of formulae, graphs and/or data files, reference is made to chapter 6, in which the parameter study SCF results for T, Y, K, TT, XX and KK joints are discussed.
   - Based on information given in tables 19 and 25, decide whether SCFs caused by carry-over effects can be neglected.
   - Based on information given in tables 20 and 26, decide whether SCFs caused by reference effects are influenced by the presence of a carry-over brace member.

5. ***Determine the total hot spot stress (range) $(\Delta)\sigma_{h.s.;tot}$ for the potential crack location(s).***
   - For the contribution of secondary bending moments, independent of the method of numerical idealization and independent of the location (crown, saddle and inbetween) considered, a minimum of

$$\sigma_{h.s.;br_{tot}} = 1.5 \cdot \sum_{i=1}^{n} SCF_{br_i;axial} \cdot \sigma_{br_i;axial}$$

     should be used in case of lattice structures [*F65*]
   - Depending upon the code of practice, a safety factor γ_m should be applied.
   - For wall thicknesses larger than 16 mm, a thickness correction should be applied.

6. ***Determine the Palmgren-Miner cumulative damage factor.***

$$D_d = \sum_1^i \frac{n_i}{N_i} \leq 1.0.$$

   - Use a design fatigue resistance curve.
   - The damage factor D_d should not exceed 1.0.

ACKNOWLEDGEMENTS

The research reported in this thesis has been carried out at the Civil Engineering Department of Delft University of Technology. Appreciation is extended to STW, ECSC and CIDECT for financial support of parts of the research projects. Appreciation is also extended to the Dutch Ministry of Economic Affairs for their additional financial contribution. Thanks are also due for donation of the hollow sections by Van Leeuwen Buizen, Zwijndrecht, The Netherlands. Also, special thanks are expressed to Prof. Dr. J. Wardenier, Prof. Dr. R.S. Puthli, Mr. C.H.M. de Koning, Mr. H. van Kakum, Ir. P. Smedley, Dipl. ing. D. Dutta, Mr. N.F. Yeomans, Mw. Dipl. Phys. C.N.M. Jansz, commission CS-W9 (tubular structures) and Diana Analysis BV (The Netherlands) for their support and friendship.

NOTATION

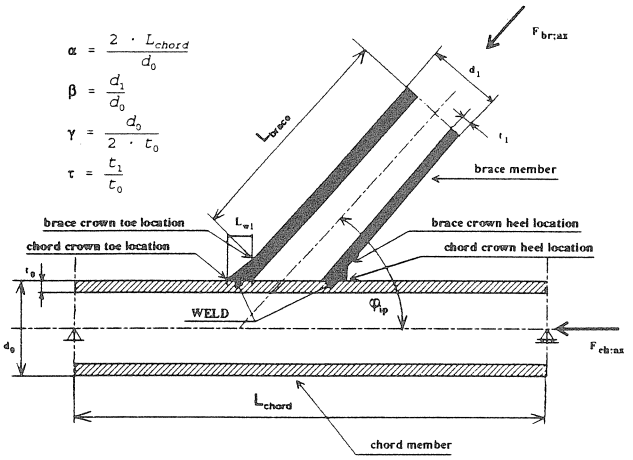

Fig. 48. Welded tubular joint.

A	Cross sectional area of member considered.
E	Youngs modulus of elasticity (E_{steel} = 2.068·10 ^{5} N/mm^2).
F	Girder load or axial load on a member.
$F_{br;ax;a}$	Axial load on brace member '*a*'.
$F_{ch;ax}$	Axial load on chord member.
L_{wl}	Length of weld footprint on chord member: *weld footprint length alternative 1.*
$M_{br;ip;a}$	In-plane bending moment on brace member '*a*'.
$M_{br;t;a}$	Torsional moment on brace member '*a*'.
$M_{ch;ip}$	In-plane bending moment on chord member.
N_f	Number of cycles to failure (through-thickness cracking).
N_{ini}	Number of cycles to initiation of cracks determined by strain gauge measurements.
R	Stress ratio σ_{min} / σ_{max} in a cycle for constant amplitude loading.
$S_{r_{h.s.}}$	Hot spot stress range: $S_{r_{h.s.}}$ = SCF · σ_r = SCF · (σ_{max} - σ_{min}).
W	Elastic section modulus of member considered.

bdc_1	Boundary condition of an isolated joint: *boundary condition method 1.*
d_0	External diameter of chord member.
d_{1-4}	External diameter of brace members 1-4.
int_1	Integration scheme of an element: *integration scheme method 1.*
$l_{r;min}$	Extrapolation region: minimum distance from the weld toe.
$l_{r;max}$	Extrapolation region: maximum distance from the weld toe.
mf_1	Mesh refinement: *alternative 1.*
snf	Conversion factor: *snf* = SCF/SNCF.
r_0	External radius of chord member.
r_{1-4}	External radius of brace members 1-4.
t_0	Wall thickness of chord member.
t_{1-4}	Wall thickness of brace members 1-4.
α	Chord length to half chord diameter ratio: $\alpha = 2L / d_0$.
α_{br}	Brace strain ratio: $\alpha_{br} = \varepsilon_{h.s.;tot} / \varepsilon_{h.s.;ax}$.
β	Brace to chord diameter ratio: $\beta = d_1 / d_0$.
τ	Brace to chord wall thickness ratio: $\tau = t_1 / t_0$.
γ	Radius to wall thickness ratio of chord member: $\gamma = d_0 / (2 \cdot t_0)$.
$\varepsilon_{ch;ax}$	Nominal axial strain in chord member.
$\varepsilon_{h.s.;tot}$	Total hot spot strain (at a fixed weld toe location).
ε_r	Nominal strain range.
ε_{tot}	Total nominal strain: $\varepsilon_{tot} = \varepsilon_{extrap;nom} = \varepsilon_{axial;nom} \pm \sqrt{\varepsilon^2_{extrap;ipb} + \varepsilon^2_{extrap;opb}}$.
$\varepsilon_{tot;num}$	Total nominal strain obtained from numerical work.
ε_y	Strain measured in a direction parallel to the weld toe (chord outerwall surface), or along the brace member perpendicular to the axis of the brace member (brace outerwall surface).
$\sigma_{ch;ax}$	Nominal axial stress in chord member.
$\sigma_{h.s.tot}$	Total hot spot stress (or geometric stress).
σ_{nom}	Nominal stress.
σ_r	Nominal stress range.
φ_{ip}	Smallest in-plane angle between chord and brace member. (Measured along the chord axis: uniplanar plane).
φ_{op}	Smallest out-of-plane angle between two brace members. (Measured perpendicular to the chord axis: multiplanar plane).
ν	Poison ratio: $\nu_{steel} = 0.30$.

SUBSCRIPTS

ax	Axial.
br	Brace member.
ch	Chord member.
exp	Experimental.
extrap	Extrapolation along a specified distance.
h.s.	Hot spot.
ip(b)	In-plane (bending).
nom	Nominal.
num	Numerical.
op(b)	Out-of-plane (bending).

ACRONYMS

API	American Petroleum Institute.
AWS	American Welding Society.
CHS	Circular (Tubular) Hollow Section.
CIDECT	Comité International pour le Développement et l'Étude de la Construction Tubulaire.
CISC	Canadian Institute of Steel Construction.
DEn	Department of Energy (UK).
ECSC	European Coal and Steel Community.
EC3	Eurocode No. 3.
FE	Finite Element.
HSE	Health and Safety Executive.
IIW	International Institute of Welding.
NAFEMS	National Agency for Finite Element Methods and Standards.
SCF	Stress concentration factor.
SNCF	Strain concentration factor.
STW	Netherlands Technology Foundation.
UEG	Underwater Engineering Group.

REFERENCES

Numerical aspects of the analysis of welded tubular joints

[*N1*]	Blaauwendraad, J. Kok, A.W.M.	Elementenmethode voor constructeurs. Part 1 and 2. ISBN 90 10 10440 0 1973. Elsevier Science publishers ltd. Amsterdam, The Netherlands.
[*N2*]	Bathe, K.J.	Finite element procedures in engineering analysis. ISBN 0-13-317305-4. Prentice-Hall, Inc., Englewood Cliffs, New Jersey, USA.
[*N3*]	Kok, A.W.M.	Numerical Mechanics. 104041-B18. Delft University of Technology, The Netherlands.
[*N4*]	NAFEMS	National Agency for Finite Element Methods and Standards. A finite element primer. ISBN 0 903640 17 1. 1986. Published by Department of Trade and Industry, National Engineering Laboratory, East Kilbride, Glasgow G75 0QU, UK.
[*N5*]	Romeijn, A. Puthli, R.S. Wardenier, J.	"Finite element modelling of multiplanar joints in tubular structures". 2nd INTERNATIONAL OFFSHORE AND POLAR ENGINEERING CONFERENCE. International Society of Offshore and Polar Engineers, P.O. Box 1107 Golden, Colorado, U.S.A. San Francisco, U.S.A., June 1992.

Fatigue behaviour of welded tubular joints

[*F1*]	American Petroleum Institute	Recommended practice for planning, designing and constructing fixed offshore platforms, API RP2A-LRFD, API RP2A-WSD, July 1, 1993.
[*F2*]	American Welding Society	Structural welding code - Steel. ANSI/AWS D1.1-94, 14th edition, Miami, USA, 1994.

[F3]	Back, J. de Vaessen, G.H.G.	Fatigue behaviour and corrosion fatigue behaviour of offshore structures. Final report ECSC Convention 7210-KB/6/602 (J.7. 1 f/76). Foundation for Materials Research in the Sea. Delft/Apeldoorn, April 1981. The Netherlands.
[F4]	Back, J. de	"Size effect and weld profile effect on fatigue of tubular joints". IIW - AIJ CONFERENCE SAFETY CRITERIA IN DESIGN OF TUBULAR STRUCTURES. February 1987, Tokyo, Japan. p. 331-341.
[F5]	Back, J. de	"Strength of tubular joints". INTERNATIONAL CONFERENCE ON STEEL IN MARINE STRUCTURES. 1981. France.
[F6]	Back, J. de	"The design aspects and fatigue behaviour of tubular joints". INTERNATIONAL CONFERENCE ON STEEL IN MARINE STRUCTURES. 1987. The Netherlands.
[F7]	Berge, S.	"Fatigue strength of tubular joints: some unresolved problems". 1993.
[F8]	Delft, D.R.V. van Noordhoek, C. Da Re, M.L.	"The results of the European fatigue tests on welded tubular joints compared with SCF formulas and design lines". INTERNATIONAL CONFERENCE ON STEEL IN MARINE STRUCTURES. 1987. The Netherlands.
[F9]	Department of Energy	Department of Energy, 1984, Offshore installation guidance on design and construction, UK.
[F10]	Dijkstra, O.D. Back, J. de	"Fatigue strength of tubular T and X joints". INTERNATIONAL CONFERENCE ON STEEL IN MARINE STRUCTURES. 1981. France.
[F11]	Dijkstra, O.D. Puthli, R.S. Snijder, H.H.	"Stress concentration factors in T and KT tubular joints using finite element analysis". Journal of Energy Resources Technology, december, 1988.
[F12]	EC	European Committee for Standardization, Eurocode 3: Design of steel structures - Part 1.1: General rules and rules for buildings. ENV 1993-1-1: 1992E, British Standards Institution, London, UK 1992.
[F13]	Efthymiou, M.	Development of SCF formulae and generalized functions for use in fatigue analysis. Report published by Shell International Petroleum Maatschappij B.V, September 1988. The Netherlands.
[F14]	European Committee for Standardization	Eurocode 3: design of steel structure - Part 1.1: General rules and rules for building. ENV 1993-1-1: 1992E, British Standards Institution of Welding Annual Assembly, The Hague, The Netherlands, 1991.
[F15]	Gibstein, M.B. Moe, M.T.	"Numerical and experimental stress analysis of tubular joints with inclined braces". INTERNATIONAL CONFERENCE ON STEEL IN MARINE STRUCTURES. 1981. France.
[F16]	Gibstein, M.B.	"Parametrical stress analysis of T joints". European Offshore Steels Research Preprints, Volume 2. Paper 26. UK Department of Energy. Abington Hall, Cambridge, UK November 1978.
[F17]	Gibstein, M.B.	"Fatigue strength of welded tubular joints tested at Det Norske Veritas Laboratories". INTERNATIONAL CONFERENCE ON STEEL IN MARINE STRUCTURES. 1981. France.
[F18]	Harrison, J.D.	"The significance of welded defects with regard to fatigue behaviour". Fatigue aspects in structural design.

ISBN 90-6275-560-7. Delft University Press. The Netherlands.

[*F19*] Hirt, M. "Interaction between research, standardization and design". Fatigue aspects in structural design. ISBN 90-6275-560-7. Delft University Press. The Netherlands.

[*F20*] Irvine, N.M. "Stress analysis of tubular joints: safety and reliability". Fatigue in offshore steel, ICE, London, 1981.

[*F21*] Irvine, N.M. "Comparison of the Performance of modern semi-empirical parametric equations for Tubular Joint Stress Concentration Factors". INTERNATIONAL CONFERENCE ON STEEL IN MARINE STRUCTURES. 1981. France.

[*F22*] International Institute of Welding Subcommission XV-E. Recommended fatigue design procedure for hollow section joints. Part 1 - Hot spot stress method for nodal joints. IIW Doc. XIII-1158-85, XV-582-85, International Institute of Welding Annual Assembly. France, 1985.

[*F23*] Koning, C.H.M. de et al Fatigue behaviour of multiplanar welded hollow section joints and reinforcement measures for repair. TNO-Building and Construction Reearch, Rijswijk, The Netherlands. Report BI-92-0079/21.4.6394. Delft University of Technology. The Netherlands. Report 6.92.17/A1/12.06. 1992. Stevinweg 1, 2628 CN Delft, The Netherlands.

[*F24*] Kuang, J.G. Potvin, A.B. Leick, R.D. "Stress concentration in tubular joint". OFFSHORE TECHNOLOGY CONFERENCE (OTC '75). paper 2205. P.O. Box 833868, Richardson. 1975. USA.

[*F25*] Kurobane, Y. Recent developments in the fatigue design rules in Japan. Fatigue aspects in structural design. ISBN 90-6275-560-7. Delft University Press. The Netherlands.

[*F26*] Lalani, M. "Developments in tubular joints technology for offshore structures". 2nd INTERNATIONAL OFFSHORE AND POLAR ENGINEERING CONFERENCE. International Society of Offshore and Polar Engineers, P.O. Box 1107 Golden, Colorado, U.S.A. San Francisco, U.S.A., June 1992.

[*F27*] Lalani, M. Tebbet, I.E. Choo, B.S. "Improved fatigue life estimation of tubular joints". 18th OFFSHORE TECHNOLOGY CONFERENCE OTC 5306. Houston, Texas, 1986.

[*F28*] Lieurade, H.P. Gerald, J. "Results of static tests on ten full scale X joints. INTERNATIONAL CONFERENCE IN STEEL MARINE STRUCTURES. 1981. France.

[*F29*] Ma, S.Y. Tebbet, I.E. "Estimations of stress concentration factor for fatigue design of welded tubular connections". OFFSHORE TECHNOLOGY CONFERENCE OTC 5666. Houston, Texas, 1986.

[*F30*] Marshall, P.W. Report "Design of welded tubular connections: basis and use of AWS code provisions". 1989. U.S.A. Civil Engineering Consultant. Shell Oil Company, Houston, Texas. U.S.A.

[*F31*] Marshall, P.W. Recent developments in the fatigue design rules in the USA. Fatigue aspects in structural design. ISBN 90-6275-560-7. Delft University Press. The Netherlands.

[*F32*] Marshall, P.W. "Design of welded tubular connections: Basis and use of AWS code provisions" Shell Oil Company, Houston, U.S.A. Developments in Civil Engineering, Volume 37. Elsevier applied science publishers ltd. Amsterdam / London / New York / Tokio.

[*F33*] Niemi, E. "Determination of stresses for fatigue analysis of welded components". Engineering design in welded constructions. Published on behalf of the International Institute of Welding 1992. ISBN 0 08 041910 0.

[*F34*] Niemi, E. Recommendations concerning stress determination for fatigue analysis of welded components. IIW Doc. XIII-1458-92 XV-797. 1992.

[*F35*] Packer, J.A. Henderson, J.E. Design guide for hollow structural section connections. ISBN 0-88811-076-6, July 1992. Canadian Institute of Steel Construction.

[*F36*] Puthli, R.S. "Geometrical non-linearity in collapse analysis of thick walled shells, with application to tubular steel joints". HERON, TU-Delft, TNO-IBBC, Volume 26, No. 1, 1981.

[*F37*] Radenkovic, D. "Stress analysis in tubular joints". INTERNATIONAL CONFERENCE ON STEEL IN MARINE STRUCTURES. 1981. France.

[*F38*] Reynolds, A.G. "The fatigue performance of tubular joints". An overview of recent work to revise Department of Energy guidance, 4th INTERNATIONAL SYMPOSIUM ON INTEGRITY OF OFFSHORE STRUCTURES, Glasgow, UK, July 1990.

[*F39*] Romeijn, A. Puthli, R.S. Wardenier, J. Koning, C.H.M. de Dutta, D. "Fatigue behaviour of multiplanar welded hollow section joints and reinforcement measures for repair". TNO-Building and Construction Research, Rijswijk, The Netherlands. Report BI-92- 0064/21.4.6394. Delft University of Technology, The Netherlands. Report 6.92.09/A1/12.08. 1992.

[*F40*] Romeijn, A. Panjeh Shahi, E. Puthli, R.S. Wardenier, J. "Fatigue strength of multiplanar welded, unstiffened hollow section joints and reinforcement measures for in-plane and multiplanar joints in repair". Stevin report 25.6.89.40/A1. Delft University of Technology. The Netherlands.

[*F41*] Romeijn, A. "Stress and strain concentration factors for T joints in circular hollow sections". STW project: DCT 80-1457 "Numerical and Experimental Investigation for the Stress Concentration Factors in Multiplanar Joints". Delft University of Technology. The Netherlands. Report 6.93.35/12.07. 1993.

[*F42*] Romeijn, A. "Stress and strain concentration factors for TT (180°) joints in circular hollow sections. STW project: DCT 80-1457 "Numerical and Experimental Investigation for the Stress Concentration Factors in Multiplanar Joints". Delft University of Technology. The Netherlands. Report 6.93.37/12.07. 1993.

[*F43*] Romeijn, A. "Stress and strain concentration factors for TT(90°) joints in circular hollow sections". STW project: DCT 80-1457 "Numerical and Experimental Investigation for the Stress Concentration Factors in Multiplanar Joints". Delft University of Technology. The Netherlands. Report 6.93.38/12.07. 1993.

[*F44*] Romeijn, A. "Stress and strain concentration factors for TT(135°) joints in circular hollow sections". STW project: DCT 80-1457 "Numerical and Experimental Investigation for the Stress Concentration Factors in Multiplanar Joints". Delft University of Technology. The Netherlands.

		Report 6.93.40/12.07. 1993.
[F45]	Romeijn, A.	"Stress and strain concentration factors for TT joints in circular hollow sections". STW project: DCT 80-1457 "Numerical and Experimental Investigation for the Stress Concentration Factors in Multiplanar Joints". Delft University of Technology. The Netherlands. Report 6.93.41/12.07. 1993.
[F46]	Romeijn, A. Puthli, R.S. Wardenier, J.	"Guidelines on the numerical determination of SCFs of Tubular Joints". 5th ISTS INTERNATIONAL SYMPOSIUM ON TUBULAR STRUCTURES, Nottingham, 1993 UK. University of Nottingham, NG7 2RD United Kingdom.
[F47]	Romeijn, A. Puthli, R.S. Koning, C. de Wardenier, J.	"Stress and strain concentration factors of multiplanar joints made of circular hollow sections". 2nd INTERNATIONAL OFFSHORE AND ENGINEERING CONFERENCE. International Society of Offshore and Polar Engineers, P.O. Box 1107 Golden, Colorado, U.S.A. San Francisco, U.S.A., June 1992.
[F48]	Romeijn, A. Puthli, R.S. Koning, C. de Wardenier, J. Dutta, D.	"Fatigue behaviour and influence of repair on multiplanar K joints made of circular hollow sections". 3th INTERNATIONAL OFFSHORE AND ENGINEERING CONFERENCE. International Society of Offshore and Polar Engineers, P.O. Box 1107 Golden, Colorado, U.S.A. Singapore, Japan, June 1993.
[F49]	Romeijn, A. Wardenier, J.	"Stress concentration factors of welded tubular joints". 6th INTERNATIONAL SYMPOSIUM ON TUBULAR STUCTURES STRUCTURES. 1994. Australia.
[F50]	Ship Structure Committee 1993	Report SSC-367 "Fatigue Technology assesment and strategies for fatigue avoidance in Marine Structures". Executive Director Ship Structure Committee. U.S. Coast Guard. 2100 Second Street, S.W. Washington, D.C. 20593-0001.
[F51]	Smedley, P.	"Stress concentration factors for ring-stiffened tubular joints". Lloyd's Register of Shipping, London, UK. 4th INTERNATIONAL SYMPOSIUM TUBULAR STRUCTURES. 1991. The Netherlands.
[F52]	Smedley, P. Fisher, P.	"Stress concentration factors for simple tubular joints". 1th INTERNATIONAL OFFSHORE AND POLAR ENGINEERING CONFERENCE. International Society of Offshore and Polar Engineers, P.O. Box 1107 Golden, Colorado, U.S.A. Edinburgh, Scotland. June 1991.
[F53]	Tebbet, I.E. Lalani, M.	"A new approach to stress concentration factor for tubular joint design". 16th OFFSHORE TECHNOLOGY CONFERENCE, Houston, Texas, 1984.
[F54]	Tebbett, I.E. Ma, S.A.	"Estimations of stress concentration for fatigue design of welded tubular connections". 20th OFFSHORE TECHNOLOGY CONFERENCE, Houston, Texas, 1988.
[F55]	Tolloczko, J.A. Lalani, M.	"The implication of new data on the fatigue life assessment of tubular joints". 20th OFFSHORE TECHNOLOGY CONFERENCE, Houston, Texas, 1988.
[F56]	UEG	Offshore Research: Publication UR 33, 1985. Design of Tubular Joints for Offshore Structures, Volume 2. ISBN 0 86017 231 7. UEG 6 Storey's Gate Westminster London SW1P 3AU. United Kingdom.
[F57]	UKOSRPII	Summary and Task Reports. HMSO, London 1987. United Kingdom.

[*F58*]	Wardenier, J.	Hollow section joints. Delft University Press. 1982. The Netherlands.
[*F59*]	Wardenier, J. et al	Design guide for circular hollow section joints under predominantly static loading. CIDECT. ISBN 3885859750. Köln, Germany, 1991.
[*F60*]	Wingerde, A.M. van Wardenier, J. Puthli, R.S. Dutta, D. Packer, J.A.	"Design recommendations and commentary regarding the fatigue behaviour of hollow section joints". 2nd INTERNATIONAL OFFSHORE AND POLAR ENGINEERING CONFERENCE. International Offshore and Polar Engineers, P.O. Box 1107 Golden, Colorado, U.S.A. San Francisco, U.S.A., June 1992.
[*F61*]	Wingerde, A.M. van	The fatigue behaviour of T- and X-joints made of square hollow sections. Heron, 37(2)(1992) 1-180.
[*F62*]	Wordsworth, A.C. Smedley, G.P.	"Stress Concentrations at unstiffened tubular joints". European Offshore Steels Research Preprints. Volume 2. Paper 31. UK Department of Energy. Abington Hall, Cambridge, UK 1978.
[*F63*]	Wordsworth, A.C.	Lloyd's Register of Shipping Research Laboratory, UK. Paper "Stress concentration factors at K and KT tubular joints". CONFERENCE FATIGUE IN OFFSHORE STRUCTURAL STEEL, ICE, London, 1981. UK.
[*F64*]	Wordsworth, A.C. Smedley, P.	Lloyd's Register of Shipping Research Laboratory, UK. Paper "Stress Concentration Factors at K and KT tubular Joints". CONFERENCE FATIGUE IN OFFSHORE STRUCTURAL STEEL, ICE, London 1981.
[*F65*]	Romeijn, A	Thesis: "Stress and strain concentration factors of welded multiplanar tubular joints". ISBN 90-407-1057-0. Delft University Press, The Netherlands.